

Marshall University

## Marshall Digital Scholar

---

Theses, Dissertations and Capstones

---

2020

### Role of ATP1A1 in Skeletal Muscle Growth and Metabolism

Laura C. Kutz  
lckutz@gmail.com

Follow this and additional works at: <https://mds.marshall.edu/etd>



Part of the [Medical Biophysics Commons](#), [Medical Physiology Commons](#), and the [Musculoskeletal, Neural, and Ocular Physiology Commons](#)

---

#### Recommended Citation

Kutz, Laura C., "Role of ATP1A1 in Skeletal Muscle Growth and Metabolism" (2020). *Theses, Dissertations and Capstones*. 1267.

<https://mds.marshall.edu/etd/1267>

This Dissertation is brought to you for free and open access by Marshall Digital Scholar. It has been accepted for inclusion in Theses, Dissertations and Capstones by an authorized administrator of Marshall Digital Scholar. For more information, please contact [zhangj@marshall.edu](mailto:zhangj@marshall.edu), [beachgr@marshall.edu](mailto:beachgr@marshall.edu).

# ROLE OF ATP1A1 IN SKELETAL MUSCLE GROWTH AND METABOLISM

A dissertation submitted to  
the Graduate College of  
Marshall University  
In partial fulfillment of  
the requirements for the degree of  
Doctor of Philosophy  
In  
Biomedical Research

by

Laura C. Kutz

Approved by

Dr. Zijian Xie, Committee Chairperson

Dr. Sandrine Pierre, Committee Co-Chairperson

Dr. Nalini Santanam

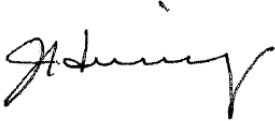
Dr. Joseph Shapiro

Dr. Judith Heiny

Marshall University  
May 2020

## APPROVAL OF THESIS

We, the faculty supervising the work of Laura C. Kutz, affirm that the dissertation, *Role of ATP1A1 in Skeletal Muscle Growth and Metabolism*, meets the high academic standards for original scholarship and creative work established by the Biomedical Sciences Program and the Graduate College of Marshall University. This work also conforms to the editorial standards of our discipline and the Graduate College of Marshall University. With our signatures, we approve the manuscript for publication.

Dr. Zijian Xie		Committee Chairperson Signing as proxy for Dr. Xie	Date 1/23/20
Dr. Sandrine Pierre		Committee Co-Chairperson	Date 11/27/2019
Dr. Nalini Santanam		Committee Member	Date 12/20/2019
Dr. Joseph Shapiro		Committee Member	Date 1/6/2020
Dr. Judith Heiny		Committee Member	Date 1.20.2020

## **DEDICATION**

This dissertation is dedicated to my advisor and mentor, Dr. Zijian Xie, who passed away before it could be published. I am proud to have been mentored by such a brilliant researcher, and I hope to honor his legacy of hard work, compassionate mentoring, and innovative research as I build my own career on the principles I learned from him and applied to this body of work.

## **ACKNOWLEDGEMENTS**

All of the hard work that went into this dissertation would not have been possible without the support of my friends and family, especially my parents Mike and Rose Mary, my brother Joey, my grandparents Mary Jo and Silas Hannah and Sally and Ralson Kutz, and my entire extended family. I also want to thank my partner Will Johnson and the entire Johnson family for their ongoing support.

## TABLE OF CONTENTS

Approval of Thesis.....	ii
Dedication.....	iii
Acknowledgements.....	iv
List of Tables.....	vii
List of Figures.....	viii
Abstract.....	x
Chapter 1.....	1
Introduction.....	1
Molecular Properties of Na/K-ATPase Isoforms in the Skeletal Muscle.....	2
Regulation of Na/K-ATPase in Skeletal Muscle Physiology.....	12
A New Role for NKA $\alpha 1$ in Skeletal Muscle Physiology.....	18
Chapter 2.....	20
Isoform-specific role of Na/K-ATPase $\alpha 1$ in skeletal muscle.....	20
Abstract.....	21
Introduction.....	21
Materials and Methods.....	23
Results.....	28
Discussion.....	34
Acknowledgements.....	40
Chapter 3.....	41
Metabolic capacity, endurance and insulin resistance are acquired by mammals via a common mechanism.....	41

Summary .....	42
Introduction .....	42
Results .....	45
Discussion.....	64
Acknowledgements.....	70
Author Contributions .....	70
Materials and Methods .....	71
Chapter 4 .....	81
Discussion and Conclusions.....	81
Isoform-specific role of NKA $\alpha$ 1 in skeletal muscle .....	81
NKA $\alpha$ 1 regulates muscle growth.....	81
NKA $\alpha$ 1 regulates muscle metabolism.....	83
Evolutionary implications .....	84
Clinical implications .....	86
Limitations.....	88
References .....	89
Appendix A.....	113
Letter from Office of Research Integrity .....	113
Appendix B.....	114
Abbreviations .....	114

## LIST OF TABLES

Table 1: NKA $\alpha$ isoform enzymatic properties .....	3
Table 2: Selected physiological parameters in Na/K-ATPase $\alpha 1$ $+/+$ vs $\alpha 1$ $+/-$ mice.....	30
Table 3: Conservation of the NKA $\alpha 1$ /Src binding sites in mammals. Bold letters indicate residues that differ from mammalian $\alpha 1$ .....	46
Table 4. Amino acid sequences of the Src binding sites of the WT rat $\alpha 1$ , WT rat $\alpha 2$ , and gain-of-function signaling mutant $\alpha 2$ NKA expressed by the AAC-19, LX- $\alpha 2$ , and LY-a2 cell lines. ....	47
Table 5: Volumes and concentrations of injections for Seahorse analysis, with final concentrations in parentheses. ....	73
Table 6: Primer sequences used in RT-qPCR.....	75

## LIST OF FIGURES

Figure 1: NKA subunits and Albers-Post mechanism .....	4
Figure 2: Schematic diagram of $\alpha$ and $\beta$ subunits of NKA .....	7
Figure 3. Na/K-ATPase $\alpha$ -isoform abundance in skeletal muscles from Na/K-ATPase $\alpha 1$ haplodeficient mice ( $\alpha 1^{+/-}$ ) and control littermates ( $\alpha 1^{+/+}$ ).....	29
Figure 4. Na/K-ATPase activity. ....	31
Figure 5. Changes in muscle mass in $\alpha 1^{+/-}$ mice. ....	32
Figure 6. Na/K-ATPase $\alpha$ -isoform abundance in skeletal muscles from C57Bl6 mice. ....	33
Figure 7. Structural changes in the soleus muscle of Na/K-ATPase $\alpha 1$ haplodeficient mice.....	34
Figure 8. A. GSK3 $\beta$ and glycogen content in the soleus muscle of Na/K-ATPase $\alpha 1$ haplodeficient mice. ....	37
Figure 9. Distance to fatigue in Na/K-ATPase $\alpha 1$ haplodeficient mice ( $\alpha 1^{+/-}$ ) and control littermates ( $\alpha 1^{+/+}$ ) during forced treadmill running. ....	38
Figure 10: Evolutionary relationships between vertebrate groups listed in Table 3.....	43
Figure 11: Importance of NKA $\alpha 1$ signaling for cell growth and metabolism. ....	48
Figure 12: Seahorse metabolic analysis of AAC-19, LX- $\alpha 2$ , and LY-a2 cells. ....	49
Figure 13: Characterization of renal epithelial-derived cell lines.....	50
Figure 14: Seahorse metabolic analysis of cells expressing a loss-of-function Src binding-mutant NKA $\alpha 1$ . ....	51
Figure 15: Cre-Lox construct for the tissue-specific ablation of $\alpha 1$ . ....	52
Figure 16: Development of skeletal muscle-specific NKA $\alpha 1$ KO mouse model.....	53
Figure 17: Soleus mass in 16-week-old $sk\alpha 1^{+/+}$ (grey, squares) and $sk\alpha 1^{-/-}$ (white, triangles) mice. ....	54

Figure 18: Exercise capacity of sk $\alpha$ 1 <sup>-/-</sup> mice. ....	55
Figure 19: Analysis of mRNA expression of metabolic genes in renal epithelial cells and skeletal muscles. ....	56
Figure 20: Oxidative stress and antioxidant response in sk $\alpha$ 1 <sup>-/-</sup> mice on Western diet. ....	58
Figure 21: Impact of skeletal muscle-specific ablation of NKA $\alpha$ 1 on reaction to Western diet..	60
Figure 22: Pharmacological targeting of $\alpha$ 1 NKA signaling through Src in diet-induced metabolic dysfunction. ....	62

## ABSTRACT

Skeletal muscle comprises approximately 30% of total body mass, and loss of muscle mass and dysfunctional muscle metabolism are implicated in multiple disease states, including type 2 diabetes, heart failure, and septic shock. As such, understanding the mechanisms of skeletal muscle growth and atrophy, including pharmaceutical targets that may prove safe and effective, is therefore an important goal of current research on skeletal muscle physiology. One potential target in skeletal muscle development and function that has not been fully explored is the Na/K-ATPase (NKA), especially the  $\alpha 1$  isoform. This isoform has a unique signaling function that has previously been shown to regulate growth, metabolism, and organogenesis and comprises only 10% of the total NKA in skeletal muscle. We therefore investigated the role of this signaling isoform in skeletal muscle. To accomplish this, we utilized a global NKA  $\alpha 1$  haplodeficient mouse ( $\alpha 1^{+/-}$ ). The oxidative soleus muscles of  $sk\alpha 1^{+/-}$  were 10% smaller than controls, while the glycolytic extensor digitorum longus mass was unchanged. This prompted us to analyze the metabolism of cells lacking NKA  $\alpha 1$ , which revealed that the  $\alpha 1$  isoform is necessary for metabolic reserve and flexibility. A second mouse model was generated with a skeletal muscle-specific ablation of NKA  $\alpha 1$ . These mice had a 35% reduction in skeletal muscle mass and a switch from oxidative to glycolytic fibers. Paradoxically, these mice were protected from diet-induced metabolic dysfunction including diet-induced insulin resistance. This provided the first genetic in vivo model of  $\alpha 1$  signaling as a major regulator of metabolism and led to the hypothesis that the evolution of the Src binding sites in  $\alpha 1$  in mammals may be linked to the development of increased metabolic reserve associated with the evolution of endothermy. These findings together confirm a vital role of NKA  $\alpha 1$  in skeletal muscle development and

metabolism, and link the evolution of endothermy to the evolution of the NKA  $\alpha$ 1 Src binding sites.

## CHAPTER 1

### INTRODUCTION

Skeletal muscle is the largest organ in the body, on average comprising between 31% and 38% of total body mass (Janssen, Heymsfield, Wang, & Ross, 2000). Furthermore, skeletal muscle accounts for an estimated 20-30% of metabolic flux at rest (Zurlo, Larson, Bogardus, & Ravussin, 1990), and is the tissue most responsive to insulin-stimulated glucose uptake (Honka et al., 2018), even when normalized to organ mass. Dysregulation of insulin signaling in skeletal muscle is sufficient to cause whole-body insulin resistance (DeFronzo & Tripathy, 2009), and muscle mass can largely predict a person's susceptibility to diabetes (Son et al., 2017). Therefore, understanding the mechanisms which regulate skeletal muscle metabolism and growth are key to treating the growing global health concerns of obesity and insulin resistance, which affect 13% and 8.5% of adults worldwide, respectively (Collaboration, 2016, 2017).

In addition to its role in metabolic regulation, skeletal muscle is vital for normal function and movement. Skeletal muscle atrophy due to aging (sarcopenia), cancer (cachexia), or disuse due to injury or bedrest impacts large numbers of people each year and currently has no approved treatment options besides physical therapy and exercise (Dhillon & Hasni, 2017; Sakuma, Aoi, & Yamaguchi, 2017; Theilen, Kunkel, & Tyagi, 2017; Weihrauch & Handschin, 2018). These changes in muscle mass can have long-term impacts on patient outcomes, with higher muscle mass associated with better outcomes (Ishizu et al., 2017; Moorthi & Avin, 2017). Understanding the mechanisms of skeletal muscle growth and atrophy, including pharmaceutical targets that may prove safe and effective, is therefore an important goal of current research on skeletal muscle physiology.

One potential target in skeletal muscle development and function that has not been fully explored is the Na/K-ATPase (NKA), especially the  $\alpha 1$  isoform. Although the oldest-known function of NKA is the active transport of  $\text{Na}^+$  and  $\text{K}^+$  across the cell membrane to create a membrane potential, the  $\alpha 1$  isoform has a more recently discovered signaling function (Cui & Xie, 2017; Pierre & Xie, 2006; Z. Xie & Askari, 2002). These studies have linked NKA  $\alpha 1$  signaling to the regulation of such vital processes as mitochondrial reactive oxygen species (ROS) production (Yan et al., 2013), cell metabolism (Banerjee et al., 2018), cell proliferation (Lai et al., 2013; Liang, Cai, Tian, Qu, & Xie, 2006; Tian et al., 2009; Ye et al., 2013), and organogenesis (Fontana, Burlaka, Khodus, Brismar, & Aperia, 2013; Khodus, Kruusmagi, Li, Liu, & Aperia, 2011; J. Li et al., 2010; X. Wang et al., 2019). The signaling NKA  $\alpha 1$  isoform has not been studied extensively in skeletal muscle, as it represents only about 13% of the total NKA in skeletal muscle (He et al., 2001). Considering the importance of skeletal muscle metabolism and growth regulation in human health and disease, we explored the potential role of NKA  $\alpha 1$  as a regulator of skeletal muscle growth and metabolism.

## **Molecular Properties of Na/K-ATPase Isoforms in the Skeletal Muscle**

### **Na/K-ATPase as an Ion Pump**

The Na/K-ATPase (NKA) is a P-type ATPase which transfers both  $\text{Na}^+$  and  $\text{K}^+$  across the cell membrane against their concentration gradients to generate a membrane potential and maintain cell volume (Blanco, 2005a; Skou & Esmann, 1992). As a P-type ATPase, NKA hydrolyzes ATP, phosphorylating the aspartate residue at position 369 on the third cytoplasmic domain of the catalytic  $\alpha$  subunit (indicated by a star in Figure 2) (Kuntzweiler, Wallick, Johnson, & Lingrel, 1995). NKA undergoes conformational changes between the E1 and E2 states to transport  $\text{K}^+$  out of and  $\text{Na}^+$  into the cells. These conformational changes were first

described by Siegel and Albers in 1967 and refined by Post et al. in 1969 and are known as the Albers-Post mechanism (Figure 1), which allows the active transport of Na<sup>+</sup> and K<sup>+</sup> out of and into the cell, thereby maintaining the electrochemical gradient (Post, Kume, Tobin, Orcutt, & Sen, 1969; Siegel & Albers, 1967). Since the discovery of NKA by Jens Skou in 1957 (Skou, 1957), its role as an ion pump in a variety of tissues has been the focus of many studies (Blanco, 2005a; Cougnon, Moseley, Radzyukevich, Lingrel, & Heiny, 2002; Gerbi et al., 1998; He et al., 2001; P. F. James et al., 1999; Thompson & McDonough, 1996).

$\alpha$ Isoform	Tissue Distribution	Associated $\beta$ Isoform	Na <sup>+</sup> Affinity (K <sub>0.5</sub> , mM)	K <sup>+</sup> Affinity (K <sub>0.5</sub> , mM)	Ouabain Inhibition (K <sub>i</sub> , M)	Ouabain Affinity (K <sub>d</sub> , M)	Species	Kinetics Source
$\alpha 1$	Ubiquitous	$\beta 1$	16.4 ± 0.7	1.9 ± 0.2	4.3±1.9×10 <sup>-5</sup>	N/A	Rat	(Blanco, Koster, Sanchez, & Mercer, 1995; Blanco, Sanchez, & Mercer, 1995)
			8.3 ± 0.6	0.92 ± 0.11	2.0±0.6×10 <sup>-7</sup>	N/A	Human	(Sanchez, Nguyen, Timmerberg, Tash, & Blanco, 2006)
		$\beta 2$	N/A	1.16 ± 0.02	N/A	1.98±0.21×10 <sup>-8</sup>	Human	(G. Crambert et al., 2000)
		$\beta 3$	N/A	1.05 ± 0.12	N/A	1.91±0.20×10 <sup>-8</sup>	Human	(G. Crambert et al., 2000)
$\alpha 2$	Myofibers, cardiomyocytes, glial cells, smooth muscle, adipose tissue	$\beta 1$	12.4 ± 0.5	3.6 ± 0.3	1.7±0.1×10 <sup>-7</sup>	N/A	Rat	(Blanco, Koster, et al., 1995; Blanco, Sanchez, et al., 1995)
			12.8 ± 2.2	1.30 ± 0.17	N/A	3.69±0.31×10 <sup>-8</sup>	Human	(G. Crambert et al., 2000)
		$\beta 2$	8.8 ± 1.0	4.8 ± 0.4	1.5±0.2×10 <sup>-7</sup>	N/A	Rat	(Blanco, Koster, et al., 1995; Blanco, Sanchez, et al., 1995)
			N/A	2.70 ± 0.3	N/A	2.65±0.65×10 <sup>-8</sup>	Human	(G. Crambert et al., 2000)
$\beta 3$	N/A	1.80 ± 0.10	N/A	2.90±0.65×10 <sup>-8</sup>	Human	(G. Crambert et al., 2000)		
$\alpha 3$	Neurons	$\beta 1$	27.9 ± 1.3	5.3 ± 0.3	3.1±0.3×10 <sup>-8</sup>	N/A	Rat	(Blanco, Sanchez, et al., 1995)
			24.7 ± 2.4	0.90 ± 0.27	N/A	1.43±0.08×10 <sup>-8</sup>	Human	(G. Crambert et al., 2000)
		$\beta 2$	17.1 ± 1.0	6.2 ± 0.4	4.7±0.4×10 <sup>-8</sup>	N/A	Rat	(Blanco, Sanchez, et al., 1995)
			N/A	1.60 ± 0.10	N/A	1.76±0.20×10 <sup>-8</sup>	Human	(G. Crambert et al., 2000)
$\beta 3$	N/A	1.33 ± 0.17	N/A	1.25±0.20×10 <sup>-8</sup>	Human	(G. Crambert et al., 2000)		
$\alpha 4$	Sperm	$\beta 1$	N/A	N/A	1.0±0.3×10 <sup>-8</sup>	N/A	Human	(Sanchez et al., 2006)
			13.5 ± 1.3	5.9 ± 1.1	6.4±2.1×10 <sup>-9</sup>	N/A	Rat	(Blanco, Melton, Sanchez, & Mercer, 1999)
		$\beta 3$	N/A	N/A	1.8±0.7×10 <sup>-8</sup>	N/A	Human	(Sanchez et al., 2006)
			12.9 ± 0.6	5.0 ± 0.3	1.0±0.3×10 <sup>-8</sup>	N/A	Rat	(Blanco et al., 1999)

**Table 1: NKA  $\alpha$  isoform enzymatic properties**

List of human and rat NKA  $\alpha$  isoforms affinities for Na<sup>+</sup> and K<sup>+</sup> (K<sub>0.5</sub>) and inhibitor constants (K<sub>i</sub>) or affinities (K<sub>d</sub>) for ouabain, depending on study design.

NKA is comprised of a catalytic  $\alpha$  subunit, a targeting  $\beta$  subunit, and in some tissues, a regulatory  $\gamma$  or FXYD subunit (Figure 1) (Blanco, 2005a). The  $\alpha$  subunit is necessary for the transport of Na<sup>+</sup> and K<sup>+</sup> (Blanco, DeTomaso, Koster, Xie, & Mercer, 1994), while the  $\beta$  subunit is required for normal trafficking and to stabilize the  $\alpha$  subunit, usually by targeting the  $\alpha 1$

subunit to the plasma membrane and thereby preventing degradation (Geering et al., 1996). The  $\gamma$  subunit is expressed in a tissue-specific manner and can bind the catalytic  $\alpha$  subunit at transmembrane segments 2 and 9 (see Figure 2). This association of the  $\gamma$  subunit with the functional  $\alpha\beta$  complex leads to decreased substrate affinity and thereby decreased ion transport activity (Gilles Crambert, Füzesi, Garty, Karlish, & Geering, 2002; G. Crambert et al., 2000). This inhibitory function is partially regulated by phosphorylation in at least some  $\gamma$  isoforms (Gilles Crambert et al., 2002; G. Crambert et al., 2000; Manoharan et al., 2015).

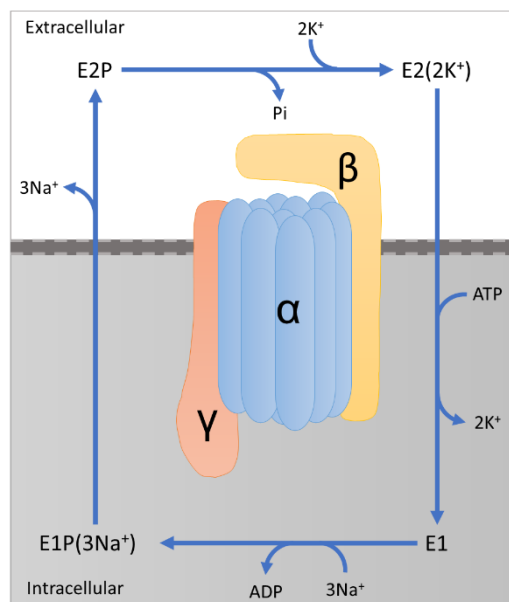


**Figure 1: NKA subunits and Albers-Post mechanism**

Schematic of the Albers-Post mechanism of NKA active Na and K and general structural representation of the catalytic  $\alpha$ , targeting  $\beta$ , and regulatory  $\gamma$  subunit.

Four isoforms of the catalytic  $\alpha$  subunit have been identified in mammals, with a tissue-specific distribution (Blanco, 2005a; Young & Lingrel, 1987). These isoforms differ slightly in enzymatic function, with decreased Na<sup>+</sup> affinity in the  $\alpha$ 3 isoform and decreased K<sup>+</sup> affinity in the  $\alpha$ 2 isoform (Blanco, Koster, et al., 1995; Blanco, Sanchez, et al., 1995; G. Crambert et al., 2000; Jewell & Lingrel, 1991; Sanchez et al., 2006), two isoforms found in excitable tissues (Table 1). While ouabain binding affinity is similar among most mammalian isoforms, with

inhibitor constants ( $K_i$ ) ranging from the 10-100 nM range (Table 1), the alteration of two amino acids on the second extracellular loop in rat and mouse  $\alpha 1$  (L111R and N122D, positions indicated by red circles in Figure 2) decreases the binding affinity of cardiotonic steroids by two orders of magnitude, to a  $K_i$  of 43  $\mu$ M (Blanco, Koster, et al., 1995; Blanco, Sanchez, et al., 1995; Blanco, Xie, & Mercer, 1993; Dostanic et al., 2003). This difference has been proposed to alter calcium signaling and muscle fatigue (Despa, Lingrel, & Bers, 2012; Radzyukevich, Lingrel, & Heiny, 2009). While some have proposed that the tissue-specific distribution of these different  $\alpha$  isoforms may be related to differences in enzymatic activities (Blanco, 2005a, 2005b), these differences do not fully explain the distribution of  $\alpha$  isoforms and the possibility that the tissue distribution may be related to other functions of NKA. For example, while excitable tissues such as skeletal muscle and neurons express multiple  $\alpha$  isoforms, the  $\alpha 2$  isoform is also expressed in adipocytes, which are not electrically excitable (Orlowski & Lingrel, 1988b). Additionally, although skeletal muscle contains both  $\alpha 1$  and  $\alpha 2$ , only 10% of the total NKA is  $\alpha 1$  (He et al., 2001). Although the  $\alpha 2$  isoform is necessary for normal muscle ion transport during muscle contraction (DiFranco, Hakimjavadi, Lingrel, & Heiny, 2015; Manoharan et al., 2015; Radzyukevich et al., 2013), it seems unlikely that this small amount of  $\alpha 1$  performs a vital ion transport function that cannot be fulfilled by  $\alpha 2$ .

The  $\beta$  and  $\gamma$  subunits also display tissue-specific isoform distributions (G. Crambert et al., 2000; Orlowski & Lingrel, 1988b). The effects of different  $\beta$  isoforms on the enzyme kinetics of the catalytic  $\alpha$  subunit could explain the distribution of the  $\beta$  isoforms in different tissues. Specifically, the expression of different  $\beta$  isoforms alters the  $\text{Na}^+$  and  $\text{K}^+$  affinities of the associated  $\alpha$  isoform (see Table 1). Similarly,  $\gamma$  isoforms exhibit distinct regulation by protein

kinases (G. Crambert et al., 2000), suggesting that the tissue-specific distribution of the  $\gamma$  isoforms could facilitate the tissue-specific regulation of NKA activity.

### **Na/K-ATPase and Skeletal Muscle Ion Homeostasis**

Skeletal muscle is an excitable tissue comprised of a heterogeneous mixture of myofibers with different contractile and metabolic properties (Goodyear, Hirshman, Smith, & Horton, 1991; Gunning & Hardeman, 1991; Stuart et al., 2013; Templeton, Sweeney, Timson, Padalino, & Dudenhoefter, 1988), from the oxidative type 1 fibers to mixed type 2a fibers and glycolytic type 2B/X fibers. Skeletal muscle contains only the ubiquitous  $\alpha 1$  isoform and the  $\alpha 2$  isoform (Blanco, 2005a; Cougnon et al., 2002; Fowles, Green, & Ouyang, 2004; He et al., 2001; O'Brien, Lingrel, & Wallick, 1994; Thompson & McDonough, 1996; Young & Lingrel, 1987). In rodents, the  $\alpha 1$  isoform is primarily found in oxidative slow-twitch fibers, while the  $\alpha 2$  isoform is most dominant in glycolytic slow-twitch fibers, with the  $\alpha 1$  isoform primarily found on the sarcolemma and the  $\alpha 2$  isoform localized to the T-tubules and neuromuscular junction (Murphy, Petersen, et al., 2006; Thompson & McDonough, 1996; L. Zhang, Morris, & Ng, 2006). However, in humans, there are conflicting reports, with Thomassen et al. reporting significantly increased  $\alpha 2$  expression in glycolytic type 2 fibers (Thomassen, Murphy, & Bangsbo, 2013) while Wyckelsma et al. reported no difference in fiber type distribution between the  $\alpha 1$  and  $\alpha 2$  isoforms (Wyckelsma et al., 2015). This discrepancy, however, appears to be at least in part due to larger variability in the Wyckelsma study. Importantly, neither study reported significantly lower expression of the  $\alpha 1$  isoform in type 2 fibers as has been seen in rodents (Murphy, Petersen, et al., 2006; Thompson & McDonough, 1996; L. Zhang et al., 2006), although in the Thomassen study, there appears to be a statistically insignificant decrease in  $\alpha 1$  expression in

type 2 fibers and this, combined with the significantly higher expression of  $\alpha 2$  in type 2 fibers, suggests a decreased  $\alpha 1/\alpha 2$  ratio in human type 2 fibers as compared to type 1 fibers.

In addition to their fiber type-specific distribution, the NKA  $\alpha 1$  and  $\alpha 2$  isoforms have distinct roles in the maintenance of skeletal muscle membrane potentials. The  $\alpha 1$  isoform comprises only 10-15% of the total NKA content in skeletal muscle, with the  $\alpha 2$  isoform making up the other 85-90% (He et al., 2001). The  $\alpha 2$  isoform is localized to the neuromuscular junction and T-tubules, while the  $\alpha 1$  isoform is localized to the sarcolemma (Cougnon et al., 2002; DiFranco et al., 2015; Heiny et al., 2010; Williams et al., 2001).

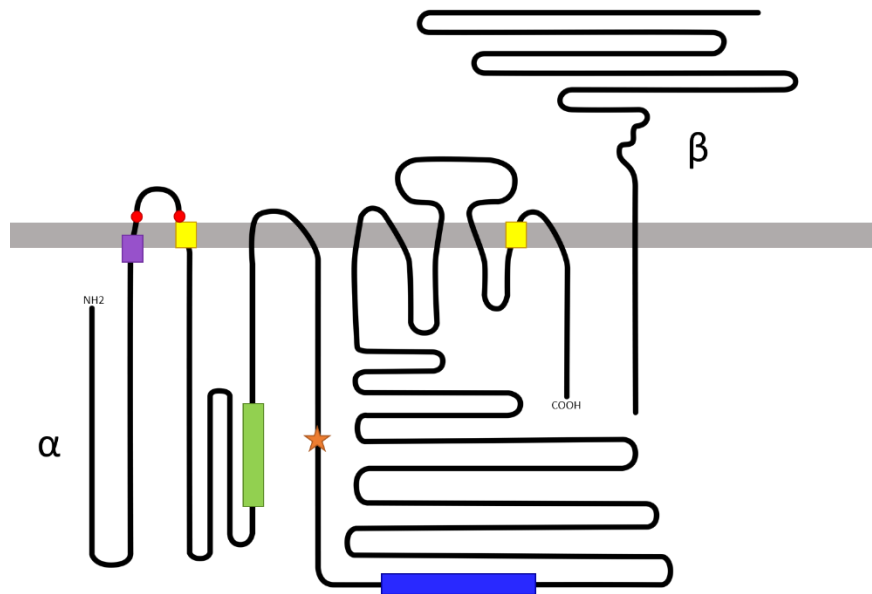


**Figure 2: Schematic diagram of  $\alpha$  and  $\beta$  subunits of NKA**

Line structure of  $\alpha$  and  $\beta$  subunits of NKA, with regions important for signaling highlighted in purple (caveolin binding motif), yellow (FXD binding regions), green (Y260 Src binding region) and blue (NaKtide Src binding region). Additionally, the positions of amino acids conferring ouabain sensitivity are denoted by red circles, and the residue at which NKA is phosphorylated during ion pumping is denoted by an orange star. The sequences of the Y260 and NaKtide regions in different isoforms from various species can be found in Table 3.

This subcellular distribution, along with the decreased  $K^+$  affinity of the  $\alpha 2$  isoform compared to the  $\alpha 1$  isoform (Table 1), leads to distinct roles for the two isoforms in maintaining the skeletal muscle membrane potential. The  $\alpha 1$  isoform has been identified as responsible for

maintaining the resting membrane potential, while the  $\alpha 2$  isoform is responsible for restoring membrane potential during muscle contraction (He et al., 2001). This role of the dominant  $\alpha 2$  isoform has been further explored with the use of a skeletal muscle-specific  $\alpha 2$  knockout mouse model (*sk $\alpha 2$ -/-*). In the absence of  $\alpha 2$ , the  $\alpha 1$  isoform is incapable of maintaining membrane potential during tetanic contractions in spite of significant compensatory upregulation of  $\alpha 1$  expression, leading to increased fatigability and dramatically decreased exercise tolerance (Radzyukevich et al., 2013). This failure to maintain the membrane potential was later attributed to the higher  $K^+$  affinity of the  $\alpha 1$  isoform, which left its enzymatic activity saturated at physiological  $K^+$  concentrations, and to the localization of  $\alpha 1$  to the sarcolemma instead of the T-tubules, where extracellular  $K^+$  diffuses more slowly and NKA activity is necessary to restore membrane potential after each depolarizing action potential (DiFranco et al., 2015; Manoharan et al., 2015). In spite of these clear functional defects, the *sk $\alpha 2$ -/-* muscles were not reported to be different in size or morphology from wild type skeletal muscles (DiFranco et al., 2015; Manoharan et al., 2015; Radzyukevich et al., 2013).

### **Hypothesized roles for the $\alpha 1$ and $\alpha 2$ isoforms in skeletal muscle**

While maintenance of the membrane potential in contracting muscles is important and  $\alpha 2$  functions as the ‘turbocharger’ to restore the membrane potential after the initiation of contraction, which isoform maintains the basal membrane potential is unclear. The basal membrane potential impacts contractility, with increased basal membrane potential correlating closely with force generation (Cairns, Hing, Slack, Mills, & Loiselle, 1997; Overgaard, Nielsen, & Clausen, 1997). Based on contractility studies in skeletal muscles from  $\alpha 1$  haplodeficient mice, He et al. hypothesized that the NKA  $\alpha 1$  isoform is responsible for maintaining the basal membrane potential. However, while global  $\alpha 1$  haplodeficiency did lead to decreased twitch

force of the extensor digitorum longus (EDL) *in vitro* (He et al., 2001), the membrane potential was not directly measured. This mouse model is a global knockdown model that has other abnormal phenotypes, including a cardiac phenotype (Moseley, Cougnon, Grupp, El Schultz, & Lingrel, 2004; Moseley et al., 2005), so it is possible that the decreased force generation observed in  $\alpha 1$  haplodeficient muscles is a result of another aspect of their phenotype, for example, a hormonal or behavioral change that could lead to weaker muscles rather than a decrease in membrane potential.

### **Src-Dependent Signaling Function**

In 1998, the lab of Zijian Xie identified a novel signaling function of the NKA when they discovered that the treatment of cardiomyocytes with the NKA-specific ligand ouabain induced cardiomyocyte hypertrophy via a dose-dependent activation of p42 MAPK (Huang, Li, & Xie, 1997; Kometiani et al., 1998). Follow up studies determined that this Src-mediated signaling function was isoform-specific (Madan et al., 2017; J. Xie et al., 2015), and that reactive oxygen species (ROS) mediated this hypertrophic pathway (Z. Xie et al., 1999). This signaling cascade has since been expanded to include transactivation of the epidermal growth factor receptor (EGFR) (Haas, Askari, & Xie, 2000), the activation of mitogen activated protein kinase (MAPK) and Akt pathways (Huang et al., 1997), the activation of the inositol triphosphate (IP3) receptor and generation of  $\text{Ca}^{2+}$  oscillations (Yuan et al., 2005), and the generation of mitochondrial reactive oxygen species (ROS) (Liu et al., 2006; Z. Xie et al., 1999), linking it to both growth and metabolism. Additionally, a positive feedback loop in which ROS are capable of activating  $\alpha 1$  signaling through Src has been identified (Yan et al., 2013), leading to the hypothesis that controlling this signaling pathway may allow for control of ROS stress in disease states.

The identification of the Src binding domains on NKA  $\alpha 1$  led to the development of NaKtide, a peptide that mimics the ability of  $\alpha 1$  to bind Src, thus acting as an inhibitor of CTS and ROS-stimulated activation of Src through NKA  $\alpha 1$  (Z. Li et al., 2009). The drug candidate pNaKtide was derived from NaKtide, with the addition of positively charged cell-penetrating peptides, generating pNaKtide. This modification allowed the pNaKtide in the extracellular space to penetrate the membrane and inhibit Src, thus disrupting the NKA  $\alpha 1$ /Src signaling complex. In vivo studies with pNaKtide have revealed that inhibiting NKA  $\alpha 1$  signaling through Src can be protective in such diverse conditions as aging (Sodhi et al., 2018), uremic cardiomyopathy (J. Liu et al., 2016), myocardial ischemia-reperfusion injury (H. Li et al., 2018), and diet-induced obesity, steatohepatitis, and insulin resistance (Sodhi et al., 2015; Sodhi et al., 2017; Srikanthan, Shapiro, & Sodhi, 2016). In all of these studies, intraperitoneal administration of pNaKtide prevented the pathological increase in ROS and ultimately prevented the development of severe pathologies.

While the in vivo studies with pNaKtide revealed a key role for  $\alpha 1$  in regulating metabolism, the ubiquitous nature of  $\alpha 1$  and the systemic administration of pNaKtide make it impossible to identify the tissue-specific impacts. In a recent study, Pratt et al. used a lentiviral transfection system to express pNaKtide specifically in adipocytes. This not only protected adipose tissue from Western diet-induced metabolic dysfunction, but also prevented the development of non-alcoholic steatohepatitis and neurodegeneration (Pratt et al., 2019). These results provide the first evidence that manipulation of  $\alpha 1$  signaling can impact cross talk between tissues. However, much remains unclear about the importance of  $\alpha 1$  and  $\alpha 1$  signaling in other tissues, and no genetic models exist to date.

In addition to this role of NKA signaling in regulating metabolism and growth, signaling by NKA  $\alpha 1$  has been recognized as a driver of development and organogenesis. In 2010, Li et al. identified the ouabain-stimulated generation of  $\text{Ca}^{2+}$  oscillations through NKA signaling as important for the development of rat kidneys (J. Li et al., 2010). This ouabain-mediated restoration of normal kidney development in malnourished fetal rats was attributed to the stimulation of the PI3K pathway through the IP3 receptor (Khodus et al., 2011; J. Li et al., 2010). More recently, studies in our lab have revealed that the caveolin binding motif found in the first transmembrane segment of the  $\alpha$  subunit (Figure 2), which is a critical component of the NKA  $\alpha 1$ /Src signaling scaffold (Bai et al., 2016; Cai et al., 2008; Quintas et al., 2010; H. Wang et al., 2004), plays a vital regulatory role in embryonic development, especially in neurogenesis (X. Wang et al.). Furthermore, studies with human induced pluripotent stem cells have shown that the loss of the caveolin binding motif leads to a loss of stemness and impaired differentiation (X. Wang et al., 2019). This control of differentiation and organogenesis by NKA  $\alpha 1$  caveolin binding motif has been linked to Wnt/ $\beta$ -catenin signaling independent of Src, but it has only been partially investigated thus far and the involvement of Src in this regulation cannot be ruled out.

These multiple signaling functions identified in other cell types offer an alternative explanation for the presence of the minor NKA  $\alpha 1$  isoform in skeletal muscle. However, this signaling function of  $\alpha 1$  has only been explored in skeletal muscle in two papers published by Kotova et al., who explored a role for the signaling function in cultured C2C12 cells (Kotova, Al-Khalili, et al., 2006; Kotova, Galuska, Essen-Gustavsson, & Chibalin, 2006). The differentiated myotubes were treated with ouabain, a NKA-specific ligand that stimulates  $\alpha 1$  signaling at low concentrations and inhibits ion pumping of all isoforms at high concentrations.

After ouabain treatment, cells showed increased glycogen synthesis via the Akt- and ERK-mediated inactivation of glycogen synthase kinase 3 $\beta$  (GSK-3 $\beta$ ) (Kotova, Al-Khalili, et al., 2006; Kotova, Galuska, et al., 2006). Because GSK-3 $\beta$  is implicated in the regulation of skeletal muscle differentiation and the progression of skeletal muscle atrophy (Leger et al., 2006; van der Velden et al., 2007; Verhees et al., 2011; W. Yang, Zhang, Li, Wu, & Zhu, 2007), this suggested a link between NKA signaling and the regulation of skeletal muscle metabolism and development. Furthermore, glycogen content correlates with exercise endurance (Overmyer et al., 2015; Xu, Ren, Lamb, & Murphy, 2018), so this regulation of glycogen content by NKA signaling could have implications for exercise performance as well. However, these hypothetical links between NKA signaling and skeletal muscle metabolism and growth have not been tested *in vitro*, and the impact of NKA signaling in skeletal muscle *in vivo* remains unclear.

## **Regulation of Na/K-ATPase in Skeletal Muscle Physiology**

### **Skeletal Muscle Development and Growth**

Myogenesis involves the progression from pluripotent stem cells to myoblasts to myotubes to myofibers, which is regulated in a time-dependent manner by skeletal muscle-specific factors such as MyoD, MRF4, myogenin, and myostatin. As myoblasts differentiate and fuse into myotubes and myofibers, cell proliferation ceases, and cells develop rudimentary contractile machinery. In normal developmental conditions, they further mature into myofibers with all of the ultrastructure of skeletal muscle including T-tubules and highly coordinated and organized contractile apparatus (Chal & Pourquie, 2017). During myogenesis, myotubes begin to express the NKA  $\alpha 2$  isoform while expression of NKA  $\alpha 1$  begins to decrease (Higham, Melikian, Karin, Ismail-Beigi, & Pressley, 1993; Orłowski & Lingrel, 1988a, 1988b), a process that corresponds with the development of T-tubules (Cougnon et al., 2002).

Even after development, skeletal muscle remains highly plastic, with the ability to expand in size and cell number after reaching maturity in response to exercise or to injury (Frontera & Ochala, 2015; Le Moal et al., 2017). Myofibers hypertrophy when they expand in size, a process that may or may not include the mobilization of satellite cells and thus the integration of more nuclei/fiber (Murach et al., 2018). Many of the regulators of this process also impact the expression and activity of NKA in isoform-specific ways (see “Hormonal Regulation of Muscle Growth and Metabolism” and “Regulation by Exercise”).

The opposite process, skeletal muscle atrophy, occurs in response to a variety of stimuli, including disuse, cancer-induced cachexia, muscular dystrophies, burn-induced cachexia, and aging-related sarcopenia (Kinugawa, Takada, Matsushima, Okita, & Tsutsui, 2015; Kravtsova, Matchkov, & Bouzinova, 2015; Matsuyama et al., 2015; Su et al., 2017). While the stimuli are different, the process of atrophy and the factors which mediate it are similar in all but muscular dystrophies. The skeletal muscle loses metabolic flexibility, becoming more glycolytic with fewer mitochondria and a disrupted mitochondrial network that leads to inefficient mitochondrial oxidation (Egawa et al., 2015; Leger et al., 2006; Su et al., 2017). Mechanistically, during skeletal muscle atrophy, mTORC is inactivated, leading to decreased AMPK activation and increased activation of GSK3 $\beta$  (Egawa et al., 2015; Leger et al., 2006; Verhees et al., 2011). Disuse-induced atrophy in the vastus lateralis of patients suffering from knee injuries was associated with a 20% decrease in NKA  $\alpha$ 1 expression and a 63% decrease in NKA  $\alpha$ 2 expression (Perry et al., 2015), an effect which has been replicated in rats and the functional implications of which are not fully understood (Kravtsova et al., 2016). However, while these key pathways have been identified as important, the master regulators of this process remain unclear.

## **Hormonal Regulation of Muscle Growth and Metabolism**

Skeletal muscle has a uniquely plastic metabolism that responds to a variety of stimuli to adjust ATP production to the metabolic demands of the muscle when at rest and active, in both fed states and starvation periods. As such, skeletal muscle is a primary target of insulin, with skeletal muscle comprising approximately 30% of insulin-stimulated glucose uptake (Honka et al., 2018). In the skeletal muscle, insulin stimulates the translocation of glucose transporter type 4 (GLUT4) to the sarcolemma, thus increasing glucose uptake (Camps et al., 1992).

Simultaneously, insulin leads to increased glycogen storage via inhibition of glycogen synthase kinase 3 $\beta$  (GSK3 $\beta$ ) and an increase in glucose utilization (Camps et al., 1992). In addition to these metabolic impacts of insulin signaling, the insulin-stimulated activation of a kinase signaling cascade, including PI3K and p42/44 MAPK, leads to increased anabolism, including the transcription of growth- and survival-associated proteins (Hoppeler, 2016; H. A. James, O'Neill, & Nair, 2017; Rhoads, Baumgard, El-Kadi, & Zhao, 2016).

Insulin signaling is also a strong stimulator of NKA activity. Insulin acts on NKA by phosphorylating the NKA  $\alpha$ 2 isoform, resulting in increased membrane abundance (Chibalin et al., 2001). This is especially interesting given the dependence of NKA activity on glycolysis that has been reported by multiple laboratories in multiple tissues (Lynch & Balaban, 1987a, 1987b; Sepp et al., 2014) and that has been confirmed in skeletal muscle (J. H. James et al., 1996; J. H. James et al., 1999; Okamoto, Wang, Rounds, Chambers, & Jacobs, 2001). Interestingly, increased lactate release as a result of insulin stimulation has been linked to increased NKA activity in humans (Novel-Chate et al., 2001), which is consistent with the association of the NKA  $\alpha$ 2 isoform with both insulin-stimulated increases in NKA membrane abundance (Al-Khalili et al., 2004; Chibalin et al., 2001).

In addition to insulin, thyroid hormone (T3) is an important regulator of skeletal muscle growth and development, as well as a known regulator of NKA abundance. Skeletal muscle is partially capable of self-regulating T3 activity through expression of iodothyronine deiodinase 2, which converts the prohormone T4 into the active T3, and iodothyronine deiodinase 3, which inactivates T3 (Brent, 2012). T3 then acts on nuclear thyroid receptors to initiate a variety of cellular processes, including myogenesis through activation of MyoD and Mrf4 (Salvatore, Simonides, Dentice, Zavacki, & Larsen, 2014) and a switch from fast glycolytic fibers to slow oxidative fibers (Simonides & van Hardeveld, 2008; D. Zhang et al., 2014). Furthermore, T3 has been found to regulate NKA activity (Harrison & Clausen, 1998), and muscles from hypothyroid rats have decreased NKA activity.

The  $\beta$  adrenergic system is also involved in skeletal muscle hypertrophy and adaptation to exercise training, and inhibition of this hormonal axis is implicated in the development of skeletal muscle atrophy (Hoppeler, 2016). Skeletal muscle expresses both  $\beta$ 1 and  $\beta$ 2 adrenergic receptors, which are both G-protein coupled receptors and have largely overlapping signaling. When epinephrine or norepinephrine binds to its receptor, adenylylase cyclase is stimulated, leading to the generation of cyclic AMP (cAMP) (Glass, 2003). Increased intracellular cAMP concentrations then lead to the activation of protein kinase A (PKA), which in turn inhibits the glycogen synthase-mediated generation of glycogen and increases glycogen degradation by activating glycogen phosphorylase via activation of phosphorylase kinase. Simultaneously, glycolysis is increased in order to produce ATP quickly (J. H. James et al., 1999; McCarter et al., 2001), although glucose transport is not impacted by  $\beta$  adrenergic stimulation (Clausen & Flatman, 1987). In addition to these short-term effects of  $\beta$  adrenergic stimulation, the activation of p42/44 MAPK via PKA activation of Rap1 and B-Raf can lead to protein transcription and

anabolic effects, making  $\beta$  adrenergic receptor agonists one of the preferred performance-enhancing drugs (Glass, 2003).

As in the case of insulin, stimulation of the  $\beta$  adrenergic receptors in skeletal muscle causes increased NKA activity (Clausen & Flatman, 1977, 1987; Kaibara, Akasu, Tokimasa, & Koketsu, 1985), which has been linked to changes in glutathionylation of specific subunits (Juel, Hostrup, & Bangsbo, 2015) and is caused specifically by the activation of  $\beta_2$  adrenergic receptors (Murphy, Bundgaard, & Clausen, 2006). Unlike insulin, where activation of NKA ion pumping is largely mediated by increasing the quantity of NKA on the sarcolemma (Chibalin et al., 2001), stimulation of NKA activity by  $\beta$  adrenergic agonists is largely mediated by increased  $\text{Na}^+$  affinity (Buchanan, Nielsen, & Clausen, 2002). This ability of  $\beta$  agonists to increase NKA activity allows for the retention of muscle contractile force at fatigue (Cairns & Dulhunty, 1993; Clausen, Andersen, & Flatman, 1993; Hostrup et al., 2014; Nielsen & Clausen, 1997), which under conditions which would elicit a fight-or-flight response could prove beneficial by preserving muscle function beyond the normal physiological scope. However,  $\beta$  agonist-mediated activation of NKA is also associated with hyperlactatemia in sepsis and hemorrhagic shock (Bundgaard et al., 2003; Levy, Desebbe, Montemont, & Gibot, 2008; McCarter et al., 2001; McCarter et al., 2002), and in fact blocking the activation of  $\beta$  adrenergic receptors or inhibiting NKA in skeletal muscle reduces circulating lactate in these conditions (J. H. James et al., 1996; Levy, Gibot, Franck, Cravoisy, & Bollaert, 2005; McCarter et al., 2001; McCarter et al., 2002).

### **Regulation by Exercise**

In addition to the hormonal regulation of skeletal muscle metabolism, such physiological processes as muscle contraction, energy depletion within the muscle as during exercise, and

depletion of glycogen stores as in endurance exercise all serve to regulate the muscle metabolism (Baker, McCormick, & Robergs, 2010; Egan & Zierath, 2013). Skeletal muscle contraction stimulates glucose uptake independent of insulin action, and the depletion of ATP during repeated muscle contractions activates AMPK signaling, leading to both short-term and long-term changes in muscle metabolism (Egan & Zierath, 2013). In addition to AMPK signaling, reactive oxygen species are released by increased mitochondrial metabolism and other, non-mitochondrial sources such as NADPH oxidase and xanthine oxidase (Davies, Quintanilha, Brooks, & Packer, 1982). This leads to changes in muscle metabolism via the activation of transcription factors including NF- $\kappa$ B, NFAT, and PGC-1 $\alpha$ , including an increased antioxidant response and increased mitochondrial capacity (Merry & Ristow, 2016).

The physiological impacts of exercise on skeletal muscle also include changes in NKA isoform expression and activity. Training in humans induces increased plasma NKA distribution and decreased release of K<sup>+</sup> into the blood with intense exercise, suggesting that this increased plasma distribution leads to increased NKA activity (Green, Chin, Ball-Burnett, & Ranney, 1993). However, this study did not address which isoforms were impacted by the exercise training. Later studies revealed increased mRNA for  $\alpha$ 1,  $\alpha$ 2, and  $\alpha$ 3 in human vastus lateralis muscles after acute exercise in both trained and untrained individuals, but increased basal expression of mRNA only in the  $\alpha$ 3 isoform (Aughey et al., 2007) Furthermore, acute exercise was shown to decrease the NKA activity measured in skeletal muscle homogenates, which in acutely exercised rats has been associated with increased glutathionylation of the NKA (Juel et al., 2015). Acute treadmill exercise was shown to increase the plasma membrane localization of all NKA isoforms ( $\alpha$ 1 and  $\alpha$ 2, as well as  $\beta$ 1 and  $\beta$ 2) in both oxidative and glycolytic myofibers isolated from rats immediately post-exercise (Juel et al., 2001). This effect could be mimicked by

the *in vivo* stimulation of skeletal muscles but was reversed in all isoforms in oxidative fibers and  $\alpha 2$  only in glycolytic fibers after 30 minutes of recovery.

However, the response of skeletal muscle metabolism to exercise is largely influenced by the effect of exercise on the acute and chronic endocrine effects of exercise, such as increased  $\beta$  adrenergic signaling during acute exercise (Pedersen, 2019) and increased long-term insulin sensitivity in exercise-trained animals (Egan & Zierath, 2013). As discussed above, these hormonal changes can have a profound impact on skeletal muscle growth and metabolism and must be included in any attempts to explain exercise-mediated changes in skeletal muscle. Additionally, exercise increases circulating levels of endogenous cardiotonic steroids (Bauer et al., 2005) but the relevance of this to physiology is only speculative. It could be involved in the regulation of skeletal muscle contractility via inhibition of the  $\alpha 2$  isoform of NKA (Radzyukevich et al., 2009), but due to the very low levels of endogenous cardiotonic steroids in exercising animals, there could be a role of cardiotonic steroid signaling through the NKA  $\alpha 1$ /Src pathway that functions even in the absence of significant ion pump inhibition and has been linked to metabolism in other systems

### **A New Role for NKA $\alpha 1$ in Skeletal Muscle Physiology**

In light of the NKA  $\alpha 1$  signaling pathways identified by multiple laboratories (Cui & Xie, 2017), the classical hypothesis for the role of  $\alpha 1$  in skeletal muscle as a regulator of basal membrane potential needs to be revisited. NKA isoform expression is regulated by the same hormones that regulate skeletal muscle growth and metabolism, and the one signaling pathway that has been associated with skeletal muscle NKA  $\alpha 1$  signaling is the activation of GSK3 $\beta$  (Kotova, Al-Khalili, et al., 2006; Kotova, Galuska, et al., 2006), which is associated with increased muscle atrophy (Leger et al., 2006; Verhees et al., 2011) and decreased proliferation

with increased differentiation (Agle et al., 2017; van der Velden et al., 2007; W. Yang et al., 2007). Furthermore, the differential regulation of  $\alpha 1$  expression in a fiber-type specific manner, with higher expression in oxidative, slow-twitch type 1 fibers with smaller twitch force generation and lower expression in glycolytic, fast-twitch type 2 fibers with larger twitch force generation challenges the hypothesis that the primary role of NKA  $\alpha 1$  in skeletal muscle is basal membrane maintenance, since larger membrane potentials are associated with larger twitch force generation (Murphy, Bundgaard, et al., 2006; Overgaard et al., 1997; Overgaard, Nielsen, Flatman, & Clausen, 1999; Thompson & McDonough, 1996; L. Zhang et al., 2006). Taken together, these studies suggest that the NKA  $\alpha 1$  isoform may have a unique, ion pumping-independent role in skeletal muscle, and may be associated with the regulation of skeletal muscle processes as diverse as growth, development, and metabolism.

## CHAPTER 2

### ISOFORM-SPECIFIC ROLE OF NA/K-ATPASE $\alpha$ 1 IN SKELETAL MUSCLE

A manuscript published in *American Journal of Physiology: Endocrinology and Metabolism*.

Laura C. Kutz<sup>1</sup>, Shreya T. Mukherji<sup>1</sup>, Xiaoliang Wang<sup>1</sup>, Amber Bryant<sup>1</sup>, Isabel Larre<sup>1</sup>, Judith A Heiny<sup>2</sup>, Jerry B. Lingrel<sup>3</sup>, Sandrine V. Pierre<sup>1</sup>, and Zijian Xie<sup>1</sup>

<sup>1</sup>Marshall Institute for Interdisciplinary Research, Marshall University, Huntington, West Virginia, 25701, USA

<sup>2</sup>Department of Pharmacology and Systems Physiology, University of Cincinnati College of Medicine, Cincinnati, OH, USA

<sup>3</sup>Department of Molecular Genetics, Biochemistry and Microbiology, University of Cincinnati College of Medicine, Cincinnati, OH, USA

## Abstract

The distribution of Na/K-ATPase  $\alpha$  isoforms in skeletal muscle is unique, with  $\alpha 1$  as the minor (15%) isoform and  $\alpha 2$  comprising the bulk of the Na/K-ATPase pool. The acute and isoform-specific role of  $\alpha 2$  in muscle performance and resistance to fatigue is well known, but the isoform-specific role of  $\alpha 1$  has not been as thoroughly investigated. *In vitro*, we reported that  $\alpha 1$  has a role in promoting cell growth that is not supported by  $\alpha 2$ . To assess whether  $\alpha 1$  serves this isoform-specific trophic role in the skeletal muscle, we used the Na/K-ATPase  $\alpha 1$  haploinsufficient ( $\alpha 1^{+/-}$ ) mice. A 30% decrease of Na/K-ATPase  $\alpha 1$  protein expression without change in  $\alpha 2$  induced a modest yet significant decrease of 10% weight in the oxidative soleus muscle. In contrast, the mixed plantaris and glycolytic extensor digitorum longus (EDL) weights were not significantly affected, likely due to their very low expression level of  $\alpha 1$  compared to the soleus. The soleus mass reduction occurred without change in total Na/K-ATPase activity or glycogen metabolism. Serum analytes including  $K^+$ , fat tissue mass, or exercise capacity were not altered in  $\alpha 1^{+/-}$  mice. The impact of  $\alpha 1$  content on soleus muscle mass is consistent with a Na/K-ATPase  $\alpha 1$ -specific role in skeletal muscle growth that cannot be fulfilled by  $\alpha 2$ . The preserved running capacity in  $\alpha 1^{+/-}$  is in sharp contrast with previously reported consequences of genetic manipulation of  $\alpha 2$ . Taken together, these results lend further support to the concept of distinct isoform-specific functions of Na/K-ATPase  $\alpha 1$  and  $\alpha 2$  in skeletal muscle.

## Introduction

The Na/K-ATPase was discovered over 60 years ago as the membrane-bound protein complex that catalyzes the active transport of  $K^+$  into and  $Na^+$  out of the cell, thereby maintaining the resting membrane potential and excitability. The minimal functional Na/K-ATPase unit is made up of two subunits,  $\alpha$  and  $\beta$ . The  $\alpha$ -subunit is the catalytic subunit and bears

the binding sites for ATP, ions and cardiotonic steroids (CTS) (Pierre & Xie, 2006). In addition to the ubiquitously present  $\alpha 1$ , three isoforms of the catalytic subunit have been characterized. Na/K-ATPase  $\alpha 2$  is found mainly in muscle, adipose and glial cells,  $\alpha 3$  mainly in neurons, and  $\alpha 4$  expression is restricted to sperm (Blanco, 2005a). This highly tissue-specific expression pattern and isoform-specific response to both physiological and pathological stimuli have long suggested that they must be serving tissue-specific functions.

Over the last fifteen years, we and others have reported that Na/K-ATPase  $\alpha 1$  serves important scaffolding and signaling functions in addition to its role as an ion pump (Pierre & Xie, 2006). Specifically,  $\alpha 1$  can interact with and modulate Src activity, which in turn affects EGF receptors through transactivation. This subsequently adjusts the assembly and activation levels of multiple protein/lipid kinases as well as the generation of reactive oxygen species (ROS) and other intracellular messengers, allowing endogenous CTS to regulate cell growth (e.g., kidney development) (Fontana et al., 2013; Kometiani et al., 1998; Yan et al., 2013). On the other hand, sustained and dysregulated activation of this signaling mechanism causes ROS stress and pathological remodeling in the heart and kidneys (Liu et al., 2006; Tian et al., 2009; Wansapura, Lasko, Lingrel, & Lorenz, 2011).

In the skeletal muscle, the role of the ion-pumping function of the dominant  $\alpha 2$  isoform in maintaining the membrane potential during contraction has been studied extensively (DiFranco et al., 2015; He et al., 2001; Heiny et al., 2010; Manoharan et al., 2015; Radzyukevich et al., 2009; Radzyukevich et al., 2013). Additionally, Radzyukevich et al. have described an improvement in exercise performance in mice expressing a ouabain-resistant mutant  $\alpha 2$  isoform, suggesting a role of endogenous CTS in the regulation of muscle contraction via the  $\alpha 2$  isoform (Radzyukevich et al., 2009). Interestingly, expression of ouabain-resistant  $\alpha 2$  or even  $\alpha 2$

knockout did not affect skeletal muscle mass (DiFranco et al., 2015; Heiny et al., 2010; Manoharan et al., 2015; Radzyukevich et al., 2009; Radzyukevich et al., 2013). In a renal epithelial cell knockdown and rescue system, we have obtained evidence that the  $\alpha 1$  isoform is important for cell growth, and that rescue with  $\alpha 2$  restores ion-pumping capacity but does not restore growth or Src-dependent signal transduction in response to ouabain binding at concentrations too low to impair enzymatic activity (J. Xie et al., 2015). Taken together, the apparent lack of impact of  $\alpha 2$  in skeletal muscle mass in genetic mouse models and the inability to support cell growth in the absence of  $\alpha 1$  *in vitro* are consistent with a model whereby  $\alpha 1$ , but not  $\alpha 2$ , plays a role in the regulation of skeletal muscle mass. To test this model, we investigated the impact of  $\alpha 1$  reduction on muscle mass in Na/K-ATPase  $\alpha 1$  haplodeficient mice ( $\alpha 1^{+/-}$ ) and control littermates ( $\alpha 1^{+/+}$ ). This mouse model has been previously used to examine  $\alpha 1$  and  $\alpha 2$ -isoform specific functions in the heart (P. F. James et al., 1999; Moseley et al., 2004; Moseley et al., 2005) and the skeletal muscle (He et al., 2001). While the latter study specifically focused on the glycolytic Extensor Digitorum Longus (EDL) muscle and the respective roles of  $\alpha 1$  and  $\alpha 2$  in the maintenance of ion homeostasis during contraction, we extended our search for a trophic role of  $\alpha 1$  to the three muscle types (oxidative, mixed and glycolytic).

## **Materials and Methods**

### **Reagents.**

The polyclonal anti-Na/K-ATPase  $\alpha 1$  antiserum NASE and polyclonal anti-Na/K-ATPase  $\alpha 2$  antiserum HERED used for Western blots were raised in rabbits and were generous gifts from Drs. T. Pressley and P. Artigas at Texas Tech University Health Sciences Center (Pressley, 1992). Antibodies for phospho-serine 9 glycogen synthase kinase 3 $\beta$  and total glycogen synthase kinase 3 $\beta$  were from Cell Signaling (catalog number 9322S and 9315S,

respectively). Anti- $\alpha$  tubulin antibody (Sigma, catalog number T5168) or anti- $\beta$  actin antibody (Santa Cruz, catalog number sc-7210) were used as a loading control. Secondary antibodies were horseradish peroxidase-conjugated anti-rabbit and anti-mouse from Santa Cruz Biotechnology Inc (catalog number sc-2004 and sc-2005, respectively).

### **Animals.**

Mice heterozygous for the Na/K-ATPase  $\alpha 1$  isoform were developed by Dr. J Lingrel's group at the University of Cincinnati (P. F. James et al., 1999). The colony was backcrossed to C57J/Bl6 mice from Jackson Labs and maintained through a heterozygous x wild type breeding scheme, resulting in  $\alpha 1$ +/- experimental animals and littermate controls. Male  $\alpha 1$ +/- mice and control littermates were housed in 12-hour light and dark cycles at constant temperature and humidity until 6 months of age. All animal procedures were approved by the Marshall University Institutional Animal Care and Use Committee.

### **Treadmill testing.**

Six-month-old male  $\alpha 1$ +/- mice and litter mate controls were placed in the six lanes of an Exer 3/6 treadmill from Columbus Instruments equipped with a shock detection system. Animals were acclimated to the treadmill for 3 days at 5 m/min for 5 minutes at a 5° angle and were subjected to the testing protocol on the fourth day. Mice began the testing protocol running at 5 m/min for five minutes and increased by 2 m/min each minute up to 25 m/min, then continued running at 25 m/min until they reached fatigue. Each shock administered and each visit to the shock grid was recorded for each animal. Fatigue was defined as 10 consecutive seconds spent on the shock grid, and the shock was discontinued to each mouse upon reaching fatigue.

### **Tissue collection.**

Mice were anesthetized with 50 mg/kg pentobarbital administered via IP injection. Tissues were dissected and weighed. Muscles used for Western blot analysis or enzymatic activity assays were flash frozen in liquid nitrogen then stored at -80° C until later use. Muscles used for histological analysis were fixed in 10% neutrally buffered formalin for 24 hours then stored in 70% ethanol until they were embedded in paraffin blocks.

### **Western blot.**

Left and right muscles of the same type from the same mouse were homogenized together in ice-cold radioimmunoprecipitation (RIPA) buffer (0.25% sodium deoxycholate, 1% Nonidet P-40, 1mM EDTA, 1mM PMSF, 1mM sodium orthovanadate, 1mM Sodium fluoride, 150 mM NaCl, 50 mM Tris-HCl, pH 7.4 and 1% protease inhibitor cocktail) with a Fisher TissueMeiser homogenizer. Homogenates were centrifuged at 14,000 X g for 15 min, supernatants were collected, and the protein content was measured using DC Protein Assay Kit from BioRad (catalog number 500-0114 and 500-0113). Equal amounts of protein of each sample were loaded, separated by SDS-PAGE, and transferred to nitrocellulose membranes. Membranes probed for  $\alpha 1$  and  $\alpha 2$  were blocked in 5% milk, then primary antibodies were added overnight at 4°C. Membranes were visualized with Western Lightning® Plus-ECL (Western Lightning) and radiographic film. Densitometric quantification was performed using ImageJ software from the National Institute of Health.

### **Membrane fractionation.**

Crude membrane fractions were prepared from frozen  $\alpha 1^{-/-}$  and  $\alpha 1^{+/+}$  gastrocnemius muscles following a procedure modified from Walas and Juel (Walas & Juel, 2012). Frozen muscles were ground into a fine powder with a mortar and pestle. The resulting powder was

homogenized in ice-cold fractionation buffer (250 mM mannitol, 30 mM L-histidine, 5 mM EGTA and 0.1% deoxycholate, adjusted to pH 6.8 with Tris-base) for 30 seconds with a Fisher Tissue Meiser handheld homogenizer. The crude homogenate was centrifuged at 3000xg for 30 minutes and the supernatant was then centrifuged at 190,000xg for 90 minutes. The pellet was resuspended in 30 mM histidine, 250 mM sucrose, and 1 mM EDTA, pH 7.4, and protein concentration was determined using the DC Protein Assay Kit from BioRad (catalog number 500-0114 and 500-0113).

#### **ATPase activity assay.**

Ouabain-sensitive ATPase activity in crude membrane fractions was determined by measuring ATP hydrolysis as previously described (Belliard et al., 2016; Belliard, Sottejeau, Duan, Karabin, & Pierre, 2013). Released inorganic phosphate (Pi) was detected using a malachite-based Biomol Green reagent. Samples containing 10 µg of protein were added to a reaction mix containing 20 mM Tris-HCL, 1 mM MgCl<sub>2</sub>, 100 mM NaCl, 20 mM KCl, and 1 mM EGTA-Tris, pH 7.2. Ouabain was added to the samples to a final concentration of 1 mM to completely inhibit both  $\alpha$ 1 and  $\alpha$ 2 isoforms of the Na/K-ATPase. After 10 minutes of preincubation at room temperature, the reaction was started by adding Mg-ATP at a final concentration of 2.25 mM and incubation at 37°C with shaking for 30 minutes. The reaction was stopped with the addition of ice-cold 8% TCA, and the concentration of Pi was measured spectrophotometrically at OD 620 nm using Biomol Green as an indicator (Enzo Life Sciences catalog # BML-AK111-250). Maximal Na/K-ATPase activity was calculated as the difference between ATPase activity obtained in the absence or presence of 1 mM ouabain.

### **Immunohistochemistry.**

Muscles were collected and then washed twice with ice-cold PBS, fixed with 10% neutrally buffered formalin for 24 hours, and embedded in paraffin. Transverse sections of the midbelly were immunostained for myosin heavy chain (Myhc) fast and Myhc slow by Wax-It, Inc., as described by Behan et al. (Behan, Cossar, Madden, & McKay, 2002) to differentiate between type 1 and type 2 fibers. Additional sections were stained for Na/K-ATPase  $\alpha 1$  by Wax-It, Inc. (Vancouver, Canada). The samples were examined on a Leica confocal SP5 microscope (Leica Microsystems, Wetzlar, Germany). The images were processed with the Leica Application Suite Advanced Fluorescence (LAS/AF) suite (Leica Microsystems, Wetzlar, Germany), FIJI platform, and the GNU Image Manipulation Program (GIMP) to obtain maximum projections, extract lateral slices, and construct figures.

### **Morphometric tissue analysis (CSA and fiber types).**

Images of muscles stained for fast and slow myosin heavy chain were obtained by Wax-It, Inc. with digital whole-slide scanning. Aperio ImageScope software was used to determine the cross sectional area (CSA) of each fiber. Fibers that had been damaged were excluded from CSA analysis. Every fiber of each type in each muscle was counted to determine the average number of fibers per muscle.

### **Glycogen content analysis.**

Glycogen was assayed in whole-muscle homogenates using a colorimetric glycogen assay kit from Abcam (catalog number ab169558) according to manufacturer's instructions.

### **Serum analytes.**

Whole blood was collected from the hepatic portal vein then allowed to clot for 15 minutes in 0.8 mL SST-MINI tubes with clot activator and gel. The blood was then centrifuged

at 2000 rpm for 15 minutes. Clear serum was transferred to 1.5 mL transport tubes and analyzed by IDEXX Bioresearch using a Beckman AU680 Chemistry System.

### **Data Analysis.**

Data presented are mean  $\pm$  S.E.M, and statistical analysis was performed using the Student's *t* test. When more than two groups were compared, one-way ANOVA was performed prior to post-hoc comparison of individual groups using Dunnet's multiple comparison test. Significance was accepted at  $P < 0.05$ .

## **Results**

### **Skeletal muscle Na/K-ATPase in $\alpha 1$ haplodeficient mice**

He et al. first reported a significant decrease in Na/K-ATPase  $\alpha 1$  expression in  $\alpha 1^{+/-}$  muscle, but their study focused on one of the three main types of muscle, the glycolytic Extensor Digitorum Longus (EDL) (He et al., 2001). In the present study, the extent of Na/K-ATPase  $\alpha 1$  expression decrease was assessed in all muscle types. Specifically, western blot analyses were performed in a representative oxidative (soleus), a mixed (plantaris) and a glycolytic (EDL) muscle. As shown in Figure 3A,  $\alpha 1$  expression in  $\alpha 1^{+/-}$  mice was decreased by 30-40% in all muscle examined ( $p < 0.05$  vs  $\alpha 1^{+/+}$ ). Further, no compensatory increase in  $\alpha 2$  expression was observed (Figure 3A), and the expression of the regulatory FXYD1 subunit was also unchanged (data not shown). The decrease of Na/K-ATPase  $\alpha 1$  was also clear after immunofluorescence labeling using a  $\alpha 1$ -specific antibody in histological preparations of soleus and EDL muscles (1B and C). To assess the impact of this reduction of  $\alpha 1$  on total Na/K-ATPase activity, a preparation of the gastrocnemius, a mixed muscle of larger size, was used. A decrease of  $\alpha 1$  without detectable change in  $\alpha 2$  expression comparable to that of the three other muscles tested was observed by Western blot (2A). As shown in Figure 4B, maximal Na/K-ATPase activity was not

different between  $\alpha 1^{+/+}$  and  $\alpha 1^{+/-}$  crude membrane fractions (ouabain-inhibited ATPase activity of  $1.91 \pm 0.23 \mu\text{mol}/\mu\text{g protein/hr}$  in  $\alpha 1^{+/+}$  membrane fractions compared to  $2.01 \pm 0.40 \mu\text{mol}/\mu\text{g protein/hr}$  in  $\alpha 1^{+/-}$  membrane fractions).

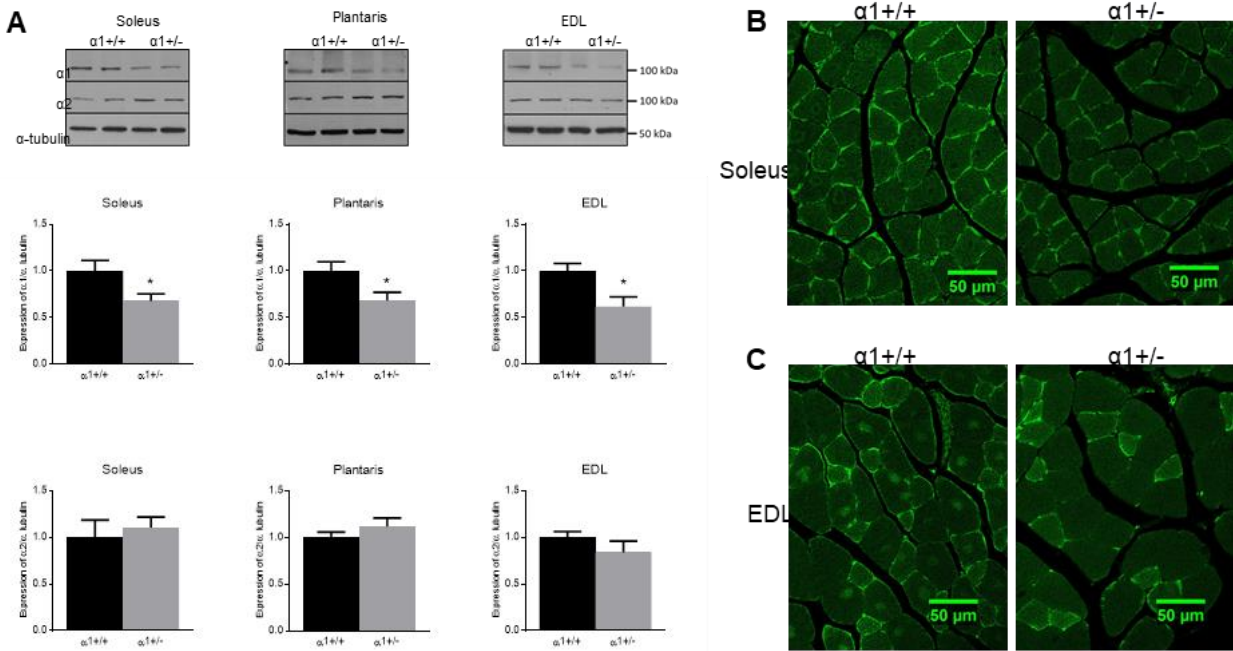


**Figure 3. Na/K-ATPase  $\alpha$ -isoform abundance in skeletal muscles from Na/K-ATPase  $\alpha 1$  haplodeficient mice ( $\alpha 1^{+/-}$ ) and control littermates ( $\alpha 1^{+/+}$ ).**

**A.** Representative Western blots for Na/K-ATPase  $\alpha 1$  and  $\alpha 2$  isoforms in soleus (oxidative), plantaris (mixed), and EDL (glycolytic) muscle homogenates are shown with  $n=2/\text{genotype}$ . The quantitative data are means  $\pm$  S.E.M. from 7-9 specimens/group normalized to the average of the  $\alpha 1^{+/+}$  controls on each gel. **B and C.** Representative immunohistochemical staining for Na/K-ATPase  $\alpha 1$  isoform in soleus (B) and EDL (C) from  $\alpha 1^{+/+}$  and  $\alpha 1^{+/-}$  mice.

**Na/K-ATPase  $\alpha 1$  reduction affects oxidative but not mixed or glycolytic muscle size.**

Based on the recent finding that removing  $\alpha 1$  causes decreased growth in an *in vitro* system (J. Xie et al., 2015), we investigated the impact of reduced  $\alpha 1$  expression on skeletal muscle size in  $\alpha 1^{+/-}$  mice compared to  $\alpha 1^{+/+}$ . Mice were age-matched at 6 months and exhibited no differences in body weight. Consistent with previous studies (P. F. James et al., 1999), there were no major abnormalities detected in basal conditions and kidney weight/body weight ratio and heart weight/body weight ratios were comparable (Table 2). Consistent with previous

observations in these animals (He et al., 2001), the mass to body weight ratio of the glycolytic EDL did not change in  $\alpha 1$ +/- mice (Figure 5). Likewise, the mass of the mixed-type plantaris was comparable (Figure 5). In contrast, the mass-to-body weight ratio of the oxidative soleus muscle was decreased by 9%, from  $0.230 \pm 0.009$  mg/g for  $\alpha 1$ +/+ mice to  $0.209 \pm 0.006$  mg/g for  $\alpha 1$ +/- mice ( $P < 0.05$ ).

	Age (days)	Body Weight (g)	Tibia Length (mm)	Heart/BW (mg/g)	Kidney/BW (mg/g)	Adipose Weight (mg)	Serum K+ (mM)	Serum Na+ (mM)	Glucose (mg/dL)
$\alpha 1$ +/+	188.1 $\pm$ 0.9	34.9 $\pm$ 0.6	16.4 $\pm$ 0.2	4.37 $\pm$ 0.08	6.82 $\pm$ 0.12	1253 $\pm$ 180	6.15 $\pm$ 0.17	153.8 $\pm$ 1.1	232 $\pm$ 37
$\alpha 1$ +/-	187.9 $\pm$ 0.7	35.5 $\pm$ 0.4	16.3 $\pm$ 0.2	4.25 $\pm$ 0.07	6.67 $\pm$ 0.11	995 $\pm$ 250	6.48 $\pm$ 0.84	152.0 $\pm$ 0.9	238 $\pm$ 36

**Table 2: Selected physiological parameters in Na/K-ATPase  $\alpha 1$  +/+ vs  $\alpha 1$  +/- mice.**

Data are presented as means  $\pm$  SEM. For body weight, age, and tibia length, n=30-40. For heart and kidney weight/body weight (BW), n=20-33. Adipose weight represents the combined weights of the epididymal and inguinal fat pads (n=7-8). Serum concentrations of K<sup>+</sup>, Na<sup>+</sup>, and glucose were measured in blood collected from the hepatic portal vein of fed mice (n=4). No significant difference was observed.

#### **Expression of Na/K-ATPase $\alpha 1$ in skeletal muscle types.**

Previous studies of Na/K-ATPase isoforms have described a muscle-type specific distribution of  $\alpha 1$  and  $\alpha 2$  in rats, with the oxidative soleus containing more  $\alpha 1$  than any other muscle type studied and the glycolytic EDL expressing the least (Thompson & McDonough, 1996). Hence, higher expression level could explain the relative high impact of  $\alpha 1$  depletion in the soleus compared to other muscle types in the mouse. This was evaluated by western blot in the oxidative soleus and red gastrocnemius, the glycolytic EDL and white gastrocnemius, and mixed plantaris muscles of C57Bl6 mice. As shown in Figure 6, expression of  $\alpha 1$  decreases as muscles become increasingly glycolytic, with the oxidative soleus expressing significantly more  $\alpha 1$  than either the mixed plantaris or the glycolytic EDL. The sharp contrast between  $\alpha 1$  expression in the soleus vs. EDL was confirmed by immunofluorescence (4C), and is consistent with a relative lack of detectable impact on growth upon reduction by 30%. A difference in  $\alpha 2$

expression between muscle types was also detected, although not as pronounced and less systematically correlated with muscle type.

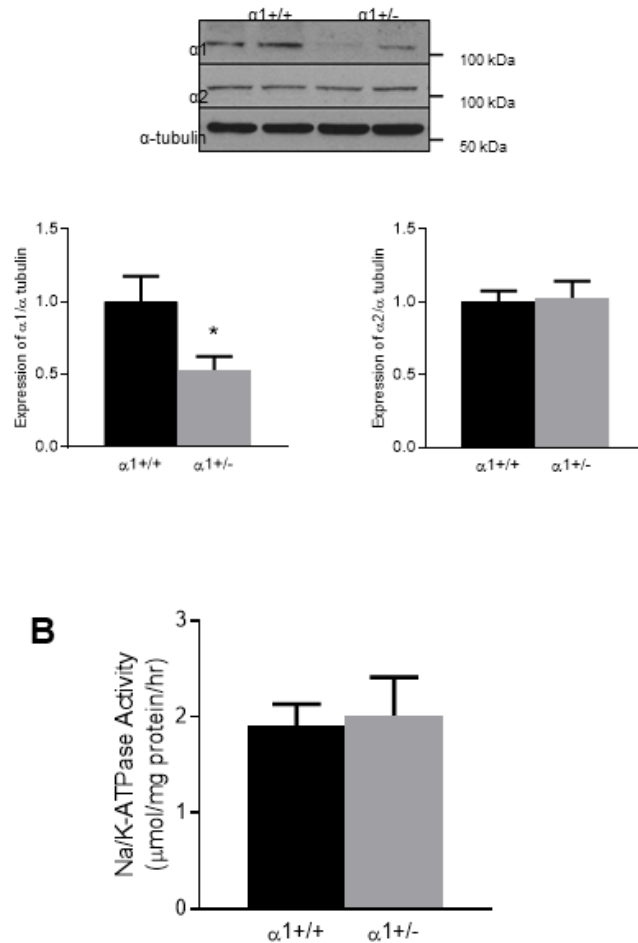


**Figure 4. Na/K-ATPase activity.**

**A.** Representative Western blots for Na/K-ATPase  $\alpha 1$  and  $\alpha 2$  isoforms in gastrocnemius muscle homogenates are shown with  $n=2/\text{genotype}$ , and the quantitative data are means  $\pm$  S.E.M. from 4 specimens/group normalized to the average of the  $\alpha 1^{+/+}$  controls on each gel. **B.** Maximal ATPase activity in crude membrane fractions from  $\alpha 1^{+/+}$  and  $\alpha 1^{-/-}$  gastrocnemius muscles. ATPase activity was measured by Pi release with a colorimetric indicator. ( $n=6-7$ )

**Decreased cross-sectional area without change in muscle fiber number in the soleus**

To determine which structural changes were associated with the decreased muscle mass in the soleus, we examined the number and size of myofibers in  $\alpha 1^{-/-}$  vs.  $\alpha 1^{+/+}$  soleus muscles after staining for fast and slow myosin heavy chain from 4 muscles per group. As shown in Figure 7A, fiber composition of the  $\alpha 1^{-/-}$  soleus was not different from  $\alpha 1^{+/+}$ . However, fiber

cross sectional area was significantly decreased by 10% in  $\alpha 1^{-/-}$  soleus muscles, suggesting that the decrease in muscle mass was due to changes in fiber size rather than number. This change in fiber size was observed in both type 1 and type 2a fibers of the soleus (Figure 7A). In contrast, the EDL exhibited no change in either fiber number or fiber cross sectional area, which is consistent with the lack of impact on overall muscle size (Figure 7B).

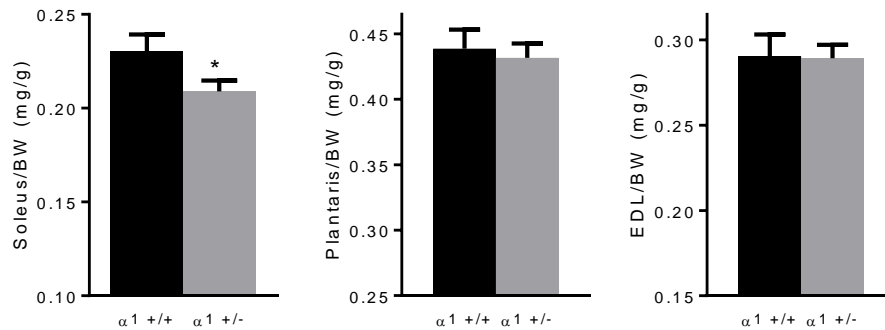


**Figure 5. Changes in muscle mass in  $\alpha 1^{-/-}$  mice.**

Muscle mass of soleus, plantaris, and EDL in  $\alpha 1^{+/+}$  and  $\alpha 1^{-/-}$  mice. The quantitative data are means  $\pm$  S.E.M. from 23  $\alpha 1^{+/+}$  or 40  $\alpha 1^{-/-}$  mice. \*p<0.05.

**Glycogen content and GSK3 $\beta$  status in the soleus**

Na/K-ATPase  $\alpha 1$  signaling pathway is a modulator of glycogen synthesis and glycogen synthase kinase 3 $\beta$  (GSK3 $\beta$ ) in skeletal muscle cells (Kotova, Al-Khalili, et al., 2006) and may therefore lead to a change in size, growth and differentiation in the soleus of  $\alpha 1^{-/-}$  mice (Agle et al., 2017; Leger et al., 2006; van der Velden et al., 2007; Verhees et al., 2011). Accordingly, we compared glycogen content and GSK3 $\beta$  in  $\alpha 1^{-/-}$  and  $\alpha 1^{+/+}$  soleus muscles. As shown in Figure 8A, Western blot analysis did not reveal any difference in GSK3 $\beta$  content or serine 9 phosphorylation between  $\alpha 1^{+/+}$  and  $\alpha 1^{-/-}$  muscles from fed mice. Consistent with this result, glycogen content was comparable in  $\alpha 1^{+/+}$  and  $\alpha 1^{-/-}$  soleus muscles (Figure 8B).

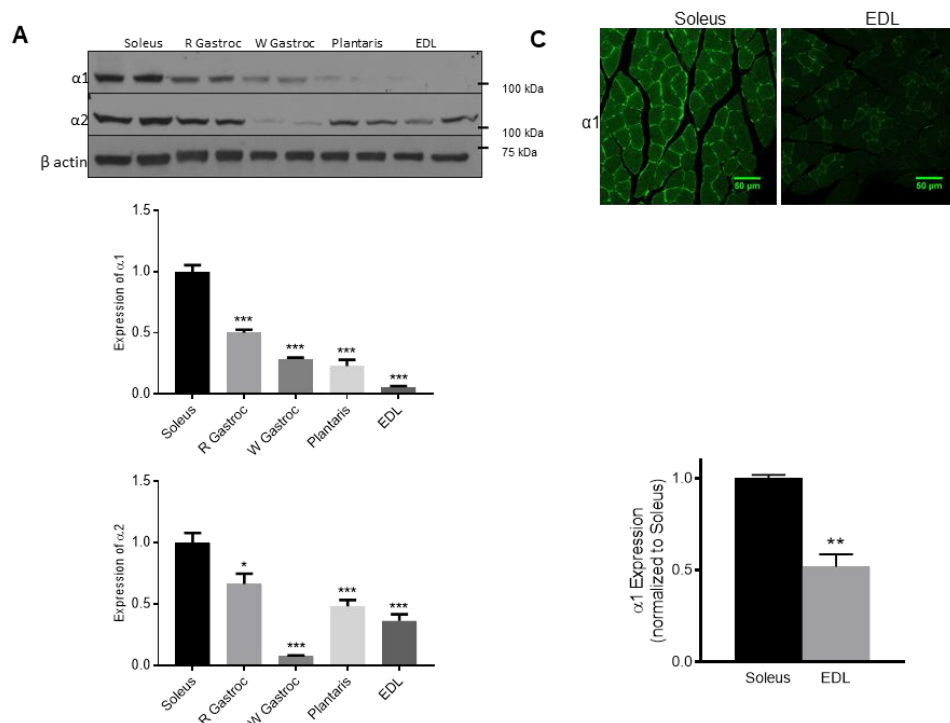


**Figure 6. Na/K-ATPase  $\alpha$ -isoform abundance in skeletal muscles from C57Bl6 mice.**

**A.** Representative Western blots for Na/K-ATPase  $\alpha$ 1 and  $\alpha$ 2 isoforms in oxidative (soleus and red gastrocnemius (R Gastroc)), mixed (plantaris), and glycolytic (EDL and white gastrocnemius (W Gastroc)) muscles are shown with  $n=2$ /muscle type. **B.** Quantitative data are means  $\pm$  S.E.M. from 6 specimens/group normalized to the average of the soleus on each gel. \*  $p<0.05$  and \*\*\* $p<0.0001$  vs soleus. **C.** Representative micrographs of immunohistological staining for Na/K-ATPase  $\alpha$ 1 in soleus (left) and EDL (right), with quantification of 3 samples/group. \*\* $p<0.001$ .

### Exercise performance

As shown in Table 2, the 10% change in muscle mass observed in some but not all muscles of the  $\alpha$ 1 $^{+/-}$  mouse was not accompanied by a noticeable change in physiological parameters related to growth (tibia length) or metabolic dysregulation (glycaemia, adipose tissue mass), or  $K^+$  homeostasis in basal conditions. To test whether the observed structural changes in  $\alpha$ 1 $^{+/-}$  soleus size affected exercise performance in 6-month-old mice, two treadmill exercise paradigms were used. A gradual increase in velocity allowed us to assess changes in tolerance to high speeds and high intensity exercise, and a prolonged time at 25 meters per minute allowed us to determine whether endurance exercise was affected. As shown in Figure 9, the number of

shocks at each speed remained unchanged, suggesting that the reduced amount of  $\alpha 1$  present in the  $\alpha 1^{+/-}$  muscle did not prevent animals from running at high speeds. Furthermore, the distance to fatigue was unchanged.

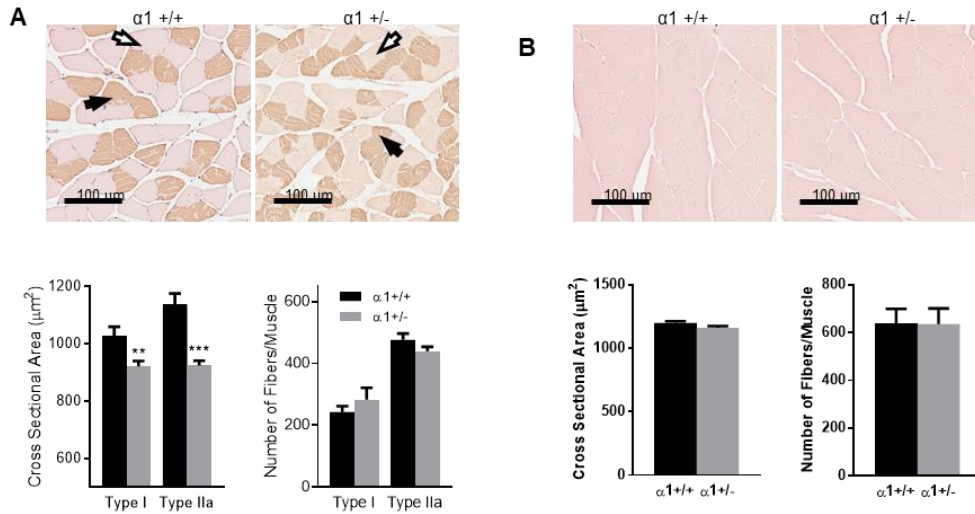


**Figure 7. Structural changes in the soleus muscle of Na/K-ATPase  $\alpha 1$  haplodeficient mice.** Soleus and EDL muscles were dissected and weighed, then cross sections of the midbelly of paraffin-embedded soleus muscles were stained for fast and slow myosin heavy chain (Myhc). Cross sectional areas (CSA) of the fibers were determined using Aperio ImageScope software. **A.** Representative micrographs of  $\alpha 1^{+/+}$  and  $\alpha 1^{+/-}$  soleus muscles, with type I and type II fibers shown with white and black arrows respectively. Quantifications of cross sectional areas of type I and type II fibers from 4 soleus muscle/group and total number of fibers of each type in each soleus muscle (n=4). \*\*  $p < 0.005$  and \*\*\*  $p < 0.0001$  vs cross sectional area in  $\alpha 1^{+/+}$  littermates. **B.** Representative micrographs of  $\alpha 1^{+/+}$  and  $\alpha 1^{+/-}$  soleus muscles. Quantifications of cross sectional areas of type II and total number of fibers of each type in each EDL muscle (n=4-5). No significant difference was observed.

## Discussion

Based on our observations in renal epithelial cell lines, Na/K-ATPase  $\alpha 1$  possesses isoform-specific functions that are not supported by  $\alpha 2$ , which results in a sizable effect on cell growth rate (J. Xie et al., 2015). Since renal epithelial cells do not normally express Na/K-ATPase  $\alpha 2$ , we took the next step of investigating this issue in a tissue expressing both isoforms. We focused on the skeletal muscle, a tissue where  $\alpha 2$  expression uniquely predominates over the minor  $\alpha 1$  isoform and with a regenerative process that occurs throughout life. Specifically, we

used the Na/K-ATPase  $\alpha 1^{+/-}$  mouse model to investigate whether a downregulation of the minor pool of Na/K-ATPase  $\alpha 1$  expressed in skeletal muscle could affect muscle mass. The data indicate that a 30-40% decrease of Na/K-ATPase  $\alpha 1$  protein expression, which does not noticeably decrease total maximum Na/K-ATPase capacity of the muscle, induces a modest yet significant decrease of 10% in the mass of the oxidative soleus (Figure 5). In contrast, the mass of the glycolytic EDL was not affected, nor was that of the mixed-type muscle plantaris (Figure 5). The very low level of  $\alpha 1$  expression in the EDL and the plantaris compared to the soleus may explain this intriguing muscle-type specific effect. Indeed, as shown in Figure 6 and consistent with previous studies in rats by Thompson and McDonough (Thompson & McDonough, 1996) and others (Chaillou et al., 2011; Fowles et al., 2004), the oxidative soleus expresses substantially more  $\alpha 1$  than the glycolytic EDL in wild-type mice. Moreover, when the western blot analysis was extended to additional representative muscles of each type, a positive correlation between  $\alpha 1$  content and oxidative metabolism was observed, suggesting that the role of  $\alpha 1$  could be particularly important in oxidative fibers. Mechanistically, we speculate that endogenous cardiotonic steroid (CTS) signaling through  $\alpha 1$  may have a role in maintaining the growth of the soleus, and the lack of this ouabain signaling could be responsible for the reduced soleus mass in  $\alpha 1^{+/-}$  mice (Figure 5). It should be noted that the mouse  $\alpha 1$  isoform has a much lower affinity for ouabain than  $\alpha 2$ , and only 0.05% of the  $\alpha 1$  isoform is bound to ouabain at the reported endogenous ouabain concentrations (Bauer et al., 2005; O'Brien et al., 1994). However, through amplification of signaling cascades, concentrations of ouabain comparable to circulating endogenous ouabain can activate signaling in cells and tissue expressing such low affinity  $\alpha 1$  (Aydemir-Koksoy, Abramowitz, & Allen, 2001; Dvela-Levitt et al., 2015; Dvela, Rosen, Ben-Ami, & Lichtstein, 2012; Fontana et al., 2013). In contrast, pumping inhibition is directly related

to the number of pumps bound to ouabain, which means that signaling could have a long-lasting impact at concentrations too low to affect the membrane potential or ion homeostasis. Although this remains to be specifically tested, a plausible model is that the higher expression level of  $\alpha 1$  in the soleus enables endogenous CTS-stimulated signaling, as seen in other cell lines and tissue types (Aydemir-Koksoy et al., 2001; Cui & Xie, 2017; Fontana et al., 2013; Kometiani et al., 1998; Tian et al., 2009). Consistent with our observation that a 50% reduction in  $\alpha 1$  expression prevents ouabain from stimulating signaling and growth in renal epithelial cells (Tian et al., 2009),  $\alpha 1$  expression in the EDL (6% of soleus) or plantaris (23% of soleus) may not allow CTS-stimulated growth through stimulation of Na/K-ATPase  $\alpha 1$  signaling. Although signaling of the CTS ouabain through Na/K-ATPase  $\alpha 1$  modulates glycogen synthesis through GSK3 $\beta$  signaling in skeletal muscle cells (Benziane et al., 2012) and may therefore lead to a change in size, growth and differentiation in the soleus of  $\alpha 1$ +/- mice (Agle et al., 2017; Leger et al., 2006; van der Velden et al., 2007; Verhees et al., 2011), we did not detect a significant change in the 6 month old mouse (Figure 8). This result certainly warrants further investigation, as a dysregulation of GSK3 $\beta$  may have occurred at an earlier time point and/or may only be discernible under agonist stimulation.

Skeletal-muscle specific ablation of Na/K-ATPase  $\alpha 2$  does not affect muscle mass (DiFranco et al., 2015; Manoharan et al., 2015; Radzyukevich et al., 2013), which suggests that the observed decrease in soleus mass in the  $\alpha 1$ +/- is likely unrelated to altered ion-pumping capacity of the cell. Consistently, we did not detect any significant decrease in Na/K-ATPase activity in crude membrane preparations from  $\alpha 1$ +/- muscles. Based on an  $\alpha 1$  contribution of about 15% of total skeletal muscle Na/K-ATPase (He et al., 2001) and a decrease of about 40% of  $\alpha 1$  in the  $\alpha 1$ +/- skeletal muscle, the expected decrease in Na/K-ATPase activity would have

been minimal (about 6%), and may have remained below the limit of detection of the assay (Heiny et al., 2010; Ingwersen et al., 2011; Walas & Juel, 2012). On the other hand, it is well established that most cells have a large reserve pump capacity and that a decrease in the number of Na/K-ATPase expressed at the cell membrane can be compensated by either a substrate-mediated stimulation of existing pumps or a mobilization of the reserve pump pool (T. Akera & Brody, 1982; Tai Akera & Brody, 1985). Finally, although we consider it unlikely because a decreased myofiber diameter as observed in  $\alpha 1^{+/-}$  muscles is not expected as a secondary adjustment for optimization of ion pumping capacity and maintenance of the membrane potential (in fact, fibers with larger rather than smaller diameters require significantly less energy to maintain their membrane potential (Jimenez, Dasika, Locke, & Kinsey, 2011; Jimenez, Dillaman, & Kinsey, 2013)), it should be noted that a change in Na/K-ATPase ion-transport activity secondary to  $\alpha 1$  depletion has not been specifically excluded in this study.

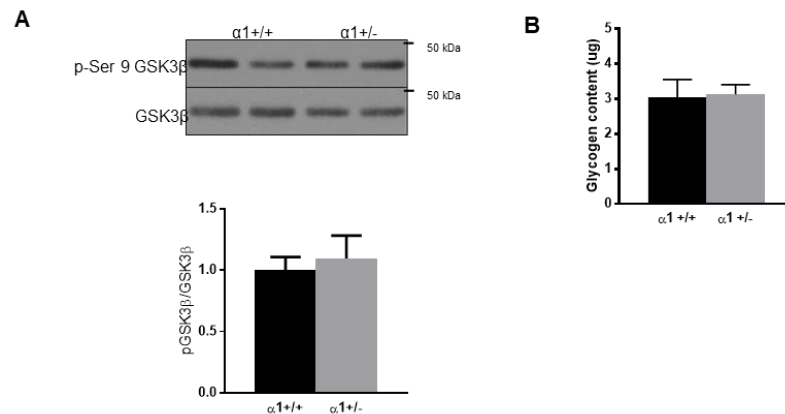


**Figure 8. A. GSK3 $\beta$  and glycogen content in the soleus muscle of Na/K-ATPase  $\alpha 1$  haplodeficient mice.**

Representative Western blots for phospho serine 9 glycogen synthase kinase 3 $\beta$  (p-Ser9 GSK3 $\beta$ ) and total glycogen synthase kinase 3 $\beta$  (GSK3 $\beta$ ) in  $\alpha 1^{+/+}$  and  $\alpha 1^{+/-}$  soleus muscles. Quantitative data are means  $\pm$  S.E.M. from 4 specimens/group. Phospho-Ser9 GSK3 $\beta$  /total GSK3 $\beta$  ratios were normalized to the average of the  $\alpha 1^{+/+}$  controls on each gel. B. Glycogen content of soleus muscles presented as means  $\pm$  S.E.M. from 6-7 samples per group.

This model of a change in muscle mass related to  $\alpha 1$ -specific signaling function is also consistent with the concept of distinct and specific roles for  $\alpha 1$  and  $\alpha 2$  in skeletal muscle initially suggested by He et al. Indeed, the authors first proposed that  $\alpha 1$  is primarily responsible for establishing a baseline membrane potential, and  $\alpha 2$  maintains the membrane potential during contraction (He et al., 2001). This role for  $\alpha 2$  was subsequently confirmed by a series of studies using skeletal muscle specific ablation of  $\alpha 2$  in mice. In those studies, muscle mass of both EDL and soleus was unchanged, but maintenance of the membrane potential during contraction was severely impaired due to an inability to clear the excitation-dependent increase in extracellular  $[K^+]_o$  (DiFranco et al., 2015; Manoharan et al., 2015; Radzyukevich et al., 2013). Taken together, those studies and the results presented here support a model where skeletal muscle  $\alpha 2$  has an isoform-specific role in the maintenance of membrane potential during contraction related to its enzymatic activity, whereas  $\alpha 1$  has, in addition to its transport function, an isoform-specific role in growth that is independent of its ion-pumping activity.

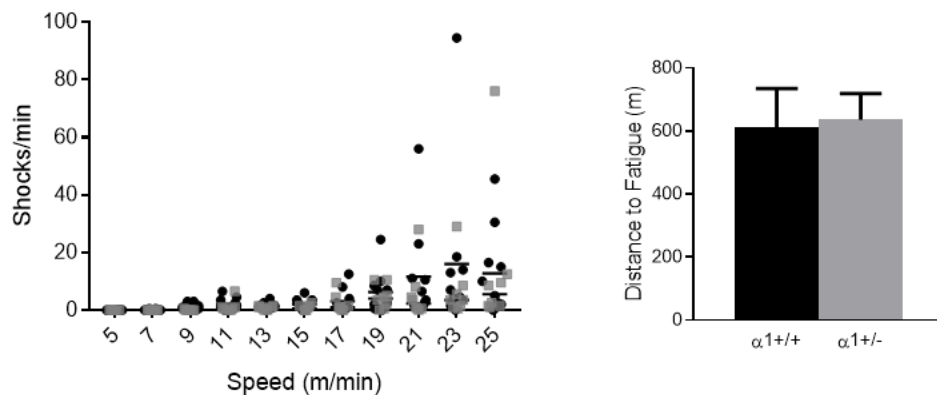


**Figure 9. Distance to fatigue in Na/K-ATPase  $\alpha 1$  haplodeficient mice ( $\alpha 1^{-/-}$ ) and control littermates ( $\alpha 1^{+/+}$ ) during forced treadmill running.**

A. Number of shocks administered per animal per minute at increasing speeds during testing of 6-month-old mice (n=7-9/group;  $\alpha 1^{+/+}$  black circles;  $\alpha 1^{-/-}$  grey squares). B. Distance to fatigue for 6-month-old  $\alpha 1^{+/+}$  and  $\alpha 1^{-/-}$  animals (n=7-9).

While the effect of  $\alpha 1$  haplodeficiency on muscle growth may seem modest at first, it is important to note that it is relevant to reported models of skeletal muscle atrophy. The soleus-specific decrease in muscle mass, accompanied by a reduction of fiber size but not fiber number, is a feature of disuse-induced atrophy induced by hind limb suspension (Egawa et al., 2015; Kravtsova et al., 2016). Although this decrease in size is relatively minor compared to some forms of atrophy, it is comparable to the 10-15% decrease in gastrocnemius mass in burn cachexia reported by Pedroso et al. (Pedroso et al., 2012). Similarly, the commonly used subcutaneous inoculation model of cancer cachexia consistently decreases muscle mass by 6-15% (Choi et al., 2013; Matsuyama et al., 2015; Murphy et al., 2011; X. Wang, Pickrell, Zimmers, & Moraes, 2012). As may have been expected with a relatively modest decrease, the  $\alpha 1^{+/-}$  mouse model does not present with major metabolic abnormalities in basal conditions (Table 2). Perhaps more surprising is the lack of defects in exercise capacity (Figure 9), given that He et al. found that the tetanic force of isolated  $\alpha 1^{+/-}$  EDL muscles is decreased *in vitro* (He et al., 2001). This apparent discrepancy is likely due to the global haplodeficiency of the  $\alpha 1^{+/-}$  mouse model, which affects other systems involved in exercise, including the nervous, cardiovascular, and endocrine systems.

Clearly, inherent limitations due to global and incomplete reduction of Na/K-ATPase  $\alpha 1$  in the  $\alpha 1^{+/-}$  model warrant future studies in a skeletal muscle-specific model. While such model seems required to fully assess the scope and significance of the proposed new isoform-specific trophic role for Na/K-ATPase  $\alpha 1$  in the skeletal muscle, several important conclusions can be drawn from the present study. First, the  $\alpha 1$ -specific trophic role observed *in vitro* is relevant *in vivo*. Second, manipulation of Na/K-ATPase  $\alpha 1$  content leads to morphological changes in the skeletal muscle that do not impact maximal running capacity, in contrast to manipulation of  $\alpha 2$

which did not affect muscle size but affected running capacity. These lend further support for the concept that Na/K-ATPase  $\alpha 1$  and  $\alpha 2$  serve distinct and isoform-specific functions in the skeletal muscle. Finally, the findings presented here suggest a novel mechanism for exercise-induced changes in muscle size and metabolism. Physiologically, exercise increases serum concentrations of endogenous Na/K-ATPase ligands such as ouabain and leads to modifications of skeletal muscle structure and function (Bauer et al., 2005; Egan & Zierath, 2013). Alteration of muscle activity during exercise through modulation of  $\alpha 2$  by endogenous Na/K-ATPase ligands has been demonstrated (Radzyukevich et al., 2009), and the present study now suggests that they may also modulate changes in oxidative skeletal muscle structure in response to exercise training through the modulation of  $\alpha 1$  signaling. These new findings suggest a possible impact of endogenous or pharmacological administration of CTS on muscle growth, which could be further investigated using the established mouse line expressing ouabain-sensitive  $\alpha 1$  (Dostanic-Larson et al., 2006).

### **Acknowledgements**

This work was supported by NIH Grant HL-109015, NIH Grant RO1 AR063710, and MIIR funds.

We thank Lanqing Wu and the Division of Animal Resources of the Marshall University Joan C. Edwards School of Medicine for animal care and husbandry, the Marshall University Molecular and Biological Imaging Center for microscopy equipment and expertise, and Carla Cook for invaluable technical support.

## CHAPTER 3

### METABOLIC CAPACITY, ENDURANCE AND INSULIN RESISTANCE ARE ACQUIRED BY MAMMALS VIA A COMMON MECHANISM

A manuscript in preparation.

Laura C Kutz<sup>1\*</sup>, Xiaoyu Cui<sup>1\*</sup>, Jeffrey X. Xie<sup>1,2</sup>, Adam J Martin<sup>1</sup>, Minqi Huang<sup>1</sup>, Shreya T Mukherji<sup>1</sup>, Xiaoliang Wang<sup>1</sup>, Jiayan Wang<sup>1</sup>, Kayleigh C Terrell<sup>1</sup>, Hua Zhu<sup>3</sup>, Judith A Heiny<sup>4</sup>, Joseph I Shapiro<sup>5</sup>, Gustavo Blanco<sup>6</sup>, Sandrine V Pierre<sup>1</sup>, Zijian Xie<sup>1</sup>

\*Co-first authors

<sup>1</sup> Marshall Institute for Interdisciplinary Research, Marshall University, Huntington, WV

<sup>2</sup> Department of Internal Medicine, University of Michigan, Ann Arbor, MI

<sup>3</sup> Department of Surgery, Wexner Medical Center, Ohio State University, Columbus, OH

<sup>4</sup> Department of Pharmacology and Systems Physiology, University of Cincinnati, Cincinnati, OH

<sup>5</sup> Joan C. Edwards School of Medicine, Marshall University, Huntington, WV

<sup>6</sup> Department of Molecular and Integrative Physiology, and The Kidney Institute, University of Kansas Medical Center, Kansas City, KS

## Summary

Mammals have acquired increased metabolic capacity to support growth and endurance. Paradoxically, they also become insulin resistant when fed with Western diet. We find that the acquisition of Src binding sites in the  $\alpha 1$  Na/K-ATPase (NKA) occurred during endothermy evolution. The loss of Src binding diminishes metabolic capacity in cell culture, which is confirmed by phenotypic changes observed in a skeletal muscle-specific  $\alpha 1$  knockout ( $sk\alpha 1^{-/-}$ ) mouse model. However,  $sk\alpha 1^{-/-}$  mice are resistant to diet-induced insulin resistance. Similar protection is observed in wild type mice treated with pNaKtide, an inhibitor of  $\alpha 1$  NKA/Src complex. These results suggest that the acquisition of Src binding by  $\alpha 1$  NKA is responsible for the dichotomy of increased metabolic capacity at the cost of decreased tolerance for Western diet. Therefore, we suggest that the  $\alpha 1$  NKA/Src complex may underlie the molecular basis of endothermy evolution and serve as a new target for metabolic syndrome therapeutics.

## Introduction

Metabolic capacity, comprised of reserve and flexibility, is vital for maintaining homeostasis when faced with changing energy demands and fuel availability. As endotherms, mammals have increased metabolic capacity compared to ectothermic animals. The aerobic scope hypothesis posits that the evolution of endothermy relied on increased metabolic capacity to facilitate not only endothermy but the increased ambulatory endurance associated with endothermy (Griffin, Humphries, Kinter, Lim, & Szweda, 2016). However, mammals also developed intolerance to overnutrition. The development of diet-induced metabolic syndrome in mammals is associated with the loss of metabolic flexibility and involves the overproduction of reactive oxygen species (ROS) and the development of chronic inflammation, leading to insulin resistance, glucose intolerance, hepatic steatosis, and obesity. Furthermore, the loss of metabolic

capacity is observed in many end-stage chronic human diseases such as heart failure, liver failure, and steatohepatitis (Galgani, Moro, & Ravussin, 2008; Peterzan, Lygate, Neubauer, & Rider, 2017; Poussin et al., 2011; Su et al., 2017; Z. V. Wang, Li, & Hill, 2014). Conversely, increased metabolic capacity is linked to improved health outcomes (Apostolopoulou et al., 2016; Carson, Hardee, & VanderVeen, 2016; Goodpaster & Sparks, 2017; Koves et al., 2008; Meex et al., 2010; Overmyer et al., 2015; Peterzan et al., 2017). Despite the importance of metabolic reserve and flexibility in mammalian pathophysiology, the mechanisms by which they are regulated are only minimally understood and the mechanism of increased metabolic capacity in mammals has yet to be identified (Goodpaster & Sparks, 2017).

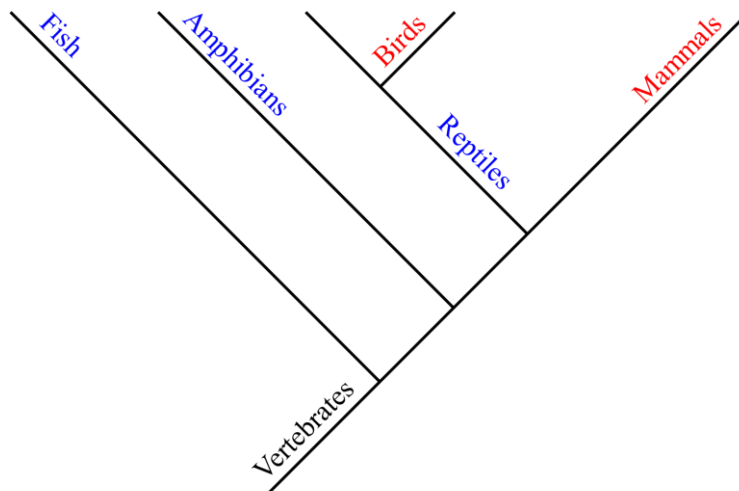


**Figure 10: Evolutionary relationships between vertebrate groups listed in Table 3.** Endotherms are written in red, ectotherms in blue.

In addition to its role as an ion transporter, the ubiquitous mammalian Na/K-ATPase (NKA)  $\alpha 1$  isoform encoded by the *ATP1A1* gene has been identified as an important signaling platform due to its ability to form a functional receptor complex with Src (Cui & Xie, 2017). The four mammalian isoforms of the  $\alpha$  subunit evolved from the invertebrate  $\alpha$  subunit and form their own clade, with mammalian ATP1A1 as the most recently evolved isoform (Kakumura et al., 2015; Saez, Lozano, & Zaldivar-Riveron, 2009; W.-K. Yang et al., 2019). Among the processes

regulated by  $\alpha 1$  NKA/Src signaling are the Warburg effect, a switch to anaerobic metabolism in cancer (Banerjee et al., 2018), and increased mitochondrial ROS production, which can further activate the  $\alpha 1$  NKA/Src pathway and generate a positive feedback loop (Yan et al., 2013). Targeting this signaling through  $\alpha 1$  NKA has been shown to attenuate metabolic syndrome (Sodhi et al., 2015; Sodhi et al., 2018; Sodhi et al., 2017; Srikanthan et al., 2016), and decreased  $\alpha 1$  NKA expression is involved with multiple disease states associated with metabolic disturbances, including heart failure (Liu, Wu, & Kennedy, 2016), cancer (Banerjee et al., 2018; Zhuang et al., 2015), diabetic neuropathy (Gerbi et al., 1998), and polycystic ovarian syndrome (Tepavcevic et al., 2015). In contrast to  $\alpha 1$  NKA, the expression of other mammalian isoforms which do not signal through Src ( $\alpha 2$ ,  $\alpha 3$ , and  $\alpha 4$ ) is restricted to specific tissues (Blanco, 2005a). In view of its links to mitochondrial ROS production and the highly conserved nature of Src binding sites in mammalian ATP1A1, we postulate that the acquisition of Src binding sites in  $\alpha 1$  NKA affords a fundamental regulatory mechanism of metabolic capacity, which supports growth, endurance, and other physiological characteristics of endothermy. Conversely, it may also represent a fundamental mechanism of metabolic dysregulation when animals are in a chronic state of nutritional over-supply.

To test these hypotheses, we developed an *in vitro* system to compare the metabolic profiles of cells expressing the wild-type Src binding  $\alpha 1$  isoform, the wild-type non-Src binding  $\alpha 2$  isoform, a previously characterized loss-of-function Src binding mutant  $\alpha 1$  isoform (Lai et al., 2013), and a previously characterized Src binding, gain-of-function  $\alpha 2$  mutant (Yu et al., 2018). We then generated a mouse model with a skeletal muscle-specific ablation of ATP1A1, taking advantage of the prior observation that the  $\alpha 2$  isoform is the primary driver of ion-pumping during skeletal muscle contraction (DiFranco et al., 2015). Moreover, in view of the well-

established role of skeletal muscle in the regulation of glucose metabolism and insulin sensitivity (Camps et al., 1992; DeFronzo & Tripathy, 2009; Holmstrom, Iglesias-Gutierrez, Zierath, & Garcia-Roves, 2012; Honka et al., 2018; Koves et al., 2008; Meex et al., 2010; Neuffer, Carey, & Dohm, 1993; Son et al., 2017; Zurlo et al., 1990), we further utilized this model to address the role of Src binding  $\alpha 1$  NKA in the development of metabolic syndrome. These genetic studies reveal a novel mechanism regulating metabolic reserve and flexibility. Moreover, they reveal a trade-off phenotype of increased endurance at the cost of increased susceptibility to Western diet and the consequent development of glucose intolerance and insulin resistance.

## **Results**

### **The impact of Src binding sites in ATP1A1 on metabolic capacity *in vitro*.**

Previous studies have identified two ATP1A1-specific Src binding sites (the NaKtide sequence and Y260, Table 3) (Banerjee et al., 2018; Lai et al., 2013; Z. Li et al., 2009; Yu et al., 2018) which are completely conserved within mammalian species. One of these binding sites, the NaKtide sequence, also appears in birds, which evolved endothermy in parallel with mammals. NaKtide contains 20 amino acid residues, the first ten of which (415S-424I) form a helical structure important for Src binding (Lai et al., 2013). While ectothermic animals (Table 3) have amino acid substitutions that disrupt the formation of the helical structure (Lai et al., 2013), most bird species contain one substitution (L419S/T) and a conserved substitution (I424V). We therefore conclude that the Src binding function of NKA  $\alpha 1$  is convergently acquired in birds and mammals and coincides with the evolution of endothermy.

Class	Species	Y260	NaKtide
Mammals	Mouse $\alpha 1$	255 RGIVVYTGDR <b>T</b> 265	415 SATW <b>F</b> ALSRIAGLCNRA <b>V</b> FQ 434
	Rat $\alpha 1$	255 RGIVVYTGDR <b>T</b> 265	415 SATW <b>F</b> ALSRIAGLCNRA <b>V</b> FQ 434
	Pig $\alpha 1$	253 RGIVVYTGDR <b>T</b> 263	413 SATW <b>L</b> ALSRIAGLCNRA <b>V</b> FQ 432
	Whale $\alpha 1$	253 RGIVVYTGDR <b>T</b> 263	413 SATW <b>L</b> ALSRIAGLCNRA <b>V</b> FQ 432
	Dolphin $\alpha 1$	253 RGIVVYTGDR <b>T</b> 263	413 SATW <b>L</b> ALSRIAGLCNRA <b>V</b> FQ 432
	Bat $\alpha 1$	253 RGIVVYTGDR <b>T</b> 263	413 SATW <b>L</b> ALSRIAGLCNRA <b>V</b> FQ 432
Birds	Chicken $\alpha 1$	253 <b>V</b> GIV <b>I</b> STGDR <b>T</b> 263	413 SATW <b>L</b> ALSRIAGLCNRA <b>V</b> FQ 432
	Finch $\alpha 1$	253 RGIV <b>I</b> STGDR <b>T</b> 263	413 SATW <b>T</b> ALSRIAGLCNRA <b>V</b> FQ 432
	Hummingbird $\alpha 1$	224 RGIV <b>I</b> STGDR <b>T</b> 234	384 SATW <b>T</b> ALS <b>R</b> VAGLCNRA <b>V</b> FQ 403
	Eagle $\alpha 1$	254 RGIV <b>I</b> STGDR <b>T</b> 264	414 SATW <b>S</b> ALS <b>R</b> VAGLCNRA <b>V</b> FQ 431
	Penguin $\alpha 1$	224 RGIV <b>I</b> STGDR <b>T</b> 234	384 SATW <b>T</b> ALS <b>R</b> VAGLCNRA <b>V</b> FQ 403
Reptiles	Bearded Dragon $\alpha 1$	224 RG <b>V</b> V <b>I</b> NTGDR <b>T</b> 234	284 <b>S</b> PTW <b>T</b> AL <b>A</b> RIAGLCNRA <b>V</b> FQ 403
	King Cobra $\alpha 1$	253 RG <b>V</b> V <b>I</b> NTGDR <b>T</b> 263	414 <b>S</b> PTW <b>T</b> AL <b>A</b> KIAGLCNRA <b>V</b> FQ 433
	Tiger Snake $\alpha 1$	257 RG <b>V</b> V <b>I</b> NTGDR <b>T</b> 267	417 <b>S</b> PSW <b>T</b> AL <b>A</b> KIAGLCNRA <b>V</b> FQ 436
	Sea Turtle $\alpha 1$	256 RG <b>V</b> V <b>I</b> NTGDR <b>T</b> 266	416 <b>S</b> LTW <b>V</b> ALS <b>R</b> VAGLCNRA <b>V</b> FQ 435
Amphibia	Frog $\alpha 1$	255 RGIVVNTGDR <b>T</b> 265	415 <b>S</b> PTW <b>T</b> ALSRIAGLCNRA <b>V</b> FQ 434
Fish	Catfish $\alpha 1$	224 RGIV <b>I</b> STGDR <b>H</b> T 234	384 <b>S</b> LTW <b>T</b> SL <b>A</b> RIAGLCNRA <b>V</b> FL 403
	Herring $\alpha 1$	258 RGIV <b>I</b> STGDR <b>K</b> T 268	418 <b>S</b> STW <b>S</b> SL <b>A</b> RIAGLCNRA <b>V</b> FL 437
	Freshwater Whipray $\alpha 1$	250 RG <b>V</b> V <b>I</b> FTGDR <b>T</b> 260	410 <b>S</b> PTW <b>S</b> ALS <b>R</b> IA <b>A</b> LCNRA <b>V</b> FK 429
	Zebrafish $\alpha 1$	256 RGIV <b>I</b> STGDR <b>T</b> 266	416 SATW <b>A</b> SL <b>A</b> R <b>V</b> AGLCNRA <b>V</b> FL 435
Mammals	Human $\alpha 2$	253 RGIV <b>I</b> A <b>T</b> GDR <b>T</b> 263	413 <b>S</b> PTW <b>T</b> ALSRIAGLCNRA <b>V</b> FK 432
	Mouse $\alpha 2$	253 RGIV <b>I</b> A <b>T</b> GDR <b>T</b> 263	413 <b>S</b> PTW <b>T</b> ALSRIAGLCNRA <b>V</b> FK 432
	Rat $\alpha 2$	253 RGIV <b>I</b> A <b>T</b> GDR <b>T</b> 263	413 <b>S</b> PTW <b>T</b> ALSRIAGLCNRA <b>V</b> FK 432
	Pig $\alpha 2$	253 RGIV <b>I</b> A <b>T</b> GDR <b>T</b> 263	413 <b>S</b> PTW <b>T</b> ALSRIAGLCNRA <b>V</b> FK 432
	Whale $\alpha 2$	253 RGIV <b>I</b> A <b>T</b> GDR <b>T</b> 263	413 <b>S</b> PTW <b>T</b> ALSRIAGLCNRA <b>V</b> FK 432
Insect	Drosophila $\alpha$	273 <b>K</b> GV <b>V</b> I <b>S</b> CGDR <b>H</b> T 283	433 <b>S</b> PG <b>F</b> KALSRIAT <b>L</b> CNRA <b>E</b> FK 452

**Table 3: Conservation of the NKA  $\alpha 1$ /Src binding sites in mammals. Bold letters indicate residues that differ from mammalian  $\alpha 1$ .**

Sequences of Src binding regions of mammalian NKA  $\alpha 1$  and homologous regions in other classes of animals and in mammalian  $\alpha 2$ .

To assess the physiological significance of ATP1A1 Src binding, we generated 3 cell lines from LLC-PK1, a porcine renal epithelial cell line, using a well-established knock down and rescue approach (Liang et al., 2006; Liang et al., 2007). AAC-19 cells expressed wild-type rat  $\alpha 1$ , LX- $\alpha 2$  cells expressed rat  $\alpha 2$  that lacks the Src binding sites, and LY-a2 expressed a mutant rat  $\alpha 2$  that was engineered to contain both Src binding sites (Table 4). Western blotting confirmed expression of these genes (Figure 13A). Detailed characterizations of these cell lines

were previously reported (Lai et al., 2013; J. Xie et al., 2015; Yu et al., 2018), and revealed that the expression of these transgenes further reduced the expression of endogenous pig  $\alpha 1$  to an undetectable level, making it possible to probe the properties of transgenes without interference from the endogenous  $\alpha 1$  NKA (Banerjee et al., 2018; Liang et al., 2006; Liu et al., 2006; J. Xie et al., 2015; Yu et al., 2018) .

Cell Line	Isoform	Y260	NaKtide
AAC-19	Rat $\alpha 1$	255 RGIVVYTGDR <u>T</u> 265	415 SATWFALSRIAGLCNRAV <u>FQ</u> 434
LX- $\alpha 2$	Rat $\alpha 2$	253 RGIV <u>I</u> ATGDRT 263	413 S <u>P</u> TW <u>T</u> ALSRIAGLCNRAV <u>F</u> <b>K</b> 432
LY-a2	Mutant $\alpha 2$	250 RGIVVYTGDR <u>T</u> 260	410 SATWFALSRIAGLCNRAV <u>FQ</u> 429
A420P	Mutant $\alpha 1$	255 RGIVVYTGDR <u>T</u> 265	415 SATW <u>P</u> ALSRIAGLCNRAV <u>FQ</u> 434

**Table 4. Amino acid sequences of the Src binding sites of the WT rat  $\alpha 1$ , WT rat  $\alpha 2$ , and gain-of-function signaling mutant  $\alpha 2$  NKA expressed by the AAC-19, LX- $\alpha 2$ , and LY-a2 cell lines.**

Underlined letters indicate residues that have been changed in mutant  $\alpha 1$  and  $\alpha 2$ , while bold letters indicate residues that differ from wild-type rat  $\alpha 1$ .

In routine culture of these cells, we noted a rapid acidification of LX- $\alpha 2$  cells' culture medium (Figure 13B), which led us to compare glucose metabolism between these cell lines. As depicted in Figure 11A, LX- $\alpha 2$  cells consumed nearly 2-fold more glucose than AAC-19 cells. Interestingly, expression of the gain-of-function Src binding mutant  $\alpha 2$  in LY-a2 cells restored glucose consumption to the level of AAC-19 controls (Figure 11A). This was substantiated by increased lactate production in LX- $\alpha 2$  compared to AAC-19 cells (Figure 11B), confirming that the increase in glucose consumption correlated with an increase in aerobic glycolysis. Again, LY-a2 cells exhibited a metabolic profile similar to that of control AAC-19 cells.

To identify whether  $\alpha 1$  NKA-mediated regulation of Src is responsible for enhanced metabolic flexibility and thus, a decreased reliance on glycolysis, cells were grown in glucose-deprived media and their proliferation was recorded. Both AAC-19 and LY-a2 cells, which express a NKA capable of binding and regulating Src, were able to proliferate under glucose-deprived conditions. In contrast, LX- $\alpha 2$  cells failed to survive altogether (Figure 11C). To

determine the degree to which LX- $\alpha$ 2 cells were reliant upon glycolysis for ATP production, we treated cells with increasing doses of the competitive glycolytic inhibitor 2-deoxy-D-glucose (2-DG) and measured the impact of inhibited glycolysis on cellular ATP levels. At low concentrations of 2-DG, only LX- $\alpha$ 2 exhibited a significant decrease in cellular ATP (Figure 11D). These data reveal that the  $\alpha$ 1 NKA/Src interaction plays a key role in regulating metabolic flexibility, but they do not address the question of metabolic reserve.

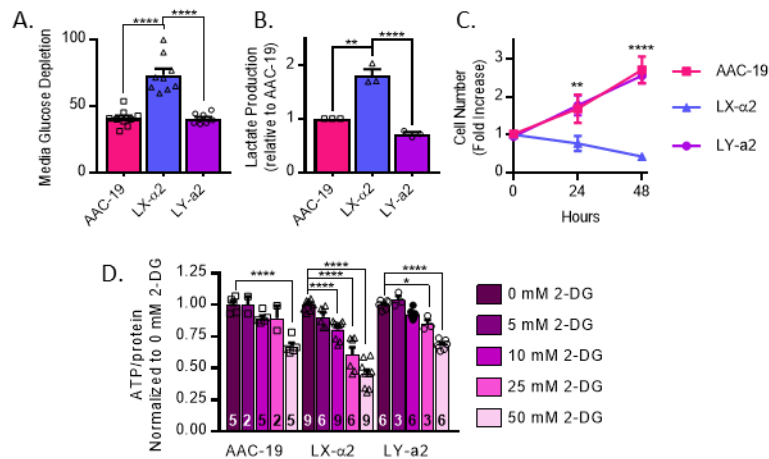


**Figure 11: Importance of NKA  $\alpha$ 1 signaling for cell growth and metabolism.**

**A.** Glucose consumption of AAC-19, LX- $\alpha$ 2, and LY-a2 cells (n=6, \*\* p<0.01). **B.** Lactate measured in the media of AAC-19, LX- $\alpha$ 2, and LY-a2 cells after 72 hours cell growth (n=3, \*\* p<0.01, \*\*\*\* p<0.0001). **C.** Growth of AAC-19 (squares), LX- $\alpha$ 2 (triangles), and LY-a2 (circles) cells in glucose-deprived media (n=6, \*\* p<0.01 vs AAC-19, \*\*\*\* p<0.0001 vs AAC-19). **D.** ATP production in AAC-19, LX- $\alpha$ 2, and LY-a2 cells in the presence of increasing concentrations of the glycolysis inhibitor 2-DG (n listed at the base of each bar, \* p<0.05 vs 0 mM 2-DG, \*\*\*\* p<0.0001 vs 0 mM 2-DG).

For this reason, we subjected these cells to Seahorse metabolic flux analyses (Figure 12).

When LX- $\alpha$ 2 cells were subjected to the mitochondrial stress test, both basal and maximal oxygen consumption rates were decreased (OCR, Figure 12B-C). Most significantly, a 65% reduction in spare capacity (Figure 12D) was noted. On the other hand, LY-a2 cells displayed a metabolic profile identical to that of  $\alpha$ 1-expressing AAC-19 cells. To probe whether the gain of Src binding also affects glycolytic properties, we measured the extracellular acidification rate of

LX- $\alpha$ 2 cells (ECAR, Figure 12E). Although LX- $\alpha$ 2 and AAC-19 cells exhibited similar basal glycolysis levels, their maximum ECAR measured in the presence of oligomycin decreased. This was in sharp contrast to AAC-19 cells in which ECAR increased (Figure 12F-G) and indicates a complete loss of metabolic reserve in LX- $\alpha$ 2 cells (Figure 12H). In all cases, LY-a2 cells exhibited a metabolic profile identical to AAC-19 controls, indicating that the loss of metabolic reserve and flexibility in the LX- $\alpha$ 2 cells was due specifically to the lack of the Src binding and not to other differences between the isoforms.

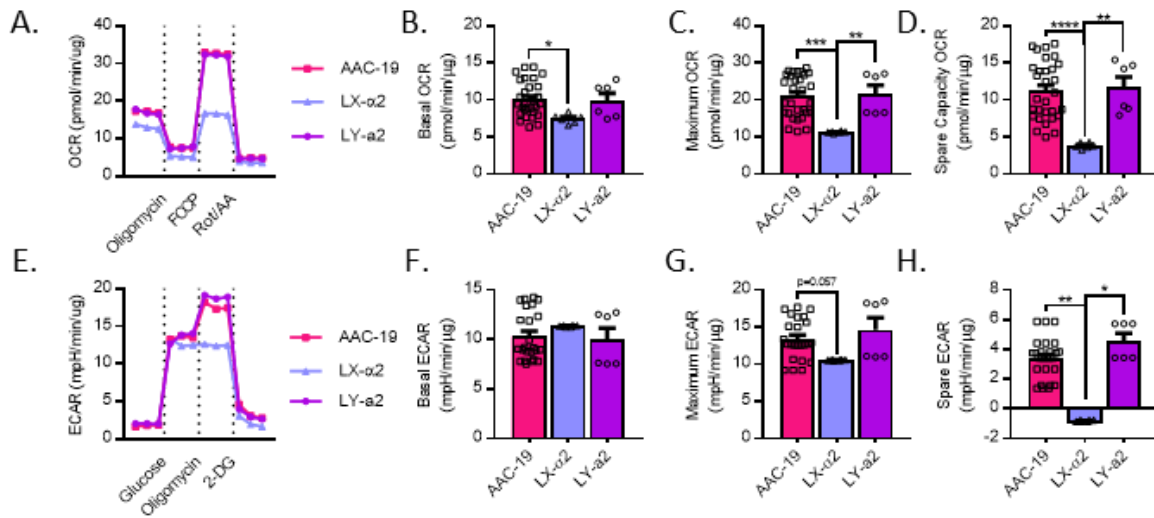


**Figure 12: Seahorse metabolic analysis of AAC-19, LX- $\alpha$ 2, and LY-a2 cells.**

**A.** Representative trace of mitochondrial stress test of AAC-19 (squares), LX- $\alpha$ 2 (triangles), and LY-a2 (circles). **B.** Basal mitochondrial respiration of AAC-19 (n=30), LX- $\alpha$ 2 (n=6), and LY-a2 (n=6). **C.** Maximum mitochondrial respiration of AAC-19 (n=30), LX- $\alpha$ 2 (n=6), and LY-a2 (n=6). **D.** Spare respiratory capacity of AAC-19 (n=30), LX- $\alpha$ 2 (n=6), and LY-a2 (n=6). **E.** Representative trace of glycolytic stress test of AAC-19 (squares), LX- $\alpha$ 2 (triangles), and LY-a2 (circles). **F.** Basal glycolysis rate of AAC-19 (n=30), LX- $\alpha$ 2 (n=6), and LY-a2 (n=6). **G.** Maximum glycolysis rate of AAC-19 (n=30), LX- $\alpha$ 2 (n=6), and LY-a2 (n=6). **H.** Spare glycolytic capacity of AAC-19 (n=30), LX- $\alpha$ 2 (n=6), and LY-a2 (n=6). \* p<0.05, \*\* p<0.01, \*\*\* p<0.005, \*\*\*\* p<0.0001.

To assess the significance of acquiring the NaKtide sequence in birds, we measured both OCR and ECAR parameters in cells expression a mutant  $\alpha$ 1 in which a mutation in the NaKtide sequence (A420P) disrupts the NaKtide/Src interaction (Lai et al., 2013). In view of the fact that

avian and mammalian NKA  $\alpha 1$  contain highly or completely conserved NaKtide sequences (Table 3), the evolutionary significance of this acquisition of Src binding was intriguing. Because birds and mammals evolved separately (Figure 10), the acquisition of this Src binding ability appears to be an example of convergent evolution between birds and mammals (Clarke & Pörtner, 2010; Wu & Wang, 2019). To assess the significance of acquiring the NaKtide sequence in birds, we measured both OCR and ECAR parameters in A420P cells, in which a mutation in the NaKtide sequence (A420P) disrupts the NaKtide/Src interaction (Lai et al., 2013). As depicted in Figure 14, loss of the NaKtide binding site in ATP1A1 significantly reduced metabolic reserve and flexibility. It abolished spare capacity of ECAR and decreased OCR by 60%. However, although both A420P and LX- $\alpha 2$  cells lost reserve metabolic capacity in OCR and ECAR, the loss in A420P cells, especially in ECAR, was less severe than that of LX- $\alpha 2$  cells. Additionally, there was no change in basal OCR and an increase in ECAR in A420P cells, which was in sharp contrast to those of LX- $\alpha 2$  cells (Figure 14). These findings led us to speculate that the acquisition of the Src binding site (NaKtide sequence) in birds facilitates the generation of metabolic reserve and flexibility, which is a major characteristic of endothermy (Clarke & Pörtner, 2010; Nespolo, Solano-Iguaran, & Bozinovic, 2017).

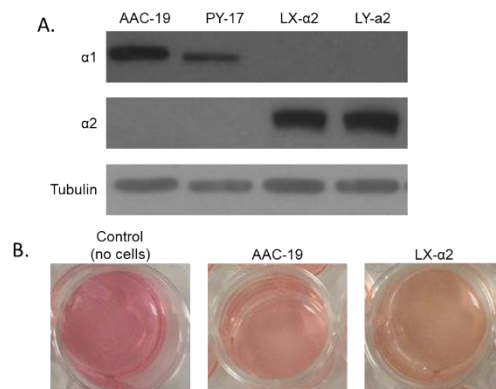


**Figure 13: Characterization of renal epithelial-derived cell lines.**

**A.** Western blot for  $\alpha 1$  and  $\alpha 2$  in AAC-19, LX- $\alpha 2$ , and LY- $\alpha 2$  cells, as well as in the knock-down PY-17 cells. **B.** Representative photos of media with no cells, AAC-19 cells, and LX- $\alpha 2$  after 24 hours of incubation.

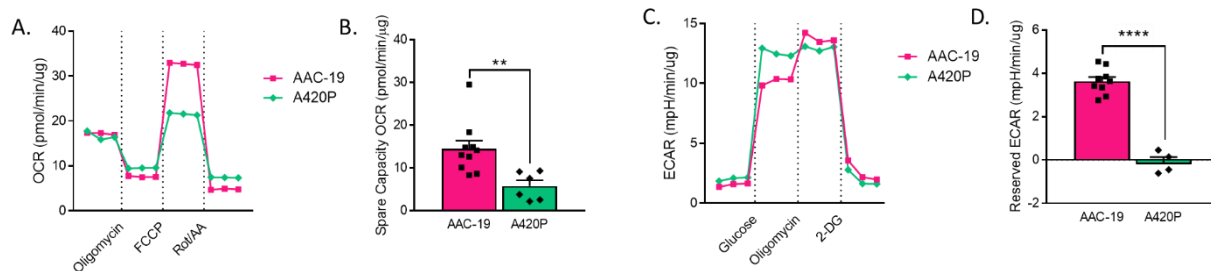


**Figure 14: Seahorse metabolic analysis of cells expressing a loss-of-function Src binding-mutant NKA  $\alpha 1$ .**

**A.** A representative trace of the mitochondrial stress test with AAC-19 (black, squares) and A420P (grey, diamonds) cells. **B.** Spare mitochondrial capacity of AAC-19 (dark grey, squares) and A420P (light grey, diamonds) cells. **C.** Representative trace of the glycolytic stress test with AAC-19 (black, squares) and A420P (grey, diamonds) cells. **D.** Reserved glycolytic capacity of AAC-19 (dark grey, squares) and A420P (light grey, diamonds) cells. (n=6-8, \*\*p<0.01, \*\*\*\*p<0.0001).

### Generation of an *in vivo* mouse model.

To address the relevance of these findings in animal physiology, we used a *MyoDiCre/Lox* system to develop a skeletal muscle-specific  $\alpha 1$  NKA knockout mouse (*sk $\alpha 1$ <sup>-/-</sup>*) as a model to assess the physiological significance of the  $\alpha 1$  NKA/Src interaction in metabolic regulation (Figure 15). Skeletal muscle was chosen as a model because it is a metabolically dynamic tissue in which only 10% of NKA is the  $\alpha 1$  isoform while the remaining 90% of NKA is the non-Src-binding  $\alpha 2$  isoform (He et al., 2001; J. Xie et al., 2015). In addition, prior transgenic studies have documented that while skeletal muscle-specific knockout of  $\alpha 2$  did not affect skeletal muscle size or fiber type composition, the resulting deficits in  $K^+$ -transport abolished their ability to match force generation to contraction stimuli (DiFranco et al., 2015; Manoharan et al., 2015; Radzyukevich et al., 2013). Given these results, the knockout of  $\alpha 1$  was expected to have a minimal effect on the pumping capacity of skeletal muscle. However, if  $\alpha 1$  NKA signaling is a key regulator of metabolic capacity as demonstrated by Figures 1 and 2,

genetic deletion of skeletal muscle  $\alpha 1$  NKA would cause a switch to more glycolytic myofibers, causing decreased exercise endurance.

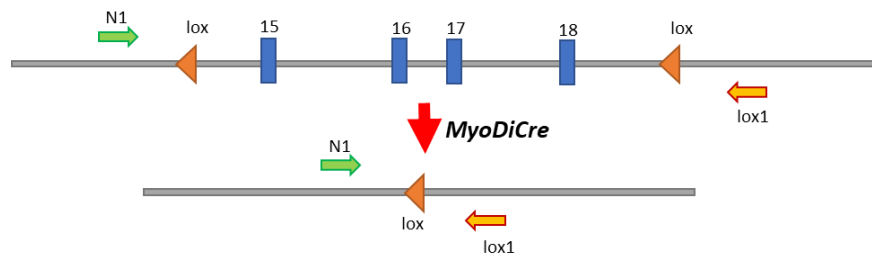


**Figure 15: Cre-Lox construct for the tissue-specific ablation of  $\alpha 1$ .**

The ablation of  $\alpha 1$  NKA in  $sk\alpha 1^{-/-}$  skeletal muscles was confirmed with both Western blot and immunohistochemistry (Figure 16A-B). Expression of the  $\alpha 2$  isoform was not changed in  $sk\alpha 1^{-/-}$  mice compared with  $sk\alpha 1^{+/+}$  controls (Figure 16A) and the total NKA activity of crude membranes as measured by ouabain-sensitive ATPase activity was also unaffected (Figure 16C), indicating that the muscles maintained their  $Na^{+}/K^{+}$  transport capacity.

$Sk\alpha 1^{-/-}$  gastrocnemius muscles were more than 35% smaller than those of  $sk\alpha 1^{+/+}$  control littermates (Figure 16D), revealing a role for  $\alpha 1$  in growth *in vivo* that mirrors that observed *in vitro* (J. Xie et al., 2015). This decrease in muscle mass was further confirmed in the soleus (Figure 17). There was also a clear change in the ratio of oxidative to glycolytic muscle fibers. Further histochemical analysis revealed proportionately more glycolytic type IIB fibers in the  $sk\alpha 1^{-/-}$  white gastrocnemius muscle, with a corresponding decrease in the number of mixed-oxidative type IIA fibers and a complete lack of oxidative type I fibers (Figure 16I). This fiber type switch suggests a transition to a metabolism reliant on glycolysis consistent with the *in vitro* cell culture data (Figures 1 and 2). Additionally, the number of fibers per muscle decreased in  $sk\alpha 1^{-/-}$  muscles (Figure 16E), with a corresponding hypertrophy of Type IIB glycolytic fibers (Figure 16F-G). This underscores the similarities between this animal model and the cell model

and further supports the notion of a shift from oxidative to glycolytic metabolism in skeletal muscle of  $sk\alpha 1^{-/-}$  mice (J. Xie et al., 2015).

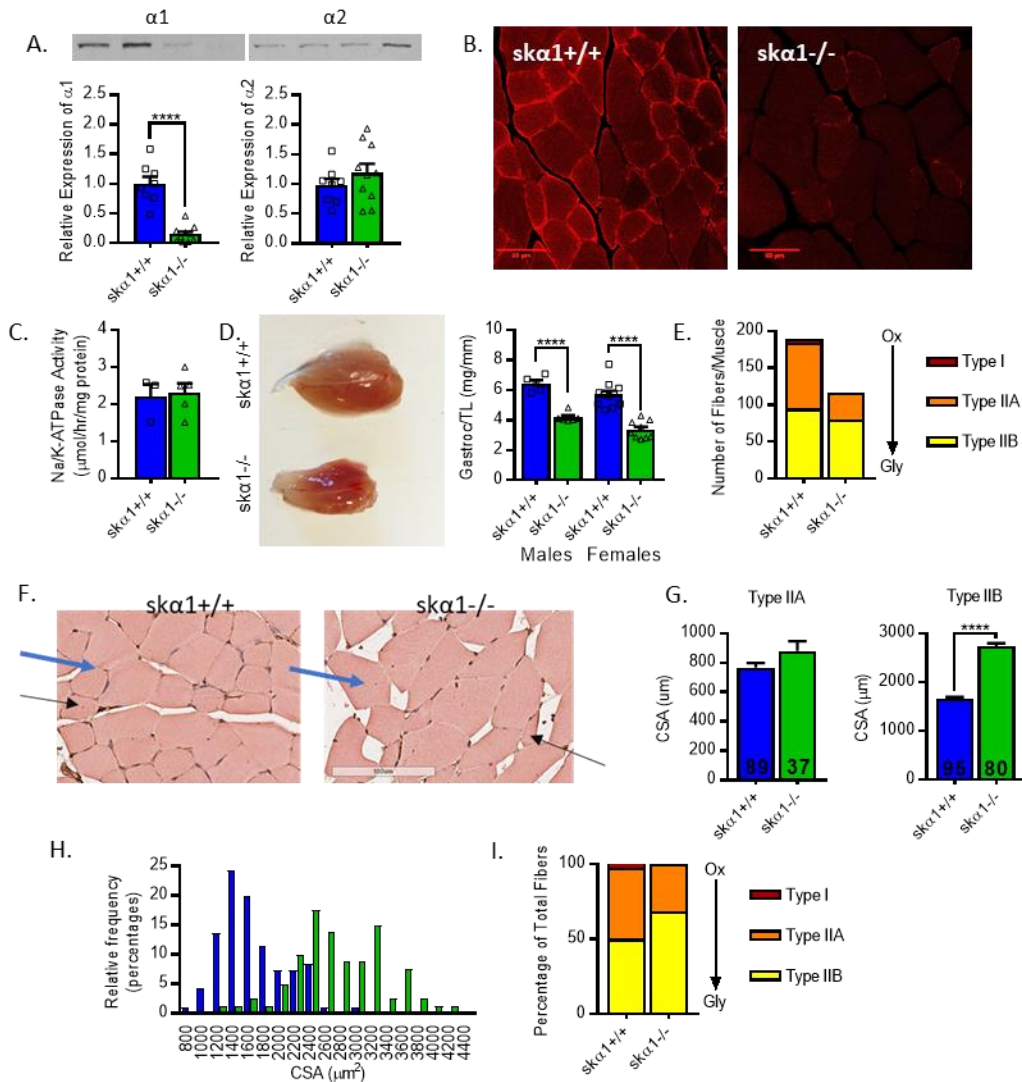


**Figure 16: Development of skeletal muscle-specific NKA  $\alpha 1$  KO mouse model.**

**A.** Western blot for NKA  $\alpha 1$  and  $\alpha 2$  in  $sk\alpha 1^{+/+}$  (n=8) and  $sk\alpha 1^{-/-}$  (n=10) muscles (\*\*\*\*p<0.0001). **B.** Immunohistochemistry of  $\alpha 1$  and  $\alpha 2$  in skeletal muscle. **C.** Ouabain-inhibited ATPase activity in crude membrane fractions from  $sk\alpha 1^{+/+}$  (n=3) and  $sk\alpha 1^{-/-}$  (n=4) muscles. **D.** Gastrocnemius muscle size in  $sk\alpha 1^{+/+}$  and  $sk\alpha 1^{-/-}$  male (n=5 and n=6, respectively) and female (n=11 and n=9, respectively) mice. (\*\*\*\* p<0.0001). **E.** Myofiber number in  $sk\alpha 1^{-/-}$  white gastrocnemius muscles. **F.** Representative micrographs of  $sk\alpha 1^{-/-}$  and  $sk\alpha 1^{+/+}$  white gastrocnemius muscles. Blue arrows indicate type IIB and black arrows indicate type IIA fibers. **G.** Mean cross sectional areas of type IIA and type IIB fibers. **H.** Histogram of fiber CSA. **I.** Proportion of fibers which are type IIA, type IIB, and type I.

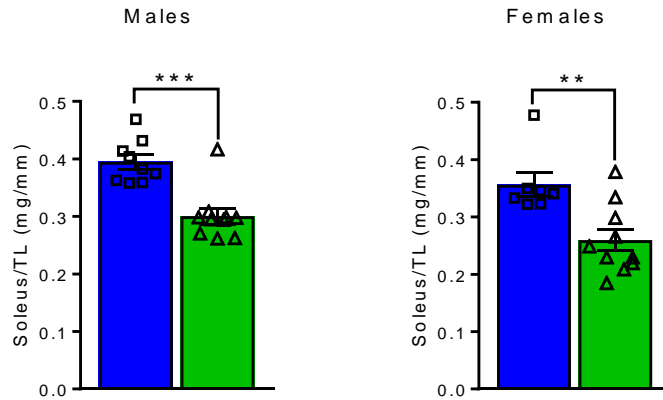


**Figure 17: Soleus mass in 16-week-old  $sk\alpha 1^{+/+}$  (grey, squares) and  $sk\alpha 1^{-/-}$  (white, triangles) mice.**

### **Impact of metabolic deficits in $sk\alpha 1^{-/-}$ muscles on exercise performance.**

Though the fiber type switch suggested a more glycolytic metabolism in  $sk\alpha 1^{-/-}$  muscles, we needed to determine the impact on muscle metabolism and performance. In a treadmill test at speeds up to 25 m/min,  $sk\alpha 1^{-/-}$  ran as well as  $sk\alpha 1^{+/+}$  controls (Figure 18A), which contrasts sharply with the phenotype observed in the  $\alpha 2$  knockout mouse (DiFranco et al., 2015; Manoharan et al., 2015; Radzyukevich et al., 2013). However,  $sk\alpha 1^{-/-}$  mice showed a 50% reduction in endurance as measured by distance to fatigue (Figure 18B), which suggests a lack of oxidative metabolic capacity and an inability to adapt to changing metabolic demands during exercise (Baker et al., 2010; Overmyer et al., 2015). Biochemically, we observed a 50% decrease in muscle glycogen content in  $sk\alpha 1^{-/-}$  gastrocnemius muscles compared to  $sk\alpha 1^{+/+}$  mice, which could contribute to their decreased endurance (Figure 18C). Furthermore, GSK3 $\beta$  expression in the gastrocnemius of  $sk\alpha 1^{-/-}$  mice was significantly increased whereas the level of inhibitory phosphorylated serine 9 (pS9) was not affected (Figure 18D-E). Thus, it is most likely that the decreased amount of glycogen in  $sk\alpha 1^{-/-}$  gastrocnemius is due to the inhibition of glycogen synthesis rather than an accelerated use of glycogen by the muscle.

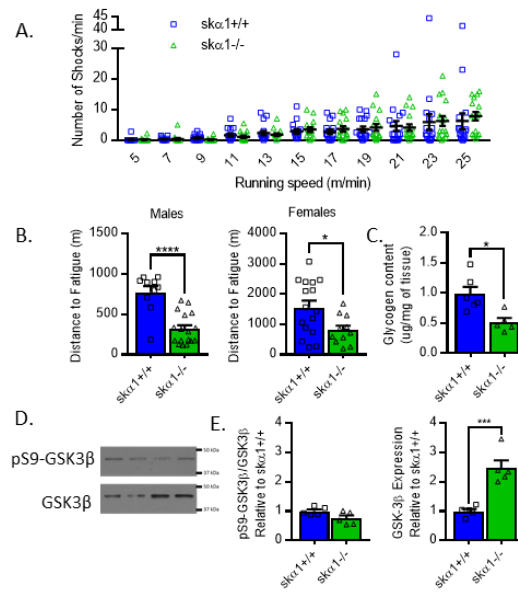


**Figure 18: Exercise capacity of *skα1*<sup>-/-</sup> mice.**

**A.** Number of shocks administered per minute per mouse at each treadmill speed to *skα1*<sup>+/+</sup> (squares, n=17) and *skα1*<sup>-/-</sup> (triangles, n=16) mice. **B.** Maximum distance run by *skα1*<sup>+/+</sup> (grey, squares) and *skα1*<sup>-/-</sup> (white, triangles) male (n=10 and 17, respectively) and female (n=16 and 11, respectively) mice. (\*p<0.05, \*\*\*\*p<0.0001). **C.** Glycogen content of gastrocnemius muscles from male *skα1*<sup>+/+</sup> (grey, squares) and *skα1*<sup>-/-</sup> (white, triangles) mice (n=5-6, \*p<0.05). **D.** Representative Western blot for phosphorylated and total glycogen synthase kinase 3β. **E.** Quantification of Western blots for phosphorylated and total glycogen synthase kinase 3β in *skα1*<sup>+/+</sup> (grey, squares) and *skα1*<sup>-/-</sup> (white, triangles) gastrocnemius muscles (n=5-6, \*\*p<0.01).

### RNA sequencing analyses of metabolic defects and transcriptional regulation of key metabolic genes.

To use an unbiased approach to probe for changes in signaling pathways involved in the regulation of skeletal muscle, we conducted RNA sequencing analyses of *skα1*<sup>-/-</sup> gastrocnemius muscles. As depicted in the heat map in Figure 19A, several groups of genes were altered in gastrocnemius of *skα1*<sup>-/-</sup> mice. We further analyzed the Gene Ontology enrichment of differentially expressed genes and visualized the result in a network map by Cytoscape. (Fig 19B). The analyses revealed changes in signaling pathways related to cell metabolism, ROS production via changes in oxygen and hypoxia sensing, protein assembly, cytoskeleton organization, and cell differentiation and morphogenesis.

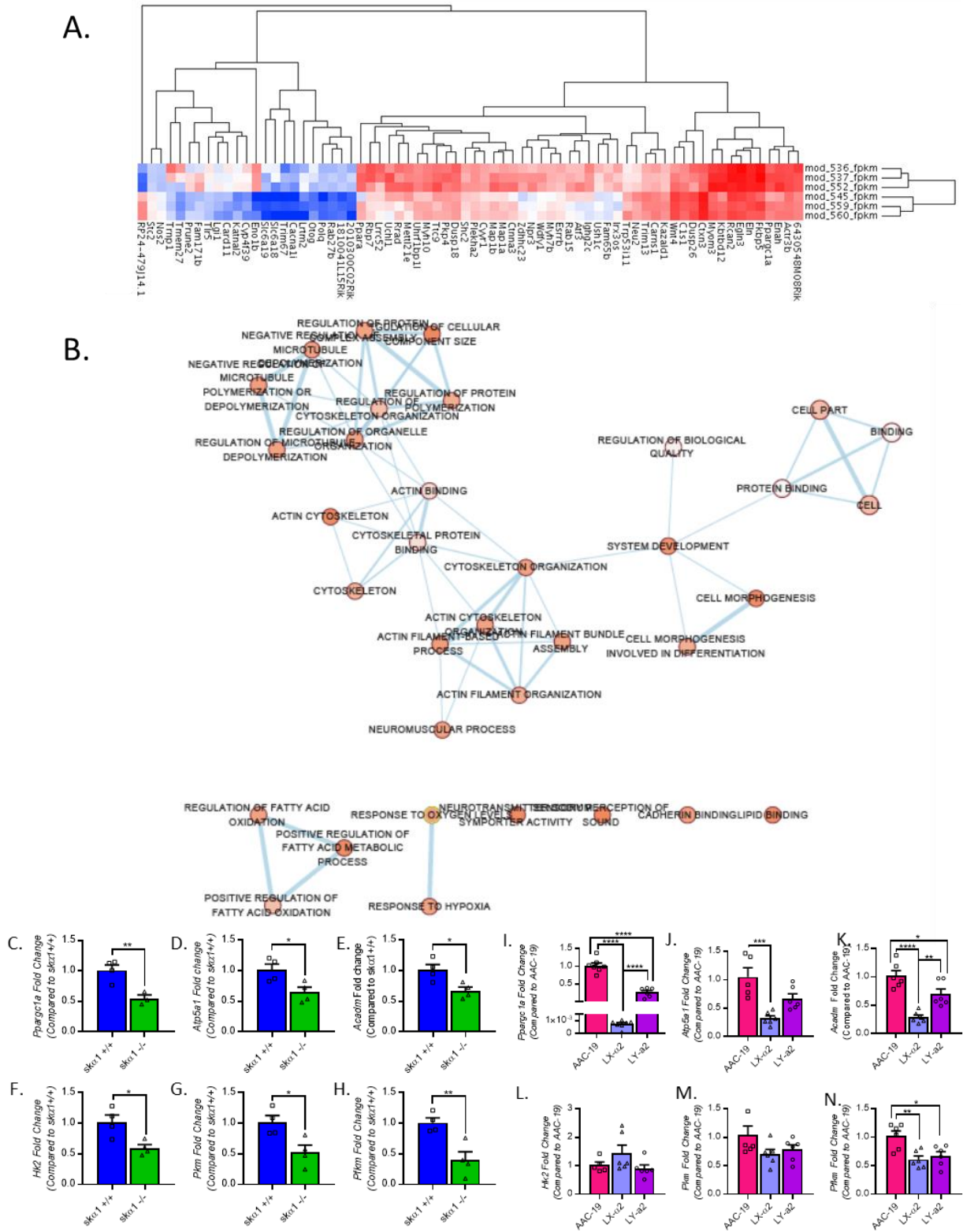


**Figure 19: Analysis of mRNA expression of metabolic genes in renal epithelial cells and skeletal muscles.**

**A (pg 56).** Heatmap of differentially expressed genes identified by RNA sequencing of  $sk\alpha 1^{+/+}$  and  $sk\alpha 1^{-/-}$  gastrocnemius muscles. **B (pg 56).** Map of pathways including differentially expressed genes identified by RNA sequencing of  $sk\alpha 1^{+/+}$  and  $sk\alpha 1^{-/-}$  gastrocnemius muscles. **C-E.** Expression of *Ppargc1a* (**C**), *Atp5a1* (**D**), and *Acadm* (**E**) in  $sk\alpha 1^{+/+}$  (grey, squares, n=4) and  $sk\alpha 1^{-/-}$  (white, triangles, n=4) white gastrocnemius muscles. **F-H.** Expression of *Hk2* (**F**), *Pkm* (**G**), and *Pfkm* (**H**) in  $sk\alpha 1^{+/+}$  (grey, squares, n=4) and  $sk\alpha 1^{-/-}$  (white, triangles, n=4) white gastrocnemius muscles. **I-K.** Expression of *Ppargc1a* (**I**), *Atp5a1* (**J**), and *Mcad* (**K**) in AAC-19 (dark grey, squares, n=6), LY- $\alpha 2$  (white, triangles, n=6), and LY-a2 (light grey, circles, n=6) cells. **L-N.** Expression of *Hk2* (**L**), *Pkm* (**M**), and *Pfkm* (**N**) AAC-19 (dark grey, squares, n=6), LY- $\alpha 2$  (white, triangles, n=6), and LY-a2 (light grey, circles, n=6) cells.

We then explored the transcriptional regulation of metabolic genes in  $sk\alpha 1^{-/-}$  and  $sk\alpha 1^{+/+}$  muscles.  $Sk\alpha 1^{-/-}$  gastrocnemius muscles exhibited decreased expression of the master regulator of mitochondrial biogenesis, *Ppargc1a* (peroxisome proliferator activated receptor  $\gamma$  coactivator 1 $\alpha$ , PGC-1 $\alpha$ ) (Figure 19C). Similarly, expression of *Atp5a1* (ATP synthase F1 subunit  $\alpha$ ) and *Acadm* (medium-chain acyl-CoA dehydrogenase) was decreased in  $sk\alpha 1^{-/-}$  gastrocnemius muscles (Figure 19D-E). Additionally, expression of the key glycolytic enzymes *Hk2* (hexokinase 2), *Pkm* (pyruvate kinase), and *Pfkm* (phosphofructo kinase) was decreased in  $sk\alpha 1^{-/-}$  muscles compared to  $sk\alpha 1^{+/+}$  muscles (Figure 19F-H). These data are further evidence of an overall decrease in metabolic capacity in  $sk\alpha 1^{-/-}$  gastrocnemius muscles.

To further determine whether the metabolic defects observed in our *in vitro* studies and those suggested by the phenotype of  $sk\alpha 1^{-/-}$  mice could have similar transcriptional mechanisms, we analyzed the mRNA expression of the same metabolic genes in AAC-19, LX- $\alpha 2$ , and LY-a2 cells. Similar to our observations in  $sk\alpha 1^{-/-}$  muscles, expression of the mitochondrial metabolism-related genes *Ppargc1a*, *Atp5a1*, and *Acadm* were down-regulated in LX- $\alpha 2$  cells compared to AAC-19 cells, and these defects were partially restored in LY-a2 cells (Figure 19I-K). In contrast, although expression of *Pfkm* was decreased in LX- $\alpha 2$  cells, we observed no change in *Hk2* or *Pkm* expression in LX- $\alpha 2$  cells (Figure 19L-N). In contrast to the mitochondrial genes, LY-a2 expression did not rescue expression of *Pfkm* (Figure 19N). The

similarities in expression of key oxidative metabolic genes between the renal epithelial cells and *skα1*<sup>-/-</sup> muscles suggest a similar molecular mechanism underlying the regulation of mitochondrial metabolism in both models. In contrast, the differences in the expression pattern of the glycolytic genes in *skα1*<sup>-/-</sup> muscle and LX- $\alpha$ 2 cells suggest distinct regulation of glycolysis in these systems.

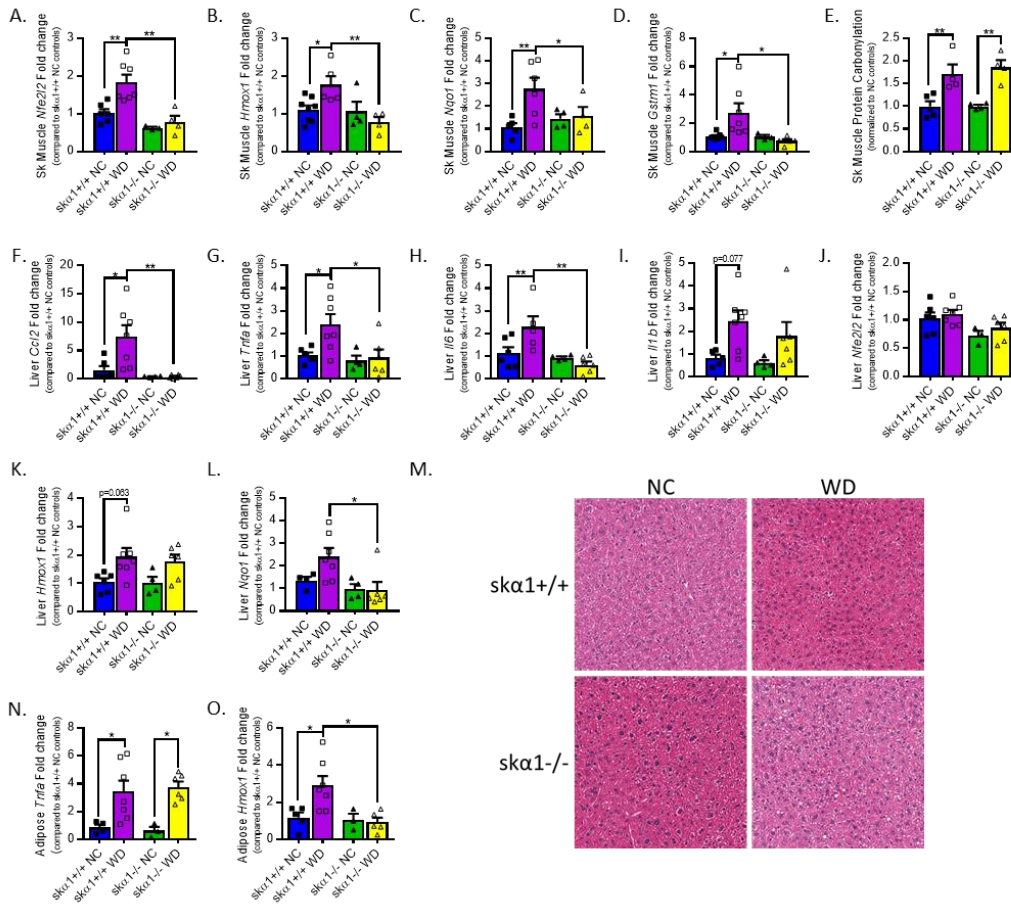


**Figure 20: Oxidative stress and antioxidant response in *skα1*<sup>-/-</sup> mice on Western diet.**

**A-D.** Expression of Nrf2-related genes in gastrocnemius muscles from *skα1*<sup>+/+</sup> (grey, squares) and *skα1*<sup>-/-</sup> (white, triangles) mice on normal chow (NC, filled symbols) and Western diet (WD, open symbols): Nuclear factor erythroid 2-related factor 2 (*Nfe2l2*, **A**), heme oxygenase 1 (*Hmox1*, **B**), NAD(P)H quinone dehydrogenase 1 (*Nqo1*, **C**), and glutathione S-transferase mu 1 (*Gstm1*, **D**) (n=4-6, \*p<0.05, \*\*p<0.01, \*\*\*p<0.005). **E.** Change in protein carbonylation in gastrocnemius muscles from *skα1*<sup>+/+</sup> (grey, squares) and *skα1*<sup>-/-</sup> (white, triangles) mice on normal chow (NC, filled symbols) and Western diet (WD, open symbols) relative to NC controls (n=4-5, \*p<0.05, \*\*\*p<0.005). **F-I.** Expression of cytokines in the livers of *skα1*<sup>+/+</sup> (grey, squares) and *skα1*<sup>-/-</sup> (white, triangles) mice on normal chow (NC, filled symbols) and Western

diet (WD, open symbols): monocyte chemoattractant protein 1 (*Ccl2*, **F**), tumor necrosis factor  $\alpha$  (*Tnfa*, **G**), interleukin 6 (*Il6*, **H**), and interleukin 1b (*Il1b*, **I**). **J-L**. Expression of Nrf2-related genes in livers of *sk $\alpha$ 1<sup>+/+</sup>* and *sk $\alpha$ 1<sup>-/-</sup>* mice on NC (grey) and WD (white): Nuclear factor erythroid 2-related factor 2 (*Nfe2l2*, **J**), heme oxygenase 1 (*Hmox1*, **K**), and NAD(P)H quinone dehydrogenase 1 (*Nqo1*, **L**). **M**. Representative images of haematoxylin and eosin stained livers from *sk $\alpha$ 1<sup>+/+</sup>* and *sk $\alpha$ 1<sup>-/-</sup>* mice fed NC or WD showing no clear evidence of steatosis. **N**. Expression of the cytokine tumor necrosis factor  $\alpha$  (*Tnfa*) in visceral epididymal adipose from *sk $\alpha$ 1<sup>+/+</sup>* (grey, squares) and *sk $\alpha$ 1<sup>-/-</sup>* (white, triangles) mice on normal chow (NC, filled symbols) and Western diet (WD, open symbols). **O**. Expression of the Nrf2-related heme-oxygenase 1 (*Hmox1*) in visceral epididymal adipose from *sk $\alpha$ 1<sup>+/+</sup>* (grey, squares) and *sk $\alpha$ 1<sup>-/-</sup>* (white, triangles) mice on normal chow (NC, filled symbols) and Western diet (WD, open symbols).

### **Skeletal muscle $\alpha$ 1 and susceptibility to diet-induced metabolic dysfunction.**

The above findings suggest that the acquisition of Src binding sites in ATP1A1 facilitates increased metabolic capacity in endotherms, which is consistent with the aerobic scope hypothesis of endotherm evolution (Clarke & Pörtner, 2010; Nespolo et al., 2017). On the other hand, this gain of metabolic reserve and flexibility may become a liability when mammals are fed a high-fat, high-fructose Western diet (WD), which increases pathological ROS stress, promotes tissue inflammation, and causes metabolic syndrome. Since skeletal muscle plays an important role in both glucose homeostasis and metabolic flux (Honka et al., 2018; Zurlo et al., 1990), this prompted us to test whether expression of ATP1A1 links the benefits of enhanced muscle metabolic capacity and endurance to increased susceptibility to diet-induced metabolic dysfunction, specifically the development of glucose intolerance and insulin resistance. Therefore, we subjected *sk $\alpha$ 1<sup>-/-</sup>* mice to WD to observe how they adapted to the metabolic stress of chronic overnutrition (Sodhi et al., 2015). Baseline body mass and body composition were similar between *sk $\alpha$ 1<sup>-/-</sup>* and *sk $\alpha$ 1<sup>+/+</sup>* mice assigned to normal chow (NC) or Western diet (WD) (data not shown). Due to their FVB-dominant mixed-strain background, even wild-type controls gained less weight than C57Bl6 mice on the same diet, a result of the well-documented FVB resistance to obesity (Nascimento-Sales et al., 2017). However, tissues collected after 12 weeks of WD revealed a significant increase in epididymal and subcutaneous adipose tissues in control

*skα1*<sup>+/+</sup> mice (Figure 21A-B). In contrast, although WD produced a modest increase in both fat tissues in *skα1*<sup>-/-</sup> mice, the apparent increase did not reach statistical significance (Figure 21A-B, *p*=0.4).

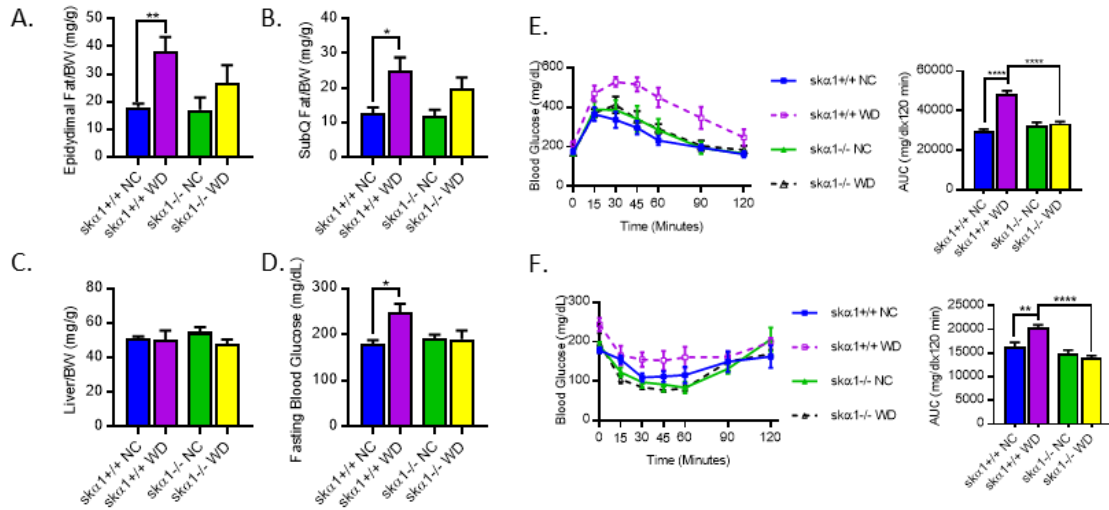


**Figure 21: Impact of skeletal muscle-specific ablation of NKA  $\alpha 1$  on reaction to Western diet.**

**A.** Epididymal fat pad mass to body weight (BW) ratio in *skα1*<sup>+/+</sup> (grey) and *skα1*<sup>-/-</sup> (white) mice after 12 weeks on a Western diet (WD) or normal chow (NC) (*skα1*<sup>+/+</sup> NC n=8, *skα1* WD n=14, *skα1*<sup>-/-</sup> NC n=4, *skα1*<sup>-/-</sup> WD n=12). **B.** Subcutaneous fat pad (SubQ)/BW ratio in *skα1*<sup>+/+</sup> (grey) and *skα1*<sup>-/-</sup> (white) mice after 12 weeks on WD or NC (*skα1*<sup>+/+</sup> NC n=8, *skα1* WD n=14, *skα1*<sup>-/-</sup> NC n=4, *skα1*<sup>-/-</sup> WD n=12). **C.** Liver mass to BW ratio in *skα1*<sup>+/+</sup> (grey) and *skα1*<sup>-/-</sup> (white) mice after 12 weeks on a WD or NC (*skα1*<sup>+/+</sup> NC n=8, *skα1* WD n=14, *skα1*<sup>-/-</sup> NC n=4, *skα1*<sup>-/-</sup> WD n=12). **D.** Fasting blood glucose in *skα1*<sup>+/+</sup> (grey) and *skα1*<sup>-/-</sup> (white) mice after 12 weeks on WD or NC (*skα1*<sup>+/+</sup> NC n=4, *skα1* WD n=5, *skα1*<sup>-/-</sup> NC n=4, *skα1*<sup>-/-</sup> WD n=4). **E.** Glucose tolerance test and area under the curve of *skα1*<sup>-/-</sup> and *skα1*<sup>+/+</sup> mice after 6 weeks on Western diet (*skα1*<sup>+/+</sup> NC n=7, *skα1* WD n=6, *skα1*<sup>-/-</sup> NC n=4, *skα1*<sup>-/-</sup> WD n=4). **F.** Insulin tolerance test of *skα1*<sup>-/-</sup> and *skα1*<sup>+/+</sup> mice after 12 weeks on Western diet (*skα1*<sup>+/+</sup> NC n=4, *skα1* WD n=5, *skα1*<sup>-/-</sup> NC n=4, *skα1*<sup>-/-</sup> WD n=4). (\* *p*<0.05, \*\* *p*<0.01, \*\*\* *p*<0.0001)

Since activation of the  $\alpha 1$  NKA/Src is associated with increased ROS production and ROS stress is central to the development of diet-induced metabolic dysfunction, we measured the activation of the nuclear factor erythroid 2-related factor 2 (Nrf2) pathway, which increases the expression of antioxidant enzymes on a WD (Devarshi, McNabney, & Henagan, 2017). As depicted in Figure 20, WD not only increased Nrf2 expression (*Nfe2l2*, Figure 20A) but also

increased the mRNA expression of the Nrf2 targets heme oxygenase 1 (*Hmox1*) and NAD(P)H quinone dehydrogenase 1 (*Nqo1*) (Figure 20B-C), indicating that WD-induced ROS stress elicited a robust antioxidant response in  $sk\alpha1^{+/+}$  muscles. This conclusion was further strengthened by the induction of glutathione S-transferase mu 1 (*Gstm1*) (Figure 20D). In contrast, no changes in the expression of these genes were observed in the gastrocnemius of  $sk\alpha1^{-/-}$  mice, suggesting that the ablation of  $\alpha1$  attenuates ROS stress, consistent with what has been reported (Yan et al., 2013). To further assess ROS signaling, we also measured protein carbonylation, an indicator of an increase in  $H_2O_2$ . As depicted in Figure 20E, a comparable increase in protein carbonylation was noted in both  $sk\alpha1^{-/-}$  and  $sk\alpha1^{+/+}$  mouse gastrocnemius.

In addition to skeletal muscle, liver plays a critically important role in the progression of metabolic syndrome, with WD-induced inflammation and oxidative stress leading to non-alcoholic steatohepatitis (NASH) and compensatory activation of the Nrf2 pathway and antioxidant responses (D. Xu et al., 2018). Therefore, we examined expression of Nrf2-targeted genes, cytokine expression, and liver morphology for evidence of oxidative stress, inflammation, and ultimately NASH. We found that the expression of the inflammatory cytokines monocyte chemoattractant protein 1 (*Ccl2*), tumor necrosis factor  $\alpha$  (*Tnfa*), and interleukin 6 (*Il6*) was highly induced in the livers of control  $sk\alpha1^{+/+}$  mice (Figure 20F-H). In sharp contrast, these changes in the liver were blunted in  $sk\alpha1^{-/-}$  mice. As depicted in Figure 20J, there was no increase in *Nfe2l2* expression, and induction of *Hmox1* expression did not reach statistical significance (Figure 20K). However, expression of *Nqo1* increased in  $sk\alpha1^{+/+}$  WD livers but not in  $sk\alpha1^{-/-}$  WD livers (Figure 20L), suggesting that  $sk\alpha1^{+/+}$  WD mice had begun the process of developing NASH but had not developed the severity seen in C57J/BL6 mice on the same diet (Sodhi et al., 2017). In accordance, there was no evidence of morphological changes in the liver

histology (Figure 20M), which is consistent with the unaltered liver weight/body weight ratio in both  $sk\alpha 1^{-/-}$  and  $sk\alpha 1^{+/+}$  mice on WD (Figure 21C).

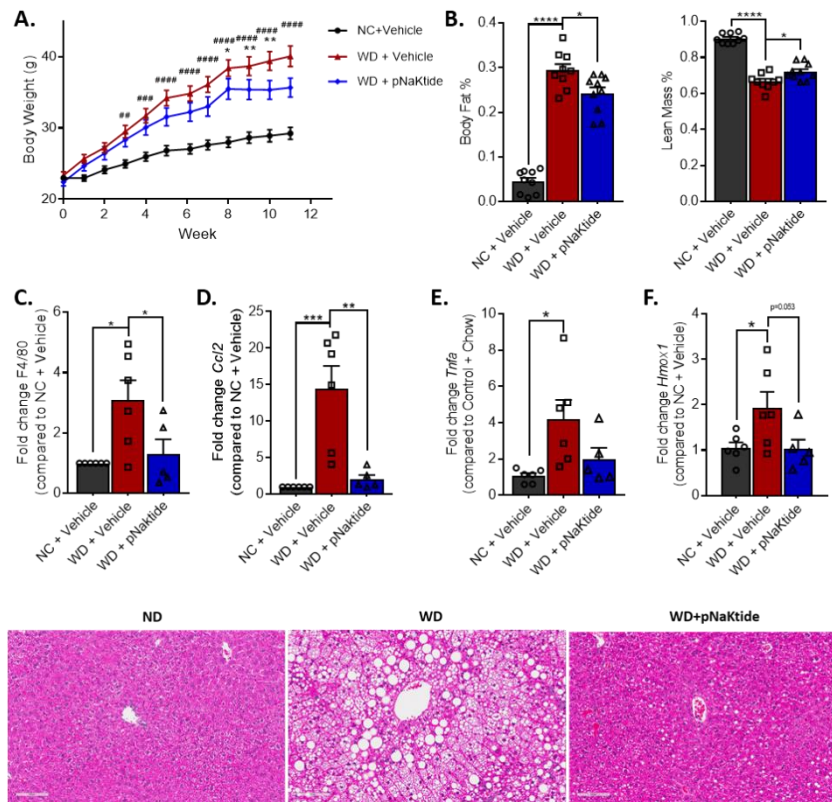


**Figure 22: Pharmacological targeting of  $\alpha 1$  NKA signaling through Src in diet-induced metabolic dysfunction.**

**A.** Weight gain in C57J/BL6 over 12 weeks of WD or NC with pNaKtide injection or vehicle injection. (n=10,  $\#\#$   $p < 0.01$ ,  $\#\#\#$   $p < 0.005$ ,  $\#\#\#\#$   $p < 0.0005$  NC+Vehicle vs WD+Vehicle; \*  $p < 0.05$ ,  $\#\#$   $p < 0.005$  WD+Vehicle vs WD+pNaKtide) **B.** Effects of pNaKtide on body composition after 12 weeks WD. **C-F.** Hepatic expression of F4/80 (**C.**), Ccl2 (**D.**), Tnfa (**E.**), and Hmox1 (**F.**) after 12 weeks diet treatment. **G.** Representative micrographs of liver sections stained with H&E to show lipid accumulation. (n=6, \*  $p < 0.05$ ,  $\#\#$   $p < 0.01$ ,  $\#\#\#$   $p < 0.005$ ,  $\#\#\#\#$   $p < 0.0005$ )

To complement the above studies, we repeated the above qPCR measurements of inflammatory cytokines and Nrf2-targeted genes in the epididymal fat pad, another important tissue in the development of glucose intolerance and insulin resistance. Interestingly, the expression of *Tnfa* was comparably induced in both  $sk\alpha 1^{+/+}$  and  $sk\alpha 1^{-/-}$  epididymal fat (Figure 20N), although expression of other cytokines was unchanged (data not shown). When the Nrf2 pathway was evaluated, WD increased expression of *Hmox1* three-fold in the epididymal fat of

sk $\alpha$ 1<sup>+/+</sup> but not sk $\alpha$ 1<sup>-/-</sup> mice (Figure 20O). However, unlike in skeletal muscle, WD did not alter the expression of other Nrf2-targeted genes (data not shown).

To further probe the impact of sk $\alpha$ 1<sup>-/-</sup> on the development of metabolic syndrome, we measured fasting blood glucose and conducted glucose tolerance tests (GTT) and insulin tolerance tests (ITT). As depicted in Figure 21D, after 12 weeks of WD, fasting glucose was significantly elevated only in WD-fed sk $\alpha$ 1<sup>+/+</sup> mice. A GTT administered after 6 weeks of WD showed increased glucose intolerance as measured by the area under the curve (AUC) only in sk $\alpha$ 1<sup>+/+</sup> mice, while WD-fed sk $\alpha$ 1<sup>-/-</sup> mice maintained normal glucose clearance (Figure 21E). An ITT administered after 12 weeks revealed impaired insulin sensitivity in sk $\alpha$ 1<sup>+/+</sup> mice but not in sk $\alpha$ 1<sup>-/-</sup> mice fed with WD as measured by AUC (Figure 21F). In both cases, glucose clearance was not different between sk $\alpha$ 1<sup>+/+</sup> and sk $\alpha$ 1<sup>-/-</sup> mice fed with normal chow but was significantly decreased in sk $\alpha$ 1<sup>+/+</sup> mice compared to sk $\alpha$ 1<sup>-/-</sup> mice fed with WD (Figures 7E-F).

**Pharmacological interruption of  $\alpha$ 1 NKA/Src binding attenuates the progression of non-alcoholic steatohepatitis.**

The above metabolic protection afforded by the genetic deletion of ATP1A1 in skeletal muscle provides compelling evidence for a role of  $\alpha$ 1 NKA-mediated Src signaling in developing diet-induced hepatic inflammation and oxidative stress, which ultimately leads to the development of NASH. To further test this hypothesis, and to evaluate whether pNaKtide, a peptide derived from  $\alpha$ 1 NKA that blocks the formation of the  $\alpha$ 1 NKA/Src complex, could be developed as a drug candidate for NASH, we treated WD-fed C57J/B16 mice with 5 mg/kg pNaKtide every other day. This treatment resulted in a significant decrease in weight gain and moderately improved body composition (Figure 22A-B). Like sk $\alpha$ 1<sup>-/-</sup>, pNaKtide treatment attenuated liver inflammation, normalizing the expression of *Ccl2*, *Tnfa*, and the macrophage

marker F4/80 (Figure 22C-E). Furthermore, pNaKtide abolished the induction of the Nrf-2 target gene *Hmox1* was decreased (Figure 22F). Finally, pNaKtide protected livers from WD-induced hepatic steatosis (Figure 22G). Because the no-observable-effect level of pNaKtide in mice is 25 mg/kg/day, we conclude from these findings that pNaKtide, by disrupting the formation of  $\alpha 1$  NKA/Src complex, is not only effective in blocking WD-induced ROS stress, inflammation, and preventing the progression of NASH, but is also well-tolerated.

## Discussion

In this study, we have made three important observations. First, we report for the first time that the evolutionary acquisition of Src binding in  $\alpha 1$  NKA facilitates increased metabolic capacity. This represents a hitherto unidentified regulatory mechanism, most likely an important evolutionary event impacting endotherm physiology. It also illustrates how the NKA gained additional fundamental functions during the evolutionary process and provides molecular insights into NKA isoform heterogeneity. Second, we were able to demonstrate the metabolic importance of the  $\alpha 1$  isoform in an *in vivo* model. The ablation of  $\alpha 1$  NKA caused a switch from oxidative to glycolytic muscle and a significant hypertrophy of glycolytic Type IIB fibers in gastrocnemius muscles (Figure 16). Consequently, it significantly reduced endurance. Paradoxically, it also afforded protection against diet-induced glucose intolerance and insulin resistance by reducing ROS stress and inflammation in three vital metabolic tissues. Therefore, it is reasonable to propose that mammals' enhanced metabolic reserve and flexibility and their susceptibility to WD-induced metabolic stress are triggered by a common mechanism –  $\alpha 1$  NKA-mediated Src regulation. Finally, these new findings, taken together with previous reports on the *in vivo* efficacy of pNaKtide in metabolic syndrome, validate the  $\alpha 1$  NKA/Src interaction as a novel therapeutic target for metabolic syndrome.

## **The evolutionary nature of NKA signaling and its significance in animal physiology.**

In addition to the Src binding sites, we have also identified a caveolin binding motif in the  $\alpha$  subunit of NKA, which is conserved in all NKA  $\alpha$  subunits within the animal kingdom (unpublished data). Recent studies demonstrate that loss of the caveolin binding motif causes the arrest of stem cell differentiation and organogenesis in mammals and *C. elegans* (unpublished data). Thus, NKA evolved with multiple functionalities. Though all animal  $\alpha$  isoforms contain the caveolin motif, Src binding is confined to endotherms, with birds possessing only the NaKtide sequence and mammals possessing both NaKtide and Y260 sequences (Table 3). Although the current work focused on the Src signaling role of ATP1A1, the possibility that other NKA isoforms have acquired other binding motifs that confer additional tissue and cell-specific functions that are independent of ion pumping should be considered.

It is important to recognize the unique nature of ATP1A1 signaling through Src for regulating metabolic capacity in mammalian cells. Specifically, our gain-of-Src-binding and loss-of-Src-binding studies indicate that the acquisition of Src binding by  $\alpha 1$  NKA is essential for generating metabolic reserve (Figure 12). This contrasts with other recognized pathways such as PPAR $\gamma$  (Rodriguez-Cuenca et al., 2012), PGC-1 $\alpha$  (Andrzejewski et al., 2017), AMPK (Schonke, Massart, & Zierath, 2018), and pyruvate dehydrogenases (S. Zhang, Hulver, McMillan, Cline, & Gilbert, 2014), which play important but nonessential roles in the generation of metabolic reserve. Similarly, NKA/Src interaction increased metabolic flexibility (Figures 1 and 2). Together, these metabolic changes represent a significant increase in metabolic capacity, allowing locomotive endurance, which the aerobic scope hypothesis posits was a selective driver for the evolution of endothermy from ectothermy (Clarke & Pörtner, 2010; Nespolo et al., 2017).

Further, we demonstrated that the skeletal muscle-specific knockout of  $\alpha 1$  produced a phenotype unique from the skeletal muscle-specific knockout of  $\alpha 2$  ( $sk\alpha 2^{-/-}$ ), which is the primary isoform necessary for the maintenance of skeletal muscle contraction, especially at high stimuli frequencies (DiFranco et al., 2015; Manoharan et al., 2015; Radzyukevich et al., 2013). This difference between  $sk\alpha 1^{-/-}$  and  $sk\alpha 2^{-/-}$  phenotypes supports the hypothesis that the  $\alpha 1$  isoform, and most likely its Src binding function, is responsible for the regulation of metabolic capacity. This was represented by the switch to more glycolytic muscle fibers (Figure 16I) and the decreased endurance (Figure 18A) in  $sk\alpha 1^{-/-}$  mice. Thus, we speculate that the evolution of Src binding in birds and mammals may have increased metabolic reserve and flexibility, which the aerobic scope hypothesis posits were necessary for the evolution of endothermy (Nespolo et al., 2017).

Notably, both Src binding sites appear to be important for regulating metabolic capacity. In addition to the cell lines used in this study (LX- $\alpha 2$ , LY-a2, AAC-19, and A420P), we also created a cell line expressing a Y260A mutant rat  $\alpha 1$ . The impact of the Y260A mutation on metabolic reserve and flexibility appears to be the mildest (Banerjee et al., 2018), followed by the A420P mutation and, finally, the complete loss of Src binding sites in the LX- $\alpha 2$  cell line.

### **NKA/Src interaction as a molecular target for developing therapeutics for metabolic syndrome.**

The first evidence linking  $\alpha 1$  NKA to ROS production came from our early studies of cardiotonic steroids in cultures of cardiac myocytes (Z. Xie et al., 1999). Subsequently, we documented that stimulation of the  $\alpha 1$  NKA/Src receptor complex by cardiotonic steroids increased ROS production in multiple cell types via both mitochondria and NADPH oxidase activation (Banerjee et al., 2018; Liu et al., 2006; Sodhi et al., 2015; Sodhi et al., 2018; Sodhi et

al., 2017; Z. Xie et al., 1999; Yan et al., 2013). These ROS then stimulate the  $\alpha 1$  NKA/Src complex, forming an amplification loop for the pathological production of ROS (Yan et al., 2013). Targeting the  $\alpha 1$  NKA/Src interaction with pNaKtide, a peptide inhibitor of the signaling complex (Z. Li et al., 2009), terminates this amplification loop, thereby preventing the generation of pathological ROS stress (Z. Li et al., 2009). These *in vitro* studies were further supported by recent *in vivo* animal studies (H. Li et al., 2018; Sodhi et al., 2015; Sodhi et al., 2017). Administration of pNaKtide restored insulin sensitivity and glucose tolerance in animals subjected to WD (Sodhi et al., 2015; Sodhi et al., 2017; Srikanthan et al., 2016). However, it is important to note that pNaKtide was used at 25 mg/kg/week in these *in vivo* studies. Because the no-observable-effect level of pNaKtide in mice is 25 mg/kg/day, these studies failed to address the safety and drug development potential of pNaKtide.

The  $sk\alpha 1^{-/-}$  phenotype provides strong genetic evidence for a role of  $\alpha 1$  NKA/Src interaction in the development of diet-induced insulin resistance, glucose intolerance, and liver inflammation (Figures 6-7). These findings, taken together with the pharmacological studies of pNaKtide, validate the  $\alpha 1$  NKA/Src interaction as a molecular target for the development of new therapeutics for metabolic syndrome. Moreover, the new pharmacological studies of pNaKtide at a much lower dose (5 mg/kg vs 25 mg/kg) provided compelling evidence of the potency and efficacy of pNaKtide in blocking liver ROS stress, inflammation, and the progression of NASH without the concern of significant side effects. Interestingly, our new findings indicate that the loss of  $\alpha 1$ -mediated Src signaling in skeletal muscle is sufficient to confer systemic protection from diet-induced glucose intolerance and insulin resistance and reduce oxidative stress and inflammation in target organs. These protective effects appear to be organ-specific, with most of the protection afforded to the liver. In view of the demonstrated role of cross-talk between

skeletal muscle, liver, and adipose, it is reasonable to suggest that skeletal muscle-specific delivery of pNaKtide might be sufficient to produce therapeutic benefits in metabolic syndrome. This will further reduce the potential of pNaKtide-induced systemic effects.

In addition to ROS stress and inflammation, the potential contribution of elevated GSK-3 $\beta$  expression in  $sk\alpha 1^{-/-}$  mouse skeletal muscles should be considered. High GSK-3 $\beta$  expression is not only consistent with the detected decrease in muscle glycogen content (Figure 18C), but could provide one of many links between the metabolic defects and decreased growth in  $sk\alpha 1^{-/-}$  muscles (Figure 16) (van der Velden et al., 2007). In addition to protecting  $sk\alpha 1^{-/-}$  mice from WD-induced insulin resistance (Figure 21), the absence of  $\alpha 1$  NKA caused a significant decrease in muscle mass (Figure 16D), a switch to glycolytic muscle fibers, and a 50% decrease in running endurance (Figure 18B), all of which could be a result of decreased metabolic capacity (Baker et al., 2010; Overmyer et al., 2015). Therefore, we propose that the evolutionary acquisition of Src binding sites in ATP1A1 came with a tradeoff: the increased metabolic reserve and flexibility enhanced mitochondrial metabolism and increased exercise endurance came at the cost of increased susceptibility to diet-induced glucose intolerance and insulin insensitivity. Interestingly, this idea that both improved mitochondrial efficiency and severely reduced mitochondrial capacity can preserve glucose homeostasis in the face of a WD has been proposed before (Finck et al., 2005; Koves et al., 2008), with Koves et al. postulating that incomplete  $\beta$ -oxidation of lipids rather than the lipids themselves leads to lipotoxicity-induced insulin resistance, a possibility that still needs to be explored in our models. Together, these new findings reveal  $\alpha 1$  NKA signaling through Src as a novel regulator for generating metabolic reserve and flexibility in mammals as well as a validated drug target. Furthermore, this offers a novel explanation for exercise-induced increases in  $\alpha 1$  NKA expression (Murphy, Petersen, et

al., 2006; H. Xu et al., 2018). This hypothesis is further supported by the reports that individuals with natural running ability have high basal levels of  $\alpha 1$  in skeletal and cardiac muscle (Chen et al., 2001; Mohr, Thomassen, Girard, Racinais, & Nybo, 2016).

### **Limitations.**

We recognize that there are a number of important unanswered questions. Decreased  $\alpha 1$  expression has been shown to decrease muscle size in a different mouse model (Kutz et al., 2018), but the growth pathways have yet to be identified. It is also important to note that in addition to skeletal muscle, other cells such as cardiomyocytes, adipocytes, and glial cells also express both  $\alpha 2$  and  $\alpha 1$  NKA. Thus, it remains to be investigated whether ablation of  $\alpha 1$  also causes a metabolic switch and reduced functionality in these cells. Moreover, although our *in vitro* studies of metabolic profile of A420P mutant  $\alpha 1$  support the contention that the acquisition of NaKtide sequence by birds would most likely impact their metabolic reserve and flexibility, this postulation remains to be experimentally tested. Finally, because the  $sk\alpha 1^{-/-}$  mice were generated on a dominant FVB mixed-strain background, which caused them to accumulate less fat mass than C57BL6 mice fed a WD (Figure 22), we recognize that the genetic background of our transgenic animal model may influence or limit our conclusions about the impact of skeletal muscle  $\alpha 1$  ablation on the development of metabolic syndrome (Nascimento-Sales et al., 2017; Sodhi et al., 2017).

Additionally, there are a few contradictions between the  $sk\alpha 1^{-/-}$  phenotype and the current accepted links between increased running endurance to better health outcomes, including improvements in insulin sensitivity and glucose tolerance (Baker et al., 2010; Overmyer et al., 2015). The association between severely attenuated mitochondrial metabolism and decreased susceptibility to diet-induced metabolic dysfunction is, however, consistent with the hypothesis

that incomplete  $\beta$  oxidation of lipids and not the lack of mitochondrial metabolism is responsible for insulin resistance (Finck et al., 2005; Koves et al., 2008). Moreover, the lack of exercise endurance in  $\text{sk}\alpha 1^{-/-}$  mice is consistent with studies that have clearly demonstrated a correlation between increased exercise endurance and  $\alpha 1$  NKA expression in the muscle of inbred rats (Chen et al., 2001).

In short, the data presented here describe a common mechanism underlying the following dichotomy: the generation of metabolic reserve and flexibility in the muscle, and consequently exercise endurance, comes at the cost of metabolic intolerance to a Western diet. These new molecular insights, together with the findings from previous studies utilizing pNaKtide, validate the  $\alpha 1$  NKA/Src interaction as a novel molecular target for the development of new pharmacological approaches to treating metabolic disorders. To this end, our new pharmacological studies warrant further development of pNaKtide and its derivatives as drug candidates for NASH and other metabolic disorders.

### **Acknowledgements**

We thank Lanqing Wu and the Division of Animal Resources of the Marshall University Joan C. Edwards School of Medicine for animal care and husbandry, Dr. Jung Han Kim for the use of equipment, and Carla Cook for invaluable technical support. We also thank David Neff and The Marshall University Molecular and Biological Imaging Center for microscopy equipment and support.

### **Author Contributions**

Conceptualization: L.C.K., X.C., J.X.X., Z.X., and S.V.P.; Methodology: L.C.K., X.C., H.Z., J.A.H., J.I.S., S.V.P., and Z.X.; Formal Analysis: L.C.K., X.C., M.H., S.T.M., and X.W.; Investigation: L.C.K., X.C., J.X.X., A.M., M. H., S.T.M., X.W., and K.T.; Resources: H.Z.,

J.A.H., and G.B.; Data Curation: L.C.K.; Writing – Original Draft: L.C.K. and Z.X. ; Writing – Reviewing & Editing: L.C.K., J.X.X., H.Z., J.I.S., G.B., S.V.P., and Z.X.; Visualization: L.C.K., J.X.X., and M.H; Project Administration: S.V.P. and Z.X.; Supervision: H.Z., J.A.H., J.I.S., and G.B.; Funding Acquisition: Z.X.

## **Materials and Methods**

### **Reagents.**

The polyclonal anti-NKA  $\alpha 1$  antiserum NASE and polyclonal anti-NKA  $\alpha 2$  antiserum HERED used for Western blots were raised in rabbits and were generous gifts from Drs. T. Pressley and P. Artigas at Texas Tech University Health Sciences Center (40). Anti- $\alpha$  tubulin antibody (Sigma, catalog number T5168) was used as a loading control. Secondary antibodies were horseradish peroxidase-conjugated anti-rabbit and anti-mouse from Santa Cruz Biotechnology Inc (catalog number sc-2004 and sc-2005, respectively).

### **Cell Culture.**

The parental LLC-PK1 cells were purchased from ATCC.

### **Site-directed mutagenesis and generation of mutant-rescued stable cell lines.**

Mutant cell lines used in this work were derived from LLC-PK1 cells. The generation of  $\alpha 1$  NKA knock down PY-17 cells from LLC-PK1 was well described (Liang et al., 2006). PY-17 cells express about 8% of  $\alpha 1$  NKA in comparison to that in LLC-PK1 cells, and do not express other isoforms of NKA. Using the well-established protocol of knockdown and rescue, we have generated a number of stable cell lines (Lai et al., 2013; J. Xie et al., 2015; Yan et al., 2013). The generation and characterization of the  $\alpha 1$ -rescued AAC-19 cells,  $\alpha 1$  mutant-rescued A420P,  $\alpha 2$ -rescued LX- $\alpha 2$ , and  $\alpha 2$  mutant-rescued cells used in this study have been reported (Lai et al., 2013; Liang et al., 2006; J. Xie et al., 2015; Yu et al., 2018). After cells reached 95-100%

confluence, they were serum-starved overnight and used for experiments unless indicated otherwise. All cell lines were cultured in DMEM plus 10% FBS with 1% penicillin/streptomycin.

#### **Cell Growth Assay.**

Cell growth assay was performed as previously described (Liang et al., 2007). Briefly, 20,000 cells/well were seeded in triplicates in 12-well plates in glucose-free DMEM containing 10% FBS and 1% penicillin/streptomycin. Cells were serum-starved for at least 12 hours to achieve cell cycle synchronization. At indicated time points, cells were trypsinized, and the number of cells was counted with hemocytometer.

#### **Biochemical measurement of ATP and lactate.**

ATP measurements were performed using CellTiter-Glo Luminescent Cell Viability Assay Kit (Promega, Madison, WI, USA, Cat # G7570). According to the protocol provided by the manufacturer, 10,000 cells per well were cultured in 96-well culture plate. After treatment with 2-DG (Sigma-Aldrich, Cat# D6134) at indicated concentrations in serum-free DMEM for 45 minutes, assay reagents were reconstituted and added into culture plate. Afterwards, reactants were transferred to opaque-walled 96-well plate, and luminescent counts were determined with microplate reader.

Lactate measurement was done as described by Barker (Barker & Summerson, 1941).

#### **Media glucose depletion.**

Media was collected from cells after 3 days incubation. Glucose concentration in the media was measured using a Glucose Colorimetric Assay Kit from Cayman Chemical (Item no. 10009582, Ann Arbor, Michigan, USA). Glucose concentrations were subtracted from the glucose concentration in fresh media to determine media glucose depletion by each cell line, and

then normalized to AAC-19 controls for each experiment, so that the final number from each experiment was derived from the following equation:

$$\text{folds to AAC} - 19 = \frac{[\text{glucose}_{\text{fresh media}}] - [\text{glucose}_{\text{experimental media}}]}{[\text{glucose}_{\text{fresh media}}] - [\text{glucose}_{\text{AAC-19 media}}]}$$

**Cell proliferation in glucose-deprived media.**

Cells were plated and grown in media consisting of glucose-free DMEM, 10% FBS, and 1% Penicillin/Streptomycin, and cell number was counted after 0, 24, 36, and 48 hours of proliferation.

**Seahorse metabolic flux analysis.**

Cells were plated in Seahorse XFp cell culture plates and subjected to both the mitochondrial stress test (Agilent Technologies, Cat # 103010-100) and the glycolytic stress test (Agilent Technologies, Cedar Creek, TX, US, Cat #103017-100) supplied by the manufacturer, with the injection of oligomycin, trifluoromethoxy carbonylcyanide phenylhydrazine (FCCP), rotenone and antimycin A, glucose, and 2-deoxyglucose (2-DG), as described in Table S3. Three measurements of oxygen consumption rate and extracellular acidification rate were taken at baseline and after each injection. The appropriate concentration of FCCP was determined by FCCP titration as recommended by the manufacturer, and all future experiments were performed with this concentration of FCCP (1.0 nM).

	Mito Stress Test	Glycolytic Stress Test
Injection 1	20 µl 10 µM Oligomycin (1.0 µM)	20 µl 100 mM Glucose (10 mM)
Injection 2	22 µl 10 µM FCCP (1.0 µM)	22 µl 10 µM Oligomycin (1.0 µM)
Injection 3	25 µl 5 µM Rotenone/Antimycin A (0.5 µM)	25 µl 500 mM 2-DG (50 mM)

**Table 5: Volumes and concentrations of injections for Seahorse analysis, with final concentrations in parentheses.**

## **Animals.**

Mice with floxed endogenous NKA  $\alpha 1$  isoform from Dr. Gustavo Blanco at Kansas University Medical Center were crossed with FVB.Cg-Myod1tm2.1(cre)Gih/Jmice purchased from Jackson Labs. Mice homozygous for floxed  $\alpha 1$  ( $\alpha 1$ flox/flox) and heterozygous for MyoDiCre (MyoDiCre/WT) were bred with  $\alpha 1$ flox/flox MyoDWT/WT mice, resulting in litters of  $\alpha 1$ flox/flox MyoDiCre/WT ( $sk\alpha 1^{-/-}$ ) mice with  $\alpha 1$ flox/flox MyoDWT/WT controls ( $sk\alpha 1^{+/+}$ ).  $Sk\alpha 1^{-/-}$  mice were born with the expected Mendelian frequency and appeared normal.  $Sk\alpha 1^{-/-}$  mice and  $sk\alpha 1^{+/+}$  control littermates were housed in 12-hour light and dark cycles at constant temperature and humidity. All animal procedures were approved by the Marshall University Institutional Animal Care and Use Committee.

## **pNaKtide diet study.**

12-week-old male C57BL/6 mice were ordered from Jackson Labs and randomized to receive normal chow + vehicle, Western diet (42% fat chow with 4.2g/L fructose water) + vehicle, or Western diet + pNaKtide for 12 weeks. pNaKtide was dissolved in phosphate-buffered saline and administered via intraperitoneal injection every 2 days, while vehicle-treated mice received phosphate-buffered saline via intraperitoneal injection every 2 days. Body composition was measured using an Echo-MRI (EchoMRI, Houston, TX, USA). Tissues were collected after 12 weeks of treatment and either fixed in 10% neutrally buffered formalin or flash frozen in liquid nitrogen for future studies.

## **Treadmill testing.**

12-week-old male and female  $sk\alpha 1^{-/-}$  mice and litter mate controls were placed in the six lanes of an Exer 3/6 treadmill from Columbus Instruments equipped with a shock detection

system. Animals were acclimated to the treadmill for 3 days at 5 m/min for 5 minutes at a 5° angle and were subjected to the testing protocol on the fourth day. Mice began the testing protocol running at 5 m/m for five minutes and increased by 2 m/min each minute up to 25 m/min, then continued running at 25 m/min until they reached fatigue. Each shock administered and each visit to the shock grid was recorded for each animal. Fatigue was defined as 10 consecutive seconds spent on the shock grid, and the shock was discontinued to each mouse upon reaching fatigue.

Gene	Forward Sequence	Reverse Sequence
Mouse <i>Actab</i>	5' GGCTGTATTCCCCTCCATCG 3'	5' CCAGTTGGTAACAATGCCATGT 3'
Mouse <i>Rn18s</i>	5' CGAAAGCATTTGCCAAGAAT 3'	5' AGTCGGCATCGTTTATGGTC 3'
Mouse <i>Ppargc1a</i>	5' CAACAATGAGCCTGCGAACA 3'	5' CTTTCATCCACGGGGAGACTG 3'
Mouse <i>Atp5a1</i>	5' CATTGGTGATGGTATTGCGC 3'	5' TCCCAAACACGACAACCTCC 3'
Mouse <i>Acadm</i>	5' TGTTAATCGGTGAAGGAGCAG 3'	5' CTATCCAGGGCATACTTCGTG 3'
Mouse <i>Hk2</i>	5' TTCGACCACATTGTCCAGTG 3'	5' CTTGAATCCCTTTGTCCACTTG 3'
Mouse <i>Pkm</i>	5' CCATTCTCTACCGTCCCTGTTG 3'	5' TCCATGTAAGCGTTGTCCAG 3'
Mouse <i>Pfkm</i>	5' GATGGCTTTGAGGGTCTGG 3'	5' CTTGGTTATGTTGGCACTGATC 3'
Mouse <i>Nfe2l2</i>	5' GGTTGCCACATTCCCAAAC 3'	5' TATCCAGGGCAAGCGACTCA 3'
Mouse <i>Hmox1</i>	5' TGACACCTGAGGTCAAGCAC 3'	5' GGCAGTATCTTGCACCAGGC 3'
Mouse <i>Nqo1</i>	5' GGCCGATTCAGAGTGGCATC 3'	5' CCAGACGGTTTCCAGACGTT 3'
Mouse <i>Gstm1</i>	5' CTGACTTTGAGAAGCAGAAGCC 3'	5' TAGGTGTTGCGATGTAGCGG 3'
Mouse <i>Ccl2</i>	5' TTTTGTCAACAAGCTCAAGAGA 3'	5' ATTAAGGCATCACAGTCCGAGT 3'
Mouse <i>Trfa</i>	5' ATGGCCTCCCTCTCATCAGT 3'	5' TGGTTTGCTACGACGTGGG 3'
Mouse <i>Il6</i>	5' TCCTCTCTGCAAGAGACTTCC 3'	5' TTGTGAAGTAGGGAAGGCCG 3'
Mouse <i>Il1b</i>	5' TGCCACCTTTTGACAGTGATG 3'	5' AAGGTCCACGGGAAAGACAC 3'
Pig <i>Gapdh</i>	5' GTGTCGGTTGTGGATCTGAC 3'	5' CTGCTTACCACCTTCTTGA 3'
Pig <i>Ppargc1a</i>	5' GCTTGACGAGCGTCATTGAG 3'	5' AACCAGAGCAGCACACTCG 3'
Pig <i>Atp5a1</i>	5' GCTGCAAAGATGCTGTCAGT 3'	5' AACAAAGGACGATCCCAAAG 3'
Pig <i>Acadm</i>	5' AACCAGACCTTCGGTAGCAG 3'	5' GCCATGTCAGCCAGCAAAA 3'
Pig <i>Hk2</i>	5' GCCTGGCTAACTTCATGGAT 3'	5' CTGGACTTGAAACCCTTGGT 3'
Pig <i>Pkm</i>	5' TCATGCTGTCTGGAGAGACG 3'	5' GGCGGAGCTCCTCAAATAAT 3'
Pig <i>Pfkm</i>	5' CGTGTTAACCTCTGGTGGTG 3'	5' TGGTAACCCTCATGGACAAA 3'

**Table 6: Primer sequences used in RT-qPCR.**

### **Tissue collection.**

Mice were anesthetized with 50 mg/kg pentobarbital administered via IP injection.

Tissues were dissected and weighed. Muscles used for Western blot analysis, qPCR, or

enzymatic activity assays were flash frozen in liquid nitrogen then stored at -80° C until later use. Muscles used for histological analysis were fixed in 10% neutrally buffered formalin for 24 hours then stored in 70% ethanol until they were embedded in paraffin blocks.

### **Western blot.**

Left and right muscles of the same type from the same mouse were homogenized together in ice-cold radioimmunoprecipitation (RIPA) buffer (0.25% sodium deoxycholate, 1% Nonidet P-40, 1mM EDTA, 1mM PMSF, 1mM sodium orthovanadate, 1mM Sodium fluoride, 150 mM NaCl, 50 mM Tris-HCl, pH 7.4 and 1% protease inhibitor cocktail) with a Fisher TissueMeiser homogenizer. Homogenates were centrifuged at 14,000 X g for 15 min, supernatants were collected, and the protein content was measured using DC Protein Assay Kit from BioRad (catalog number 500-0114 and 500-0113). Equal amounts of protein of each sample were loaded, separated by SDS-PAGE, and transferred to nitrocellulose membranes. Membranes probed for  $\alpha 1$  and  $\alpha 2$  were blocked in 5% milk, then primary antibodies were added overnight at 4°C. Membranes were visualized with Western Lightning® Plus-ECL (Western Lightning) and radiographic film. Densitometric quantification was performed using ImageJ software from the National Institute of Health.

### **RT-qPCR.**

RNA was extracted from tissues and cells using TRIzol Reagent (Life Technologies Corporation, Carlsbad, CA, USA) according to manufacturer's instructions. The amount and quality of extracted RNA was measured using the Nanodrop 2000 (Thermo Scientific, Waltham, MA, USA). SuperScript III First-Strand Synthesis SuperMix for qRT-PCR (Life Technologies Corporation, Carlsbad, CA, USA) was used to synthesize first-strand cDNA. Gene expression was analyzed by real-time quantitative RT-PCR using the LightCycler 480 SYBR Green I

Master mix (Roche, Indianapolis, IN, USA) using a LightCycler 480 Instrument II (Roche, Indianapolis, IN, USA). Relative expression was calculated using the comparative Ct method with data normalized to *Actab* (liver and skeletal muscle), *Rn18s* (adipose), or *Gapdh* (AAC-19, LX- $\alpha$ 2, and LY-a2 cell lines) as previously described (Livak & Schmittgen, 2001). Primer sequences are listed in Table S3.

### **RNA sequencing and data analysis.**

RNA was extracted from whole gastrocnemius muscles using a combination of TRIzol Reagent (Life Technologies Corporation, Carlsbad, CA, USA) and an RNeasy kit (Qiagen, Hillden, Germany) the method described by Bhatnagar, Panguluri, and Kumar (2012). RNA sequencing was performed by Novogene (Sacramento, CA, USA). A heatmap of the top 70 differential expressed genes were visualized by log<sub>2</sub> normalized fragments per kilobase million (Fpkm), using cytoscape 3.7.1 (Shannon et al., 2003) and clusterMaker2 (Morris et al., 2011). Gene Ontology (GO) enrichment were analyzed using BiNGO (Maere, Heymans, & Kuiper, 2005), and then visualized using EnrichmentMap (Merico, Isserlin, Stueker, Emili, & Bader, 2010).

### **Membrane fractionation.**

Crude membrane fractions were prepared from frozen  $\alpha$ 1<sup>+/-</sup> and  $\alpha$ 1<sup>+/+</sup> gastrocnemius muscles following a procedure modified from Walas and Juel (Walas & Juel, 2012). Frozen muscles were ground into a fine powder with a mortar and pestle. The resulting powder was homogenized in ice-cold fractionation buffer (250 mM mannitol, 30 mM L-histidine, 5 mM EGTA and 0.1% deoxycholate, adjusted to pH 6.8 with Tris-base) for 30 seconds with a Fisher Tissue Meiser handheld homogenizer. The crude homogenate was centrifuged at 3000xg for 30 minutes and the supernatant was then centrifuged at 190,000xg for 90 minutes. The pellet was

resuspended in 30 mM histidine, 250 mM sucrose, and 1 mM EDTA, pH 7.4, and protein concentration was determined using the DC Protein Assay Kit from BioRad (catalog number 500-0114 and 500-0113).

#### **ATPase activity assay.**

Ouabain-sensitive ATPase activity in crude membrane fractions was determined by measuring ATP hydrolysis as previously described (Belliard et al., 2016; Belliard et al., 2013). Released inorganic phosphate (Pi) was detected using a malachite-based Biomol Green reagent. Samples containing 10 µg of protein were added to a reaction mix containing 20 mM Tris-HCL, 1 mM MgCl<sub>2</sub>, 100 mM NaCl, 20 mM KCl, and 1 mM EGTA-Tris, pH 7.2. Ouabain was added to the samples to a final concentration of 1 mM to completely inhibit both  $\alpha$ 1 and  $\alpha$ 2 isoforms of the NKA. After 10 minutes of preincubation at room temperature, the reaction was started by adding Mg-ATP at a final concentration of 2.25 mM and incubation at 37°C with shaking for 30 minutes. The reaction was stopped with the addition of ice-cold 8% TCA, and the concentration of Pi was measured spectrophotometrically at OD 620 nm using Biomol Green as an indicator (Enzo Life Sciences catalog # BML-AK111-250). Maximal NKA activity was calculated as the difference between ATPase activity obtained in the absence or presence of 1 mM ouabain.

#### **Immunohistochemistry.**

Muscles were collected and then washed twice with ice-cold PBS, fixed with 10% neutrally buffered formalin for 24 hours, and embedded in paraffin. Transverse sections of the midbelly were immunostained for myosin heavy chain (Myhc) fast and Myhc slow by Wax-It, Inc., as described by Behan et al. (Behan et al., 2002) to differentiate between type 1 and type 2 fibers. Additional sections were stained for NKA  $\alpha$ 1 by Wax-It, Inc. (Vancouver, Canada). The samples were examined on a Leica confocal SP5 microscope (Leica Microsystems, Wetzlar,

Germany). The images were processed with the Leica Application Suite Advanced Fluorescence (LAS/AF) suite (Leica Microsystems, Wetzlar, Germany), FIJI platform, and the GNU Image Manipulation Program (GIMP) to obtain maximum projections, extract lateral slices, and construct figures.

#### **Morphometric tissue analysis (CSA and fiber types).**

Images of muscles stained for fast and slow myosin heavy chain were obtained by Wax-It, Inc. with digital whole-slide scanning. Aperio ImageScope software was used to determine the cross sectional area (CSA) of each fiber. Fibers that had been damaged were excluded from CSA analysis. Every fiber of each type in each muscle was counted to determine the average number of fibers per muscle.

#### **Western diet study.**

6-8-week-old male mice were placed on a 42% fat diet with 4.2g/L fructose water with controls on a normal chow diet for 12 weeks. Glucose tolerance tests were performed at 6 weeks and insulin tolerance tests were performed at 12 weeks. Tissues were collected and weighed after 12 weeks of diet treatment, and flash frozen in liquid nitrogen or fixed in 10% neutrally buffered formalin for 24 hours then transferred to 70% ethanol for shipment to Wax-It, Inc., for paraffin embedding and hematoxylin and eosin staining.

#### **pNaKtide diet study.**

12-week-old male C57BL/6 mice were ordered from Jackson Labs and randomized to receive normal chow + vehicle, Western diet (42% fat chow with 4.2g/L fructose water) + vehicle, or Western diet + pNaKtide for 12 weeks. pNaKtide was dissolved in phosphate-buffered saline and administered via intraperitoneal injection every 2 days, while vehicle-treated mice received phosphate-buffered saline via intraperitoneal injection every 2 days. Body

composition was measured using an Echo-MRI (EchoMRI, Houston, TX, USA). Tissues were dissected and flash frozen in liquid N<sub>2</sub> for biochemical analysis or fixed in 10% neutrally buffered formalin for histological analysis.

## CHAPTER 4

### DISCUSSION AND CONCLUSIONS

#### **Isoform-specific role of NKA $\alpha 1$ in skeletal muscle**

These studies reveal that the NKA  $\alpha 1$  isoform has an isoform-specific role in skeletal muscle that cannot be filled by the  $\alpha 2$  isoform, in spite of its low expression as a proportion of the total NKA pool in skeletal muscle (He et al., 2001). While NKA  $\alpha 2$  is indeed vital for normal contractility (DiFranco et al., 2015; Radzyukevich et al., 2013), the skeletal muscle-specific ablation of  $\alpha 2$  has no impact on skeletal muscle growth. In contrast, our  $sk\alpha 1^{-/-}$  mice had a 35% decrease in muscle mass and abnormal muscle structure (Figure 17), revealing that the growth of skeletal muscle is regulated by NKA  $\alpha 1$  in an isoform-specific manner. Similarly, no clear metabolic defects were described in skeletal muscles lacking NKA  $\alpha 2$ , although the studies of the role of  $\alpha 2$  in skeletal muscle did not specifically evaluate markers of altered metabolism (DiFranco et al., 2015; Manoharan et al., 2015; Radzyukevich et al., 2013).

Additionally, the treadmill running studies reported by Radzyukevich et al. (2013) reveal a severe defect in running ability in mice with a skeletal muscle-specific ablation of  $\alpha 2$  which is absent in  $sk\alpha 1^{-/-}$  mice (Figure 18). This further confirms the isoform specificity of the ‘turbocharger’ role of NKA  $\alpha 2$  in maintaining the membrane potential during muscle contraction, as ablation of NKA  $\alpha 1$  did not impact running even at speeds of 25 meters per minute but did impact endurance, which is associated with metabolic defects rather than ion transport defect.

#### **NKA $\alpha 1$ regulates muscle growth**

One of the most striking results of these studies is the impact of a reduction or ablation of NKA  $\alpha 1$  on muscle growth. While this was the first time that a direct relationship between NKA

$\alpha 1$  and skeletal muscle growth was reported, a similar role for  $\alpha 1$  in growth regulation has been shown in other models, including renal epithelial cell growth and cardiomyocyte proliferation *in vitro* (Huang et al., 1997; Liu et al., 2006; Tian et al., 2009; J. Xie et al., 2015; Z. Xie et al., 1999) and renal development *in vivo* (Fontana et al., 2013). While the exact mechanism of that regulation was not clarified in this body of work, the importance of the Src binding site for the ability of NKA  $\alpha 1$  to regulate cell proliferation has been established in other models (Lai et al., 2013; Yu et al., 2018). Additionally, NKA  $\alpha 1$  signaling in skeletal muscle cells has been linked to Src- and Erk-mediated GSK3 $\beta$  inactivation (Kotova, Al-Khalili, et al., 2006; Kotova, Galuska, et al., 2006). Inactivation of GSK3 $\beta$ , in turn, has been linked to myogenesis and the growth of skeletal muscles (Agle et al., 2017; Leger et al., 2006; van der Velden et al., 2007), while the activation of GSK3 $\beta$  is associated with skeletal muscle atrophy (Verhees et al., 2011; W. Yang et al., 2007).

The possibility that GSK3 $\beta$  is involved is compelling, but it cannot fully explain the  $sk\alpha 1^{-/-}$  phenotype. The  $\alpha 1^{+/-}$  model had decreased muscle mass in spite of apparently normal GSK3 $\beta$  expression (Figure 8), suggesting that the growth defects in this model of reduced NKA  $\alpha 1$  expression was not mediated by GSK3 $\beta$ . Furthermore, the impact of altered GSK3 $\beta$  expression are much smaller than the effects of altered NKA  $\alpha 1$  expression, even when paired with altered GSK3 $\alpha$  expression to eliminate compensation by the other isoform. This suggests that the  $sk\alpha 1^{-/-}$  phenotype is mediated by multiple pathways, of which GSK3 $\beta$  is merely one. The fact that the ablation of the dominant  $\alpha 2$  isoform does not have the same impact on skeletal muscle growth supports the hypothesis that mechanism by which  $\alpha 1$  regulates skeletal muscle growth and development is independent of ion pumping (DiFranco et al., 2015; Manoharan et al., 2015; Radzyukevich et al., 2013).

Another possible mechanism by which  $\alpha 1$  could regulate myogenesis is via the Wnt signaling pathway. The caveolin binding motif of  $\alpha 1$  has been shown to regulate embryonic organogenesis via Wnt/ $\beta$ -catenin signaling, and although myogenesis was not specifically evaluated, this process represents a possible mechanism for the regulation of muscle growth by NKA  $\alpha 1$ . Although this hypothesis is compelling, additional studies are necessary to understand which aspects of muscle development are impacted, such as the cardiotoxin method of evaluating muscle growth and repair (Garry, Antony, & Garry, 2016; Guardiola et al., 2017) or *in vitro* studies of myoblast proliferation and differentiation.

### **NKA $\alpha 1$ regulates muscle metabolism**

Previous studies have found links between NKA activity and metabolic control of glycolysis, both under physiological and pathological conditions (Banerjee et al., 2018; J. H. James et al., 1996; J. H. James et al., 1999; Lynch & Balaban, 1987a, 1987b; Okamoto et al., 2001; Sepp et al., 2014). This set of studies is unique in that it identified a direct link between the NKA  $\alpha 1$  isoform and regulation of metabolic flexibility and spare capacity, both key components of skeletal muscle metabolism. The decrease in oxidative muscle size observed in  $\alpha 1^{+/-}$  mice (Figure 5) and the switch from oxidative to glycolytic fibers in  $sk\alpha 1^{-/-}$  mice (Figure 16) both suggest decreased metabolic flexibility when NKA  $\alpha 1$  expression is decreased or ablated. The functional importance of this metabolic regulation is supported by the lack of endurance exhibited by  $sk\alpha 1^{-/-}$  mice when subjected to forced treadmill running (Figure 18). However, this metabolic flexibility appears to come at the cost of intolerance to a Western diet (Figures 19-20). Furthermore, our studies with renal epithelial-derived cell lines expressing Src binding-mutant  $\alpha 1$  and  $\alpha 2$  suggest that this link is mediated by the  $\alpha 1$ -specific NKA/Src interaction.

This regulation of skeletal muscle metabolism by the NKA  $\alpha$ 1/Src signaling complex has implications for our understanding of exercise-induced metabolic adaptations and skeletal muscle hypertrophy. Exercise has been shown to increase circulating levels of endogenous cardiotonic steroids (Bauer et al., 2005), but what role this spike in NKA ligands plays in physiological adaptations to exercise has not been explored. The generation of mice with ouabain-resistant NKA  $\alpha$ 2 revealed that increased circulating ouabain during exercise reduces exercise capacity due to reduced ion transport (Radzyukevich et al., 2009). However, in light of these new revelations about the role of NKA  $\alpha$ 1-mediated signaling in skeletal muscle growth and metabolism, the possibility that increased circulating cardiotonic steroids during exercise could stimulate NKA  $\alpha$ 1/Src signaling and thereby mediate skeletal muscle metabolic responses to exercise should be investigated. The metabolic adaptations to exercise training in several existing animals, such as global  $\alpha$ 1 haplodeficient mice, skeletal muscle-specific  $\alpha$ 1 knockout mice, and mice expressing ouabain sensitive  $\alpha$ 1, could be evaluated and contrasted to determine what role endogenous ouabain signaling through NKA  $\alpha$ 1 plays in exercise-induced metabolic adaptations. Additionally, generation of a mouse model with a skeletal muscle-specific rescue of  $\alpha$ 1 expression with a signaling-null  $\alpha$ 1, such as the A420P mutant used in Figure 14, would allow us to differentiate between the ion transport function and the Src-mediated signaling function of NKA  $\alpha$ 1 in skeletal muscle.

### **Evolutionary implications**

If this novel role of NKA  $\alpha$ 1 in skeletal muscle is in fact mediated by Src signaling, it could indicate the evolution of a novel regulator of metabolic flexibility and metabolism in mammals and birds that is not seen in other classes of animals. The convergent evolution of the NaKtide sequence in birds and mammals is intriguing, especially with the metabolic phenotype

observed in A420P cells, which have a conserved Y260 region and disrupted Src binding only in the NaKtide region. Unlike the LX- $\alpha$ 2 cells which have no Src binding capacity and have decreased basal mitochondrial metabolism and unchanged basal glycolytic metabolism (Figure 13), A420P cells have unchanged basal mitochondrial metabolism and increased basal glycolytic metabolism (Figure 67). This suggests that the acquisition of the NaKtide region alone is enough to increase basal metabolism, which according to the aerobic scope hypothesis was a key component of the development of endothermy (Clarke & Pörtner, 2010; Nespolo et al., 2017). For these reasons, the evolutionary implications of the Src binding capacity of NKA  $\alpha$ 1 in endotherms bear further investigation.

Additionally, the metabolic reserve and flexibility afforded by Src binding appear to come at the cost of intolerance to nutritional oversupply. Based on the work done by Sodhi et al, NKA signaling through Src appears to facilitate adipogenesis and the storage of lipids, as well as the development of T2D (Sodhi et al., 2015; Sodhi et al., 2018). Administration of pNaKtide, a small peptide inhibitor of NKA-mediated Src activation based on the NaKtide sequence, prevents the development of metabolic syndrome on a Western diet and attenuates aging (Sodhi et al., 2015; Sodhi et al., 2018). These affects are attributed to the disruption of the ROS-mediated feed-forward NKA  $\alpha$ 1 activation loop (Yan et al., 2013).

Similarly, sk $\alpha$ 1<sup>-/-</sup> mice which lack this signaling pathway and subsequent metabolic control are resistant to the metabolic effects of the Western diet (Figures 19-20). This resistance does not come without a price. Indeed, under normal, healthy conditions, these mice exhibit decreased exercise performance and display multiple hallmarks of decreased metabolic flexibility and increased metabolic dysfunction, including a severe decrease in endurance exercise tolerance (Figure 18), a switch to more glycolytic fibers (Figure 16), and decreased

glycogen storage (Figure 18). Therefore, we can hypothesize that the addition of this new mechanism for regulating metabolism may also have introduced a mechanism by which metabolism can become dysregulated, resulting in metabolic disease.

### **Clinical implications**

These studies provide the first genetic evidence of NKA  $\alpha 1$  as an important regulator of metabolism *in vivo*. Although previous studies using pNaKtide have linked NKA  $\alpha 1$  signaling to metabolism and metabolic disorders (J. Liu et al., 2016; Sodhi et al., 2015; Sodhi et al., 2018; Sodhi et al., 2017; Srikanthan et al., 2016), it is possible that pNaKtide may have off-target effects on Src independent of NKA  $\alpha 1$  itself. Additionally, these studies involved the systemic disruption of the NKA  $\alpha 1$ /Src signaling complex, which makes it difficult to identify the specific impact of altered NKA  $\alpha 1$ /Src signaling on individual tissues. Furthermore, the identification of NKA as a regulator of metabolic flexibility in skeletal muscle could lead to the development of novel treatments for metabolic disorders which target the NKA/Src signaling axis, or to the application of existing drugs such as digoxin that are capable of targeting NKA for a different therapeutic goal.

Additionally, the identification of NKA as a regulator of skeletal muscle growth is similarly useful in treating muscle wasting due to cachexia, sarcopenia, and disuse by stimulating NKA signaling through Src, thereby increasing the activation of key growth pathways and increasing muscle mass and metabolic flexibility. Moreover, because NKA signaling contributes to the regulation of both metabolism and growth in skeletal muscle, it could be a useful therapeutic goal for populations who are in need of addressing both muscle wasting and metabolism, such as elderly patients suffering from type 2 diabetes in addition to sarcopenia, or patients with burn cachexia whose muscle metabolism can be controlled with CTS which can

also contribute to increasing muscle growth and decreasing wasting (Dhillon & Hasni, 2017; Pedroso et al., 2012; Sakuma et al., 2017). Furthermore, if exercise-induced increases in metabolic flexibility and mitochondrial metabolism are mediated by increased circulating cardiostimulatory steroids which increase NKA  $\alpha 1$  signaling through Src in skeletal muscle, it may be possible to mimic the health benefits of exercise pharmacologically using exogenous cardiostimulatory steroids for those who are unable to exercise, such as patients on bedrest.

The striking impact of NKA  $\alpha 1$  ablation on skeletal muscle size and morphology provides compelling evidence that NKA  $\alpha 1$  signaling regulates skeletal muscle growth and development. However, without identifying the specific aspects of skeletal muscle development that are impacted, it is difficult to recognize which developmental and degenerative muscle conditions might benefit from the pharmacological targeting of this pathway. The commonly used cardiotoxin injury model of skeletal muscle regeneration could provide insight into the aspects of skeletal muscle growth and differentiation that are mediated by NKA  $\alpha 1$  and could identify the muscle wasting conditions that are most likely to benefit from NKA  $\alpha 1$ -targeted therapeutics. Additionally, the viability of such therapeutic options should be validated using animal models of muscle wasting diseases such as the hindlimb suspension model of disuse-induced atrophy, the mdx mouse model of Duchenne's muscular dystrophy, and the cancer cachexia model in tumor-inoculated immunodeficient mice.

While differences in  $\alpha 1$  expression have been identified in multiple disease states, we have yet to evaluate the impacts of genetically altering  $\alpha 1$  expression in other tissues. Whether altered  $\alpha 1$  expression contributes to the progression of these diseases or is a protective mechanism is also unclear. The sk $\alpha 1$ <sup>-/-</sup> mice were protected from Western diet-induced metabolic dysfunction (Figures 20 and 21), suggesting that although NKA  $\alpha 1$  plays a vital role in

the development of normal metabolism in skeletal muscle, it also plays a key role in the pathological dysregulation of metabolism. Given that metabolism is dysregulated in many of the diseases in which  $\alpha 1$  expression is altered, including heart failure (L. Liu et al., 2016), diabetic neuropathy (Gerbi et al., 1998), and polycystic ovarian syndrome (Tepavcevic et al., 2015), reduced expression of NKA  $\alpha 1$  may actually be protective as the loss of the NKA  $\alpha 1$ /Src signaling complex appears to be protective in our model. These studies of the interaction between skeletal muscle-specific NKA  $\alpha 1$  ablation and Western diet-induced metabolic dysregulation are intriguing and bring up the possibility that ablation of the NKA/Src receptor complex in other tissues in other disease states could enhance our understanding of the interaction of this signaling mechanism and human disease, thus leading to further uses of NKA  $\alpha 1$  as a pharmacological target. This is supported by the similarities between the effects of  $\alpha 1$  ablation and treatment with pNaKtide to ‘short circuit’ Src signaling.

### **Limitations**

One mechanism that these studies fail to address is the impact of NKA  $\alpha 1$  ablation on calcium signaling, which is critical in skeletal muscle (Hostrup et al., 2014). Additionally, while the effects we see with decreased or ablated NKA expression in skeletal muscle are consistent with the effects of the disruption of NKA  $\alpha 1$ /Src signaling complex in other cell types *in vitro* (Banerjee et al., 2018; Lai et al., 2013; J. Xie et al., 2015; Yu et al., 2018), we did not perform experiments that specifically interrupted this complex in skeletal muscle. To do this, a system of signaling-null rescue of NKA  $\alpha 1$  expression would be ideal.

## REFERENCES

- Agley, C. C., Lewis, F. C., Jaka, O., Lazarus, N. R., Velloso, C., Francis-West, P., . . . Harridge, S. D. R. (2017). Active GSK3beta and an intact beta-catenin TCF complex are essential for the differentiation of human myogenic progenitor cells. *Sci Rep*, 7(1), 13189. doi:10.1038/s41598-017-10731-1
- Akera, T., & Brody, T. M. (1982). Myocardial membranes: regulation and function of the sodium pump. *Annu Rev Physiol*, 44, 375-388. doi:10.1146/annurev.ph.44.030182.002111
- Akera, T., & Brody, T. M. (1985). Estimating sodium pump activity in beating heart muscle. *Trends in Pharmacological Sciences*, 6(Supplement C), 156-159. doi:[https://doi.org/10.1016/0165-6147\(85\)90074-4](https://doi.org/10.1016/0165-6147(85)90074-4)
- Al-Khalili, L., Kotova, O., Tsuchida, H., Ehren, I., Feraille, E., Krook, A., & Chibalin, A. V. (2004). ERK1/2 mediates insulin stimulation of Na(+),K(+)-ATPase by phosphorylation of the alpha-subunit in human skeletal muscle cells. *J Biol Chem*, 279(24), 25211-25218. doi:10.1074/jbc.M402152200
- Andrzejewski, S., Klimcakova, E., Johnson, R. M., Tabaries, S., Annis, M. G., McGuirk, S., . . . St-Pierre, J. (2017). PGC-1alpha Promotes Breast Cancer Metastasis and Confers Bioenergetic Flexibility against Metabolic Drugs. *Cell Metab*, 26(5), 778-787.e775. doi:10.1016/j.cmet.2017.09.006
- Apostolopoulou, M., Strassburger, K., Herder, C., Knebel, B., Kotzka, J., Szendroedi, J., & Roden, M. (2016). Metabolic flexibility and oxidative capacity independently associate with insulin sensitivity in individuals with newly diagnosed type 2 diabetes. *Diabetologia*, 59(10), 2203-2207. doi:10.1007/s00125-016-4038-9
- Aughey, R. J., Murphy, K. T., Clark, S. A., Garnham, A. P., Snow, R. J., Cameron-Smith, D., . . . McKenna, M. J. (2007). Muscle Na<sup>+</sup>-K<sup>+</sup>-ATPase activity and isoform adaptations to intense interval exercise and training in well-trained athletes. *J Appl Physiol* (1985), 103(1), 39-47. doi:10.1152/jappphysiol.00236.2006
- Aydemir-Koksoy, A., Abramowitz, J., & Allen, J. C. (2001). Ouabain-induced signaling and vascular smooth muscle cell proliferation. *J Biol Chem*, 276(49), 46605-46611. doi:10.1074/jbc.M106178200

- Bai, Y., Wu, J., Li, D., Morgan, E. E., Liu, J., Zhao, X., . . . Liu, L. (2016). Differential roles of caveolin-1 in ouabain-induced Na<sup>+</sup>/K<sup>+</sup>-ATPase cardiac signaling and contractility. *Physiol Genomics*, 48(10), 739-748. doi:10.1152/physiolgenomics.00042.2016
- Baker, J. S., McCormick, M. C., & Robergs, R. A. (2010). Interaction among Skeletal Muscle Metabolic Energy Systems during Intense Exercise. *J Nutr Metab*, 2010, 905612. doi:10.1155/2010/905612
- Banerjee, M., Cui, X., Li, Z., Yu, H., Cai, L., Jia, X., . . . Xie, Z. (2018). Na/K-ATPase Y260 Phosphorylation-mediated Src Regulation in Control of Aerobic Glycolysis and Tumor Growth. *Sci Rep*, 8(1), 12322. doi:10.1038/s41598-018-29995-2
- Barker, S. B., & Summerson, W. H. (1941). The Colorimetric Determination of Lactic Acid in Biological Material. *Journal of Biological Chemistry*, 138(2), 535-554.
- Bauer, N., Muller-Ehmsen, J., Kramer, U., Hambarchian, N., Zobel, C., Schwinger, R. H., . . . Schoner, W. (2005). Ouabain-like compound changes rapidly on physical exercise in humans and dogs: effects of beta-blockade and angiotensin-converting enzyme inhibition. *Hypertension*, 45(5), 1024-1028. doi:10.1161/01.HYP.0000165024.47728.f7
- Behan, W. M., Cossar, D. W., Madden, H. A., & McKay, I. C. (2002). Validation of a simple, rapid, and economical technique for distinguishing type 1 and 2 fibres in fixed and frozen skeletal muscle. *J Clin Pathol*, 55(5), 375-380.
- Belliard, A., Gulati, G. K., Duan, Q., Alves, R., Brewer, S., Madan, N., . . . Pierre, S. V. (2016). Ischemia/reperfusion-induced alterations of enzymatic and signaling functions of the rat cardiac Na<sup>+</sup>/K<sup>+</sup>-ATPase: protection by ouabain preconditioning. *Physiol Rep*, 4(19). doi:10.14814/phy2.12991
- Belliard, A., Sottejeau, Y., Duan, Q., Karabin, J. L., & Pierre, S. V. (2013). Modulation of cardiac Na<sup>+</sup>,K<sup>+</sup>-ATPase cell surface abundance by simulated ischemia-reperfusion and ouabain preconditioning. *Am J Physiol Heart Circ Physiol*, 304(1), H94-103. doi:10.1152/ajpheart.00374.2012
- Benziane, B., Bjornholm, M., Pirkmajer, S., Austin, R. L., Kotova, O., Viollet, B., . . . Chibalin, A. V. (2012). Activation of AMP-activated protein kinase stimulates Na<sup>+</sup>,K<sup>+</sup>-ATPase activity in skeletal muscle cells. *J Biol Chem*, 287(28), 23451-23463. doi:10.1074/jbc.M111.331926

- Bhatnagar, S., Panguluri, S. K., & Kumar, A. (2012). Gene profiling studies in skeletal muscle by quantitative real-time polymerase chain reaction assay. *Methods Mol Biol*, 798, 311-324. doi:10.1007/978-1-61779-343-1\_18
- Blanco, G. (2005a). Na,K-ATPase subunit heterogeneity as a mechanism for tissue-specific ion regulation. *Semin Nephrol*, 25(5), 292-303. doi:10.1016/j.semnephrol.2005.03.004
- Blanco, G. (2005b). The NA/K-ATPase and its isozymes: what we have learned using the baculovirus expression system. *Front Biosci*, 10, 2397-2411.
- Blanco, G., DeTomaso, A. W., Koster, J., Xie, Z. J., & Mercer, R. W. (1994). The alpha-subunit of the Na,K-ATPase has catalytic activity independent of the beta-subunit. *J Biol Chem*, 269(38), 23420-23425.
- Blanco, G., Koster, J. C., Sanchez, G., & Mercer, R. W. (1995). Kinetic properties of the alpha 2 beta 1 and alpha 2 beta 2 isozymes of the Na,K-ATPase. *Biochemistry*, 34(1), 319-325. doi:10.1021/bi00001a039
- Blanco, G., Melton, R. J., Sanchez, G., & Mercer, R. W. (1999). Functional characterization of a testes-specific alpha-subunit isoform of the sodium/potassium adenosinetriphosphatase. *Biochemistry*, 38(41), 13661-13669. doi:10.1021/bi991207b
- Blanco, G., Sanchez, G., & Mercer, R. W. (1995). Comparison of the enzymatic properties of the Na,K-ATPase alpha 3 beta 1 and alpha 3 beta 2 isozymes. *Biochemistry*, 34(31), 9897-9903. doi:10.1021/bi00031a011
- Blanco, G., Xie, Z. J., & Mercer, R. W. (1993). Functional expression of the alpha 2 and alpha 3 isoforms of the Na,K-ATPase in baculovirus-infected insect cells. *Proc Natl Acad Sci U S A*, 90(5), 1824-1828. doi:10.1073/pnas.90.5.1824
- Brent, G. A. (2012). Mechanisms of thyroid hormone action. *J Clin Invest*, 122(9), 3035-3043. doi:10.1172/jci60047
- Buchanan, R., Nielsen, O. B., & Clausen, T. (2002). Excitation- and beta(2)-agonist-induced activation of the Na(+)-K(+) pump in rat soleus muscle. *J Physiol*, 545(1), 229-240. doi:10.1113/jphysiol.2002.023325
- Bundgaard, H., Kjeldsen, K., Suarez Krabbe, K., van Hall, G., Simonsen, L., Qvist, J., . . . Klarlund Pedersen, B. (2003). Endotoxemia stimulates skeletal muscle Na<sup>+</sup>-K<sup>+</sup>-ATPase

- and raises blood lactate under aerobic conditions in humans. *Am J Physiol Heart Circ Physiol*, 284(3), H1028-1034. doi:10.1152/ajpheart.00639.2002
- Cai, T., Wang, H., Chen, Y., Liu, L., Gunning, W. T., Quintas, L. E., & Xie, Z. J. (2008). Regulation of caveolin-1 membrane trafficking by the Na/K-ATPase. *J Cell Biol*, 182(6), 1153-1169. doi:10.1083/jcb.200712022
- Cairns, S. P., & Dulhunty, A. F. (1993). Beta-adrenergic potentiation of E-C coupling increases force in rat skeletal muscle. *Muscle Nerve*, 16(12), 1317-1325. doi:10.1002/mus.880161208
- Cairns, S. P., Hing, W. A., Slack, J. R., Mills, R. G., & Loiselle, D. S. (1997). Different effects of raised [K<sup>+</sup>]<sub>o</sub> on membrane potential and contraction in mouse fast- and slow-twitch muscle. *Am J Physiol*, 273(2 Pt 1), C598-611. doi:10.1152/ajpcell.1997.273.2.C598
- Camps, M., Castello, A., Munoz, P., Monfar, M., Testar, X., Palacin, M., & Zorzano, A. (1992). Effect of diabetes and fasting on GLUT-4 (muscle/fat) glucose-transporter expression in insulin-sensitive tissues. Heterogeneous response in heart, red and white muscle. *Biochem J*, 282 ( Pt 3), 765-772.
- Carson, J. A., Hardee, J. P., & VanderVeen, B. N. (2016). The emerging role of skeletal muscle oxidative metabolism as a biological target and cellular regulator of cancer-induced muscle wasting. *Semin Cell Dev Biol*, 54, 53-67. doi:10.1016/j.semcdb.2015.11.005
- Chaillou, M., Rigoard, P., Fares, M., Francois, C., Sottejeau, Y., & Maixent, J. M. (2011). Relation between alpha-isoform and phosphatase activity of Na<sup>+</sup>,K<sup>+</sup>-ATPase in rat skeletal muscle fiber types. *Cell Mol Biol (Noisy-le-grand)*, 57 Suppl, O11520-1527.
- Chal, J., & Pourquie, O. (2017). Making muscle: skeletal myogenesis in vivo and in vitro. *Development*, 144(12), 2104-2122. doi:10.1242/dev.151035
- Chen, J., Feller, G. M., Barbato, J. C., Periyasamy, S., Xie, Z. J., Koch, L. G., . . . Britton, S. L. (2001). Cardiac performance in inbred rat genetic models of low and high running capacity. *J Physiol*, 535(Pt 2), 611-617.
- Chibalin, A. V., Kovalenko, M. V., Ryder, J. W., Féraillé, E., Wallberg-Henriksson, H., & Zierath, J. R. (2001). Insulin- and Glucose-Induced Phosphorylation of the Na<sup>+</sup>,K<sup>+</sup>-Adenosine Triphosphatase  $\alpha$ -Subunits in Rat Skeletal Muscle. *Endocrinology*, 142(8), 3474-3482. doi:10.1210/endo.142.8.8294

- Choi, E., Carruthers, K., Zhang, L., Thomas, N., Battaglino, R. A., Morse, L. R., & Widrick, J. J. (2013). Concurrent muscle and bone deterioration in a murine model of cancer cachexia. *Physiol Rep*, 1(6), e00144. doi:10.1002/phy2.144
- Clarke, A., & Pörtner, H.-O. (2010). Temperature, metabolic power and the evolution of endothermy. *Biological Reviews*, 85(4), 703-727. doi:10.1111/j.1469-185X.2010.00122.x
- Clausen, T., Andersen, S. L., & Flatman, J. A. (1993). Na(+)-K+ pump stimulation elicits recovery of contractility in K(+)-paralysed rat muscle. *J Physiol*, 472, 521-536. doi:10.1113/jphysiol.1993.sp019960
- Clausen, T., & Flatman, J. A. (1977). The effect of catecholamines on Na-K transport and membrane potential in rat soleus muscle. *J Physiol*, 270(2), 383-414. doi:10.1113/jphysiol.1977.sp011958
- Clausen, T., & Flatman, J. A. (1987). Effects of insulin and epinephrine on Na<sup>+</sup>-K<sup>+</sup> and glucose transport in soleus muscle. *Am J Physiol*, 252(4 Pt 1), E492-499. doi:10.1152/ajpendo.1987.252.4.E492
- Collaboration, N. R. F. (2016). Worldwide trends in diabetes since 1980: a pooled analysis of 751 population-based studies with 4.4 million participants. *Lancet*, 387(10027), 1513-1530. doi:10.1016/s0140-6736(16)00618-8
- Collaboration, N. R. F. (2017). Worldwide trends in body-mass index, underweight, overweight, and obesity from 1975 to 2016: a pooled analysis of 2416 population-based measurement studies in 128&#xb7;9 million children, adolescents, and adults. *The Lancet*, 390(10113), 2627-2642. doi:10.1016/S0140-6736(17)32129-3
- Cougnon, M. H., Moseley, A. E., Radzyukevich, T. L., Lingrel, J. B., & Heiny, J. A. (2002). Na,K-ATPase alpha- and beta-isoform expression in developing skeletal muscles: alpha(2) correlates with t-tubule formation. *Pflugers Arch*, 445(1), 123-131. doi:10.1007/s00424-002-0898-6
- Crambert, G., Füzesi, M., Garty, H., Karlsh, S., & Geering, K. (2002). Phospholemman (FXD1) associates with Na,K-ATPase and regulates its transport properties. *Proceedings of the National Academy of Sciences*, 99(17), 11476-11481. doi:10.1073/pnas.182267299

- Crambert, G., Hasler, U., Beggah, A. T., Yu, C., Modyanov, N. N., Horisberger, J. D., . . . Geering, K. (2000). Transport and pharmacological properties of nine different human Na, K-ATPase isozymes. *J Biol Chem*, *275*(3), 1976-1986. doi:10.1074/jbc.275.3.1976
- Cui, X., & Xie, Z. (2017). Protein Interaction and Na/K-ATPase-Mediated Signal Transduction. *Molecules*, *22*(6). doi:10.3390/molecules22060990
- Davies, K. J., Quintanilha, A. T., Brooks, G. A., & Packer, L. (1982). Free radicals and tissue damage produced by exercise. *Biochem Biophys Res Commun*, *107*(4), 1198-1205. doi:10.1016/s0006-291x(82)80124-1
- DeFronzo, R. A., & Tripathy, D. (2009). Skeletal muscle insulin resistance is the primary defect in type 2 diabetes. *Diabetes Care*, *32 Suppl 2*, S157-163. doi:10.2337/dc09-S302
- Despa, S., Lingrel, J. B., & Bers, D. M. (2012). Na(+)/K(+)-ATPase alpha2-isoform preferentially modulates Ca2(+) transients and sarcoplasmic reticulum Ca2(+) release in cardiac myocytes. *Cardiovasc Res*, *95*(4), 480-486. doi:10.1093/cvr/cvs213
- Devarshi, P. P., McNabney, S. M., & Henagan, T. M. (2017). Skeletal Muscle Nucleo-Mitochondrial Crosstalk in Obesity and Type 2 Diabetes. *Int J Mol Sci*, *18*(4). doi:10.3390/ijms18040831
- Dhillon, R. J., & Hasni, S. (2017). Pathogenesis and Management of Sarcopenia. *Clin Geriatr Med*, *33*(1), 17-26. doi:10.1016/j.cger.2016.08.002
- DiFranco, M., Hakimjavadi, H., Lingrel, J. B., & Heiny, J. A. (2015). Na,K-ATPase alpha2 activity in mammalian skeletal muscle T-tubules is acutely stimulated by extracellular K+. *J Gen Physiol*, *146*(4), 281-294. doi:10.1085/jgp.201511407
- Dostanic-Larson, I., Lorenz, J. N., Van Huysse, J. W., Neumann, J. C., Moseley, A. E., & Lingrel, J. B. (2006). Physiological role of the alpha1- and alpha2-isoforms of the Na+-K+-ATPase and biological significance of their cardiac glycoside binding site. *Am J Physiol Regul Integr Comp Physiol*, *290*(3), R524-528. doi:10.1152/ajpregu.00838.2005
- Dostanic, I., Lorenz, J. N., Schultz Jel, J., Grupp, I. L., Neumann, J. C., Wani, M. A., & Lingrel, J. B. (2003). The alpha2 isoform of Na,K-ATPase mediates ouabain-induced cardiac inotropy in mice. *J Biol Chem*, *278*(52), 53026-53034. doi:10.1074/jbc.M308547200

- Dvela-Levitt, M., Cohen-Ben Ami, H., Rosen, H., Ornoy, A., Hochner-Celnikier, D., Granat, M., & Lichtstein, D. (2015). Reduction in maternal circulating ouabain impairs offspring growth and kidney development. *J Am Soc Nephrol*, *26*(5), 1103-1114. doi:10.1681/asn.2014020130
- Dvela, M., Rosen, H., Ben-Ami, H. C., & Lichtstein, D. (2012). Endogenous ouabain regulates cell viability. *Am J Physiol Cell Physiol*, *302*(2), C442-452. doi:10.1152/ajpcell.00336.2011
- Egan, B., & Zierath, J. R. (2013). Exercise metabolism and the molecular regulation of skeletal muscle adaptation. *Cell Metab*, *17*(2), 162-184. doi:10.1016/j.cmet.2012.12.012
- Egawa, T., Goto, A., Ohno, Y., Yokoyama, S., Ikuta, A., Suzuki, M., . . . Goto, K. (2015). Involvement of AMPK in regulating slow-twitch muscle atrophy during hindlimb unloading in mice. *Am J Physiol Endocrinol Metab*, *309*(7), E651-662. doi:10.1152/ajpendo.00165.2015
- Finck, B. N., Bernal-Mizrachi, C., Han, D. H., Coleman, T., Sambandam, N., LaRiviere, L. L., . . . Kelly, D. P. (2005). A potential link between muscle peroxisome proliferator-activated receptor- $\alpha$  signaling and obesity-related diabetes. *Cell Metab*, *1*(2), 133-144. doi:10.1016/j.cmet.2005.01.006
- Fontana, J. M., Burlaka, I., Khodus, G., Brismar, H., & Aperia, A. (2013). Calcium oscillations triggered by cardiotoxic steroids. *Febs j*, *280*(21), 5450-5455. doi:10.1111/febs.12448
- Fowles, J. R., Green, H. J., & Ouyang, J. (2004). Na<sup>+</sup>-K<sup>+</sup>-ATPase in rat skeletal muscle: content, isoform, and activity characteristics. *J Appl Physiol (1985)*, *96*(1), 316-326. doi:10.1152/jappphysiol.00745.2002
- Frontera, W. R., & Ochala, J. (2015). Skeletal muscle: a brief review of structure and function. *Calcif Tissue Int*, *96*(3), 183-195. doi:10.1007/s00223-014-9915-y
- Galgani, J. E., Moro, C., & Ravussin, E. (2008). Metabolic flexibility and insulin resistance. *Am J Physiol Endocrinol Metab*, *295*(5), E1009-1017. doi:10.1152/ajpendo.90558.2008
- Garry, G. A., Antony, M. L., & Garry, D. J. (2016). Cardiotoxin Induced Injury and Skeletal Muscle Regeneration. *Methods Mol Biol*, *1460*, 61-71. doi:10.1007/978-1-4939-3810-0\_6

- Geering, K., Beggah, A., Good, P., Girardet, S., Roy, S., Schaer, D., & Jaunin, P. (1996). Oligomerization and maturation of Na,K-ATPase: functional interaction of the cytoplasmic NH<sub>2</sub> terminus of the beta subunit with the alpha subunit. *J Cell Biol*, *133*(6), 1193-1204. doi:10.1083/jcb.133.6.1193
- Gerbi, A., Maixent, J. M., Barbey, O., Jamme, I., Pierlovisi, M., Coste, T., . . . Raccach, D. (1998). Alterations of Na,K-ATPase isoenzymes in the rat diabetic neuropathy: protective effect of dietary supplementation with n-3 fatty acids. *J Neurochem*, *71*(2), 732-740.
- Glass, D. J. (2003). Signalling pathways that mediate skeletal muscle hypertrophy and atrophy. *Nat Cell Biol*, *5*(2), 87-90. doi:10.1038/ncb0203-87
- Goodpaster, B. H., & Sparks, L. M. (2017). Metabolic Flexibility in Health and Disease. *Cell Metab*, *25*(5), 1027-1036. doi:10.1016/j.cmet.2017.04.015
- Goodyear, L. J., Hirshman, M. F., Smith, R. J., & Horton, E. S. (1991). Glucose transporter number, activity, and isoform content in plasma membranes of red and white skeletal muscle. *Am J Physiol*, *261*(5 Pt 1), E556-561.
- Green, H. J., Chin, E. R., Ball-Burnett, M., & Ranney, D. (1993). Increases in human skeletal muscle Na(+)-K(+)-ATPase concentration with short-term training. *Am J Physiol*, *264*(6 Pt 1), C1538-1541. doi:10.1152/ajpcell.1993.264.6.C1538
- Griffin, T. M., Humphries, K. M., Kinter, M., Lim, H. Y., & Szweda, L. I. (2016). Nutrient sensing and utilization: Getting to the heart of metabolic flexibility. *Biochimie*, *124*, 74-83. doi:10.1016/j.biochi.2015.10.013
- Guardiola, O., Andolfi, G., Tirone, M., Iavarone, F., Brunelli, S., & Minchiotti, G. (2017). Induction of Acute Skeletal Muscle Regeneration by Cardiotoxin Injection. *J Vis Exp*(119). doi:10.3791/54515
- Gunning, P., & Hardeman, E. (1991). Multiple mechanisms regulate muscle fiber diversity. *Faseb j*, *5*(15), 3064-3070.
- Haas, M., Askari, A., & Xie, Z. (2000). Involvement of Src and epidermal growth factor receptor in the signal-transducing function of Na<sup>+</sup>/K<sup>+</sup>-ATPase. *J Biol Chem*, *275*(36), 27832-27837. doi:10.1074/jbc.M002951200

- Harrison, A. P., & Clausen, T. (1998). Thyroid hormone-induced upregulation of Na<sup>+</sup> channels and Na<sup>(+)</sup>-K<sup>+</sup> pumps: implications for contractility. *Am J Physiol*, 274(3), R864-867. doi:10.1152/ajpregu.1998.274.3.R864
- He, S., Shelly, D. A., Moseley, A. E., James, P. F., James, J. H., Paul, R. J., & Lingrel, J. B. (2001). The alpha(1)- and alpha(2)-isoforms of Na-K-ATPase play different roles in skeletal muscle contractility. *Am J Physiol Regul Integr Comp Physiol*, 281(3), R917-925.
- Heiny, J. A., Kravtsova, V. V., Mandel, F., Radzyukevich, T. L., Benziane, B., Prokofiev, A. V., . . . Krivoi, II. (2010). The nicotinic acetylcholine receptor and the Na,K-ATPase alpha2 isoform interact to regulate membrane electrogenesis in skeletal muscle. *J Biol Chem*, 285(37), 28614-28626. doi:10.1074/jbc.M110.150961
- Higham, S. C., Melikian, J., Karin, N. J., Ismail-Beigi, F., & Pressley, T. A. (1993). Na,K-ATPase expression in C2C12 cells during myogenesis: minimal contribution of alpha 2 isoform to Na,K transport. *J Membr Biol*, 131(2), 129-136.
- Holmstrom, M. H., Iglesias-Gutierrez, E., Zierath, J. R., & Garcia-Roves, P. M. (2012). Tissue-specific control of mitochondrial respiration in obesity-related insulin resistance and diabetes. *Am J Physiol Endocrinol Metab*, 302(6), E731-739. doi:10.1152/ajpendo.00159.2011
- Honka, M. J., Latva-Rasku, A., Bucci, M., Virtanen, K. A., Hannukainen, J. C., Kalliokoski, K. K., & Nuutila, P. (2018). Insulin-stimulated glucose uptake in skeletal muscle, adipose tissue and liver: a positron emission tomography study. *Eur J Endocrinol*, 178(5), 523-531. doi:10.1530/eje-17-0882
- Hoppeler, H. (2016). Molecular networks in skeletal muscle plasticity. *J Exp Biol*, 219(Pt 2), 205-213. doi:10.1242/jeb.128207
- Hostrup, M., Kalsen, A., Ortenblad, N., Juel, C., Morch, K., Rzeppa, S., . . . Bangsbo, J. (2014). beta2-adrenergic stimulation enhances Ca<sup>2+</sup> release and contractile properties of skeletal muscles, and counteracts exercise-induced reductions in Na<sup>+</sup>-K<sup>+</sup>-ATPase V<sub>max</sub> in trained men. *J Physiol*, 592(24), 5445-5459. doi:10.1113/jphysiol.2014.277095
- Huang, L., Li, H., & Xie, Z. (1997). Ouabain-induced hypertrophy in cultured cardiac myocytes is accompanied by changes in expression of several late response genes. *J Mol Cell Cardiol*, 29(2), 429-437. doi:10.1006/jmcc.1996.0320

- Ingwersen, M. S., Kristensen, M., Pilegaard, H., Wojtaszewski, J. F., Richter, E. A., & Juel, C. (2011). Na,K-ATPase activity in mouse muscle is regulated by AMPK and PGC-1alpha. *J Membr Biol*, 242(1), 1-10. doi:10.1007/s00232-011-9365-7
- Ishizu, Y., Ishigami, M., Kuzuya, T., Honda, T., Hayashi, K., Ishikawa, T., . . . Goto, H. (2017). Low skeletal muscle mass predicts early mortality in cirrhotic patients with acute variceal bleeding. *Nutrition*, 42, 87-91. doi:10.1016/j.nut.2017.06.004
- James, H. A., O'Neill, B. T., & Nair, K. S. (2017). Insulin Regulation of Proteostasis and Clinical Implications. *Cell Metab*, 26(2), 310-323. doi:10.1016/j.cmet.2017.06.010
- James, J. H., Fang, C. H., Schrantz, S. J., Hasselgren, P. O., Paul, R. J., & Fischer, J. E. (1996). Linkage of aerobic glycolysis to sodium-potassium transport in rat skeletal muscle. Implications for increased muscle lactate production in sepsis. *J Clin Invest*, 98(10), 2388-2397. doi:10.1172/jci119052
- James, J. H., Wagner, K. R., King, J. K., Leffler, R. E., Upputuri, R. K., Balasubramaniam, A., . . . Fischer, J. E. (1999). Stimulation of both aerobic glycolysis and Na(+)-K(+)-ATPase activity in skeletal muscle by epinephrine or amylin. *Am J Physiol*, 277(1 Pt 1), E176-186.
- James, P. F., Grupp, I. L., Grupp, G., Woo, A. L., Askew, G. R., Croyle, M. L., . . . Lingrel, J. B. (1999). Identification of a specific role for the Na,K-ATPase alpha 2 isoform as a regulator of calcium in the heart. *Mol Cell*, 3(5), 555-563.
- Janssen, I., Heymsfield, S. B., Wang, Z., & Ross, R. (2000). Skeletal muscle mass and distribution in 468 men and women aged 18–88 yr. *Journal of Applied Physiology*, 89(1), 81-88. doi:10.1152/jappl.2000.89.1.81
- Jewell, E. A., & Lingrel, J. B. (1991). Comparison of the substrate dependence properties of the rat Na,K-ATPase alpha 1, alpha 2, and alpha 3 isoforms expressed in HeLa cells. *J Biol Chem*, 266(25), 16925-16930.
- Jimenez, A. G., Dasika, S. K., Locke, B. R., & Kinsey, S. T. (2011). An evaluation of muscle maintenance costs during fiber hypertrophy in the lobster *Homarus americanus*: are larger muscle fibers cheaper to maintain? *J Exp Biol*, 214(Pt 21), 3688-3697. doi:10.1242/jeb.060301
- Jimenez, A. G., Dillaman, R. M., & Kinsey, S. T. (2013). Large fibre size in skeletal muscle is metabolically advantageous. *Nat Commun*, 4, 2150. doi:10.1038/ncomms3150

- Juel, C., Grunnet, L., Holse, M., Kenworthy, S., Sommer, V., & Wulff, T. (2001). Reversibility of exercise-induced translocation of Na<sup>+</sup>-K<sup>+</sup> pump subunits to the plasma membrane in rat skeletal muscle. *Pflugers Arch*, 443(2), 212-217. doi:10.1007/s004240100674
- Juel, C., Hostrup, M., & Bangsbo, J. (2015). The effect of exercise and beta2-adrenergic stimulation on glutathionylation and function of the Na,K-ATPase in human skeletal muscle. *Physiol Rep*, 3(8). doi:10.14814/phy2.12515
- Kaibara, K., Akasu, T., Tokimasa, T., & Koketsu, K. (1985). Beta-adrenergic modulation of the Na<sup>+</sup>-K<sup>+</sup> pump in frog skeletal muscles. *Pflugers Arch*, 405(1), 24-28.
- Kakumura, K., Takabe, S., Takagi, W., Hasegawa, K., Konno, N., Bell, J. D., . . . Hyodo, S. (2015). Morphological and molecular investigations of the holocephalan elephant fish nephron: the existence of a countercurrent-like configuration and two separate diluting segments in the distal tubule. *Cell Tissue Res*, 362(3), 677-688. doi:10.1007/s00441-015-2234-4
- Khodus, G. R., Kruusmagi, M., Li, J., Liu, X. L., & Aperia, A. (2011). Calcium signaling triggered by ouabain protects the embryonic kidney from adverse developmental programming. *Pediatr Nephrol*, 26(9), 1479-1482. doi:10.1007/s00467-011-1816-y
- Kinugawa, S., Takada, S., Matsushima, S., Okita, K., & Tsutsui, H. (2015). Skeletal Muscle Abnormalities in Heart Failure. *Int Heart J*, 56(5), 475-484. doi:10.1536/ihj.15-108
- Kometiani, P., Li, J., Gnudi, L., Kahn, B. B., Askari, A., & Xie, Z. (1998). Multiple signal transduction pathways link Na<sup>+</sup>/K<sup>+</sup>-ATPase to growth-related genes in cardiac myocytes. The roles of Ras and mitogen-activated protein kinases. *J Biol Chem*, 273(24), 15249-15256.
- Kotova, O., Al-Khalili, L., Talia, S., Hooke, C., Fedorova, O. V., Bagrov, A. Y., & Chibalin, A. V. (2006). Cardiotoxic steroids stimulate glycogen synthesis in human skeletal muscle cells via a Src- and ERK1/2-dependent mechanism. *J Biol Chem*, 281(29), 20085-20094. doi:10.1074/jbc.M601577200
- Kotova, O., Galuska, D., Essen-Gustavsson, B., & Chibalin, A. V. (2006). Metabolic and signaling events mediated by cardiotoxic steroid ouabain in rat skeletal muscle. *Cell Mol Biol (Noisy-le-grand)*, 52(8), 48-57.
- Koves, T. R., Ussher, J. R., Noland, R. C., Slentz, D., Mosedale, M., Ilkayeva, O., . . . Muoio, D. M. (2008). Mitochondrial overload and incomplete fatty acid oxidation contribute to

- skeletal muscle insulin resistance. *Cell Metab*, 7(1), 45-56.  
doi:10.1016/j.cmet.2007.10.013
- Kravtsova, V. V., Matchkov, V. V., & Bouzinova, E. V. (2015). Isoform-specific Na,K-ATPase alterations precede disuse-induced atrophy of rat soleus muscle. *2015*, 720172.  
doi:10.1155/2015/720172
- Kravtsova, V. V., Petrov, A. M., Matchkov, V. V., Bouzinova, E. V., Vasiliev, A. N., Benziane, B., . . . Krivoi, II. (2016). Distinct alpha2 Na,K-ATPase membrane pools are differently involved in early skeletal muscle remodeling during disuse. *J Gen Physiol*, 147(2), 175-188. doi:10.1085/jgp.201511494
- Kuntzweiler, T. A., Wallick, E. T., Johnson, C. L., & Lingrel, J. B. (1995). Amino acid replacement of Asp369 in the sheep alpha 1 isoform eliminates ATP and phosphate stimulation of [3H]ouabain binding to the Na<sup>+</sup>, K<sup>(+)</sup>-ATPase without altering the cation binding properties of the enzyme. *J Biol Chem*, 270(27), 16206-16212.  
doi:10.1074/jbc.270.27.16206
- Kutz, L. C., Mukherji, S. T., Wang, X., Bryant, A., Larre, I., Heiny, J. A., . . . Xie, Z. (2018). Isoform-specific role of Na/K-ATPase alpha1 in skeletal muscle. *Am J Physiol Endocrinol Metab*. doi:10.1152/ajpendo.00275.2017
- Lai, F., Madan, N., Ye, Q., Duan, Q., Li, Z., Wang, S., . . . Xie, Z. (2013). Identification of a mutant alpha1 Na/K-ATPase that pumps but is defective in signal transduction. *J Biol Chem*, 288(19), 13295-13304. doi:10.1074/jbc.M113.467381
- Le Moal, E., Pialoux, V., Juban, G., Groussard, C., Zouhal, H., Chazaud, B., & Mounier, R. (2017). Redox Control of Skeletal Muscle Regeneration. *Antioxid Redox Signal*, 27(5), 276-310. doi:10.1089/ars.2016.6782
- Leger, B., Cartoni, R., Praz, M., Lamon, S., Deriaz, O., Crettenand, A., . . . Russell, A. P. (2006). Akt signalling through GSK-3beta, mTOR and Foxo1 is involved in human skeletal muscle hypertrophy and atrophy. *J Physiol*, 576(Pt 3), 923-933.  
doi:10.1113/jphysiol.2006.116715
- Levy, B., Desebbe, O., Montemont, C., & Gibot, S. (2008). Increased aerobic glycolysis through beta2 stimulation is a common mechanism involved in lactate formation during shock states. *Shock*, 30(4), 417-421. doi:10.1097/SHK.0b013e318167378f

- Levy, B., Gibot, S., Franck, P., Cravoisy, A., & Bollaert, P. E. (2005). Relation between muscle Na<sup>+</sup>/K<sup>+</sup> ATPase activity and raised lactate concentrations in septic shock: a prospective study. *Lancet*, *365*(9462), 871-875. doi:10.1016/s0140-6736(05)71045-x
- Li, H., Yin, A., Cheng, Z., Feng, M., Zhang, H., Xu, J., . . . Qian, L. (2018). Attenuation of Na/K-ATPase/Src/ROS amplification signal pathway with pNaktide ameliorates myocardial ischemia-reperfusion injury. *Int J Biol Macromol*, *118*(Pt A), 1142-1148. doi:10.1016/j.ijbiomac.2018.07.001
- Li, J., Khodus, G. R., Kruusmagi, M., Kamali-Zare, P., Liu, X. L., Eklof, A. C., . . . Aperia, A. (2010). Ouabain protects against adverse developmental programming of the kidney. *Nat Commun*, *1*, 42. doi:10.1038/ncomms1043
- Li, Z., Cai, T., Tian, J., Xie, J. X., Zhao, X., Liu, L., . . . Xie, Z. (2009). NaKtide, a Na/K-ATPase-derived peptide Src inhibitor, antagonizes ouabain-activated signal transduction in cultured cells. *J Biol Chem*, *284*(31), 21066-21076. doi:10.1074/jbc.M109.013821
- Liang, M., Cai, T., Tian, J., Qu, W., & Xie, Z. J. (2006). Functional characterization of Src-interacting Na/K-ATPase using RNA interference assay. *J Biol Chem*, *281*(28), 19709-19719. doi:10.1074/jbc.M512240200
- Liang, M., Tian, J., Liu, L., Pierre, S., Liu, J., Shapiro, J., & Xie, Z. J. (2007). Identification of a pool of non-pumping Na/K-ATPase. *J Biol Chem*, *282*(14), 10585-10593. doi:10.1074/jbc.M609181200
- Liu, J., Tian, J., Chaudhry, M., Maxwell, K., Yan, Y., Wang, X., . . . Shapiro, J. I. (2016). Attenuation of Na/K-ATPase Mediated Oxidant Amplification with pNaKtide Ameliorates Experimental Uremic Cardiomyopathy. *Sci Rep*, *6*, 34592. doi:10.1038/srep34592
- Liu, L., Li, J., Liu, J., Yuan, Z., Pierre, S. V., Qu, W., . . . Xie, Z. (2006). Involvement of Na<sup>+</sup>/K<sup>+</sup>-ATPase in hydrogen peroxide-induced hypertrophy in cardiac myocytes. *Free Radic Biol Med*, *41*(10), 1548-1556. doi:10.1016/j.freeradbiomed.2006.08.018
- Liu, L., Wu, J., & Kennedy, D. J. (2016). Regulation of Cardiac Remodeling by Cardiac Na<sup>(+)</sup>/K<sup>(+)</sup>-ATPase Isoforms. *Front Physiol*, *7*, 382. doi:10.3389/fphys.2016.00382
- Livak, K. J., & Schmittgen, T. D. (2001). Analysis of relative gene expression data using real-time quantitative PCR and the 2<sup>(-Delta Delta C(T))</sup> Method. *Methods*, *25*(4), 402-408. doi:10.1006/meth.2001.1262

- Lynch, R. M., & Balaban, R. S. (1987a). Coupling of aerobic glycolysis and Na<sup>+</sup>-K<sup>+</sup>-ATPase in renal cell line MDCK. *Am J Physiol*, 253(2 Pt 1), C269-276. doi:10.1152/ajpcell.1987.253.2.C269
- Lynch, R. M., & Balaban, R. S. (1987b). Energy metabolism of renal cell lines, A6 and MDCK: regulation by Na-K-ATPase. *Am J Physiol*, 252(2 Pt 1), C225-231. doi:10.1152/ajpcell.1987.252.2.C225
- Madan, N., Xu, Y., Duan, Q., Banerjee, M., Larre, I., Pierre, S. V., & Xie, Z. (2017). Src-independent ERK signaling through the rat alpha3 isoform of Na/K-ATPase. *Am J Physiol Cell Physiol*, 312(3), C222-c232. doi:10.1152/ajpcell.00199.2016
- Maere, S., Heymans, K., & Kuiper, M. (2005). BiNGO: a Cytoscape plugin to assess overrepresentation of gene ontology categories in biological networks. *Bioinformatics*, 21(16), 3448-3449. doi:10.1093/bioinformatics/bti551
- Manoharan, P., Radzyukevich, T. L., Hakim Javadi, H., Stiner, C. A., Landero Figueroa, J. A., Lingrel, J. B., & Heiny, J. A. (2015). Phospholemman is not required for the acute stimulation of Na(+)-K(+)-ATPase alpha(2)-activity during skeletal muscle fatigue. *Am J Physiol Cell Physiol*, 309(12), C813-822. doi:10.1152/ajpcell.00205.2015
- Matsuyama, T., Ishikawa, T., Okayama, T., Oka, K., Adachi, S., Mizushima, K., . . . Itoh, Y. (2015). Tumor inoculation site affects the development of cancer cachexia and muscle wasting. *Int J Cancer*, 137(11), 2558-2565. doi:10.1002/ijc.29620
- McCarter, F. D., James, J. H., Luchette, F. A., Wang, L., Friend, L. A., King, J. K., . . . Fischer, J. E. (2001). Adrenergic blockade reduces skeletal muscle glycolysis and Na(+), K(+)-ATPase activity during hemorrhage. *J Surg Res*, 99(2), 235-244. doi:10.1006/jsre.2001.6175
- McCarter, F. D., Nierman, S. R., James, J. H., Wang, L., King, J. K., Friend, L. A., & Fischer, J. E. (2002). Role of skeletal muscle Na<sup>+</sup>-K<sup>+</sup> ATPase activity in increased lactate production in sub-acute sepsis. *Life Sci*, 70(16), 1875-1888. doi:10.1016/s0024-3205(02)01475-3
- Meex, R. C., Schrauwen-Hinderling, V. B., Moonen-Kornips, E., Schaart, G., Mensink, M., Phielix, E., . . . Hesselink, M. K. (2010). Restoration of muscle mitochondrial function and metabolic flexibility in type 2 diabetes by exercise training is paralleled by increased myocellular fat storage and improved insulin sensitivity. *Diabetes*, 59(3), 572-579. doi:10.2337/db09-1322

- Merico, D., Isserlin, R., Stueker, O., Emili, A., & Bader, G. D. (2010). Enrichment map: a network-based method for gene-set enrichment visualization and interpretation. *PLoS One*, 5(11), e13984. doi:10.1371/journal.pone.0013984
- Merry, T. L., & Ristow, M. (2016). Do antioxidant supplements interfere with skeletal muscle adaptation to exercise training? *J Physiol*, 594(18), 5135-5147. doi:10.1113/jp270654
- Mohr, M., Thomassen, M., Girard, O., Racinais, S., & Nybo, L. (2016). Muscle variables of importance for physiological performance in competitive football. *Eur J Appl Physiol*, 116(2), 251-262. doi:10.1007/s00421-015-3274-x
- Moorthi, R. N., & Avin, K. G. (2017). Clinical relevance of sarcopenia in chronic kidney disease. *Curr Opin Nephrol Hypertens*, 26(3), 219-228. doi:10.1097/mnh.0000000000000318
- Morris, J. H., Apeltsin, L., Newman, A. M., Baumbach, J., Wittkop, T., Su, G., . . . Ferrin, T. E. (2011). clusterMaker: a multi-algorithm clustering plugin for Cytoscape. *BMC Bioinformatics*, 12, 436. doi:10.1186/1471-2105-12-436
- Moseley, A. E., Cougnon, M. H., Grupp, I. L., El Schultz, J., & Lingrel, J. B. (2004). Attenuation of cardiac contractility in Na,K-ATPase alpha1 isoform-deficient hearts under reduced calcium conditions. *J Mol Cell Cardiol*, 37(5), 913-919. doi:10.1016/j.yjmcc.2004.06.005
- Moseley, A. E., Huddleson, J. P., Bohanan, C. S., James, P. F., Lorenz, J. N., Aronow, B. J., & Lingrel, J. B. (2005). Genetic profiling reveals global changes in multiple biological pathways in the hearts of Na, K-ATPase alpha 1 isoform haploinsufficient mice. *Cell Physiol Biochem*, 15(1-4), 145-158.
- Murach, K. A., Fry, C. S., Kirby, T. J., Jackson, J. R., Lee, J. D., White, S. H., . . . Peterson, C. A. (2018). Starring or Supporting Role? Satellite Cells and Skeletal Muscle Fiber Size Regulation. *Physiology (Bethesda)*, 33(1), 26-38. doi:10.1152/physiol.00019.2017
- Murphy, K. T., Bundgaard, H., & Clausen, T. (2006). Beta3-adrenoceptor agonist stimulation of the Na<sup>+</sup>, K<sup>+</sup> -pump in rat skeletal muscle is mediated by beta2- rather than beta3-adrenoceptors. *Br J Pharmacol*, 149(6), 635-646. doi:10.1038/sj.bjp.0706896
- Murphy, K. T., Chee, A., Gleeson, B. G., Naim, T., Swiderski, K., Koopman, R., & Lynch, G. S. (2011). Antibody-directed myostatin inhibition enhances muscle mass and function in tumor-bearing mice. *Am J Physiol Regul Integr Comp Physiol*, 301(3), R716-726. doi:10.1152/ajpregu.00121.2011

- Murphy, K. T., Petersen, A. C., Goodman, C., Gong, X., Leppik, J. A., Garnham, A. P., . . . McKenna, M. J. (2006). Prolonged submaximal exercise induces isoform-specific Na<sup>+</sup>-K<sup>+</sup>-ATPase mRNA and protein responses in human skeletal muscle. *Am J Physiol Regul Integr Comp Physiol*, 290(2), R414-424. doi:10.1152/ajpregu.00172.2005
- Nascimento-Sales, M., Fredo-da-Costa, I., Borges Mendes, A. C. B., Melo, S., Ravache, T. T., Gomez, T. G. B., . . . Christoffolete, M. A. (2017). Is the FVB/N mouse strain truly resistant to diet-induced obesity? *Physiol Rep*, 5(9). doi:10.14814/phy2.13271
- Nespolo, R. F., Solano-Iguaran, J. J., & Bozinovic, F. (2017). Phylogenetic Analysis Supports the Aerobic-Capacity Model for the Evolution of Endothermy. *Am Nat*, 189(1), 13-27. doi:10.1086/689598
- Neufer, P. D., Carey, J. O., & Dohm, G. L. (1993). Transcriptional regulation of the gene for glucose transporter GLUT4 in skeletal muscle. Effects of diabetes and fasting. *J Biol Chem*, 268(19), 13824-13829.
- Nielsen, O. B., & Clausen, T. (1997). Regulation of Na<sup>(+)</sup>-K<sup>+</sup> pump activity in contracting rat muscle. *J Physiol*, 503 ( Pt 3), 571-581. doi:10.1111/j.1469-7793.1997.571bg.x
- Novel-Chate, V., Rey, V., Chiolero, R., Schneiter, P., Leverve, X., Jequier, E., & Tappy, L. (2001). Role of Na<sup>+</sup>-K<sup>+</sup>-ATPase in insulin-induced lactate release by skeletal muscle. *Am J Physiol Endocrinol Metab*, 280(2), E296-300. doi:10.1152/ajpendo.2001.280.2.E296
- O'Brien, W. J., Lingrel, J. B., & Wallick, E. T. (1994). Ouabain binding kinetics of the rat alpha two and alpha three isoforms of the sodium-potassium adenosine triphosphate. *Arch Biochem Biophys*, 310(1), 32-39.
- Okamoto, K., Wang, W., Rounds, J., Chambers, E. A., & Jacobs, D. O. (2001). ATP from glycolysis is required for normal sodium homeostasis in resting fast-twitch rodent skeletal muscle. *Am J Physiol Endocrinol Metab*, 281(3), E479-488. doi:10.1152/ajpendo.2001.281.3.E479
- Orlowski, J., & Lingrel, J. B. (1988a). Differential expression of the Na,K-ATPase alpha 1 and alpha 2 subunit genes in a murine myogenic cell line. Induction of the alpha 2 isozyme during myocyte differentiation. *J Biol Chem*, 263(33), 17817-17821.

- Orlowski, J., & Lingrel, J. B. (1988b). Tissue-specific and developmental regulation of rat Na,K-ATPase catalytic alpha isoform and beta subunit mRNAs. *J Biol Chem*, 263(21), 10436-10442.
- Overgaard, K., Nielsen, O. B., & Clausen, T. (1997). Effects of reduced electrochemical Na<sup>+</sup> gradient on contractility in skeletal muscle: role of the Na<sup>+</sup>-K<sup>+</sup> pump. *Pflugers Arch*, 434(4), 457-465. doi:10.1007/s004240050421
- Overgaard, K., Nielsen, O. B., Flatman, J. A., & Clausen, T. (1999). Relations between excitability and contractility in rat soleus muscle: role of the Na<sup>+</sup>-K<sup>+</sup> pump and Na<sup>+</sup>/K<sup>+</sup> gradients. *J Physiol*, 518(Pt 1), 215-225. doi:10.1111/j.1469-7793.1999.0215r.x
- Overmyer, K. A., Evans, C. R., Qi, N. R., Minogue, C. E., Carson, J. J., Chermside-Scabbo, C. J., . . . Burant, C. F. (2015). Maximal oxidative capacity during exercise is associated with skeletal muscle fuel selection and dynamic changes in mitochondrial protein acetylation. *Cell Metab*, 21(3), 468-478. doi:10.1016/j.cmet.2015.02.007
- Pedersen, B. K. (2019). Physical activity and muscle-brain crosstalk. *Nat Rev Endocrinol*, 15(7), 383-392. doi:10.1038/s41574-019-0174-x
- Pedroso, F. E., Spalding, P. B., Cheung, M. C., Yang, R., Gutierrez, J. C., Bonetto, A., . . . Zimmers, T. A. (2012). Inflammation, organomegaly, and muscle wasting despite hyperphagia in a mouse model of burn cachexia. *J Cachexia Sarcopenia Muscle*, 3(3), 199-211. doi:10.1007/s13539-012-0062-x
- Perry, B. D., Levinger, P., Morris, H. G., Petersen, A. C., Garnham, A. P., Levinger, I., & McKenna, M. J. (2015). The effects of knee injury on skeletal muscle function, Na<sup>+</sup>, K<sup>+</sup>-ATPase content, and isoform abundance. *Physiol Rep*, 3(2). doi:10.14814/phy2.12294
- Peterzan, M. A., Lygate, C. A., Neubauer, S., & Rider, O. J. (2017). Metabolic remodeling in hypertrophied and failing myocardium: a review. *Am J Physiol Heart Circ Physiol*, 313(3), H597-h616. doi:10.1152/ajpheart.00731.2016
- Pierre, S. V., & Xie, Z. (2006). The Na,K-ATPase receptor complex: its organization and membership. *Cell Biochem Biophys*, 46(3), 303-316.
- Post, R. L., Kume, S., Tobin, T., Orcutt, B., & Sen, A. K. (1969). Flexibility of an active center in sodium-plus-potassium adenosine triphosphatase. *J Gen Physiol*, 54(1), 306-326. doi:10.1085/jgp.54.1.306

- Poussin, C., Ibberson, M., Hall, D., Ding, J., Soto, J., Abel, E. D., & Thorens, B. (2011). Oxidative phosphorylation flexibility in the liver of mice resistant to high-fat diet-induced hepatic steatosis. *Diabetes*, *60*(9), 2216-2224. doi:10.2337/db11-0338
- Pratt, R. D., Brickman, C., Nawab, A., Cottrill, C., Snoad, B., Lakhani, H. V., . . . Sodhi, K. (2019). The Adipocyte Na/K-ATPase Oxidant Amplification Loop is the Central Regulator of Western Diet-Induced Obesity and Associated Comorbidities. *Sci Rep*, *9*(1), 7927. doi:10.1038/s41598-019-44350-9
- Pressley, T. A. (1992). Phylogenetic conservation of isoform-specific regions within alpha-subunit of Na(+)-K(+)-ATPase. *Am J Physiol*, *262*(3 Pt 1), C743-751.
- Quintas, L. E., Pierre, S. V., Liu, L., Bai, Y., Liu, X., & Xie, Z. J. (2010). Alterations of Na<sup>+</sup>/K<sup>+</sup>-ATPase function in caveolin-1 knockout cardiac fibroblasts. *J Mol Cell Cardiol*, *49*(3), 525-531. doi:10.1016/j.yjmcc.2010.04.015
- Radzyukevich, T. L., Lingrel, J. B., & Heiny, J. A. (2009). The cardiac glycoside binding site on the Na,K-ATPase alpha2 isoform plays a role in the dynamic regulation of active transport in skeletal muscle. *Proc Natl Acad Sci U S A*, *106*(8), 2565-2570. doi:10.1073/pnas.0804150106
- Radzyukevich, T. L., Neumann, J. C., Rindler, T. N., Oshiro, N., Goldhamer, D. J., Lingrel, J. B., & Heiny, J. A. (2013). Tissue-specific role of the Na,K-ATPase alpha2 isozyme in skeletal muscle. *J Biol Chem*, *288*(2), 1226-1237. doi:10.1074/jbc.M112.424663
- Rhoads, R. P., Baumgard, L. H., El-Kadi, S. W., & Zhao, L. D. (2016). Physiology and Endocrinology Symposium: Roles for insulin-supported skeletal muscle growth. *J Anim Sci*, *94*(5), 1791-1802. doi:10.2527/jas.2015-0110
- Rodriguez-Cuenca, S., Carobbio, S., Velagapudi, V. R., Barbarroja, N., Moreno-Navarrete, J. M., Tinahones, F. J., . . . Vidal-Puig, A. (2012). Peroxisome proliferator-activated receptor gamma-dependent regulation of lipolytic nodes and metabolic flexibility. *Mol Cell Biol*, *32*(8), 1555-1565. doi:10.1128/mcb.06154-11
- Saez, A. G., Lozano, E., & Zaldivar-Riveron, A. (2009). Evolutionary history of Na,K-ATPases and their osmoregulatory role. *Genetica*, *136*(3), 479-490. doi:10.1007/s10709-009-9356-0

- Sakuma, K., Aoi, W., & Yamaguchi, A. (2017). Molecular mechanism of sarcopenia and cachexia: recent research advances. *Pflugers Arch*, *469*(5-6), 573-591. doi:10.1007/s00424-016-1933-3
- Salvatore, D., Simonides, W. S., Dentice, M., Zavacki, A. M., & Larsen, P. R. (2014). Thyroid hormones and skeletal muscle--new insights and potential implications. *Nat Rev Endocrinol*, *10*(4), 206-214. doi:10.1038/nrendo.2013.238
- Sanchez, G., Nguyen, A. N., Timmerberg, B., Tash, J. S., & Blanco, G. (2006). The Na,K-ATPase alpha4 isoform from humans has distinct enzymatic properties and is important for sperm motility. *Mol Hum Reprod*, *12*(9), 565-576. doi:10.1093/molehr/gal062
- Schonke, M., Massart, J., & Zierath, J. R. (2018). Effects of high-fat diet and AMP-activated protein kinase modulation on the regulation of whole-body lipid metabolism. *J Lipid Res*, *59*(7), 1276-1282. doi:10.1194/jlr.D082370
- Sepp, M., Sokolova, N., Jugai, S., Mandel, M., Peterson, P., & Vendelin, M. (2014). Tight coupling of Na<sup>+</sup>/K<sup>+</sup>-ATPase with glycolysis demonstrated in permeabilized rat cardiomyocytes. *PLoS One*, *9*(6), e99413. doi:10.1371/journal.pone.0099413
- Shannon, P., Markiel, A., Ozier, O., Baliga, N. S., Wang, J. T., Ramage, D., . . . Ideker, T. (2003). Cytoscape: a software environment for integrated models of biomolecular interaction networks. *Genome Res*, *13*(11), 2498-2504. doi:10.1101/gr.1239303
- Siegel, G. J., & Albers, R. W. (1967). Sodium-potassium-activated adenosine triphosphatase of Electrophorus electric organ. IV. Modification of responses to sodium and potassium by arsenite plus 2,3-dimercaptopropanol. *J Biol Chem*, *242*(21), 4972-4979.
- Simonides, W. S., & van Hardeveld, C. (2008). Thyroid hormone as a determinant of metabolic and contractile phenotype of skeletal muscle. *Thyroid*, *18*(2), 205-216. doi:10.1089/thy.2007.0256
- Skou, J. C. (1957). The influence of some cations on an adenosine triphosphatase from peripheral nerves. *Biochim Biophys Acta*, *23*(2), 394-401.
- Skou, J. C., & Esmann, M. (1992). The Na,K-ATPase. *J Bioenerg Biomembr*, *24*(3), 249-261.

- Sodhi, K., Maxwell, K., Yan, Y., Liu, J., Chaudhry, M. A., Getty, M., . . . Shapiro, J. I. (2015). pNaKtide inhibits Na/K-ATPase reactive oxygen species amplification and attenuates adipogenesis. *Sci Adv*, *1*(9), e1500781. doi:10.1126/sciadv.1500781
- Sodhi, K., Nichols, A., Mallick, A., Klug, R. L., Liu, J., Wang, X., . . . Shapiro, J. I. (2018). The Na/K-ATPase Oxidant Amplification Loop Regulates Aging. *Sci Rep*, *8*(1), 9721. doi:10.1038/s41598-018-26768-9
- Sodhi, K., Srikanthan, K., Goguet-Rubio, P., Nichols, A., Mallick, A., Nawab, A., . . . Shapiro, J. I. (2017). pNaKtide Attenuates Steatohepatitis and Atherosclerosis by Blocking Na/K-ATPase/ROS Amplification in C57Bl6 and ApoE Knockout Mice Fed a Western Diet. *Sci Rep*, *7*(1), 193. doi:10.1038/s41598-017-00306-5
- Son, J. W., Lee, S. S., Kim, S. R., Yoo, S. J., Cha, B. Y., Son, H. Y., & Cho, N. H. (2017). Low muscle mass and risk of type 2 diabetes in middle-aged and older adults: findings from the KoGES. *Diabetologia*, *60*(5), 865-872. doi:10.1007/s00125-016-4196-9
- Srikanthan, K., Shapiro, J. I., & Sodhi, K. (2016). The Role of Na/K-ATPase Signaling in Oxidative Stress Related to Obesity and Cardiovascular Disease. *Molecules*, *21*(9). doi:10.3390/molecules21091172
- Stuart, C. A., McCurry, M. P., Marino, A., South, M. A., Howell, M. E., Layne, A. S., . . . Stone, M. H. (2013). Slow-twitch fiber proportion in skeletal muscle correlates with insulin responsiveness. *J Clin Endocrinol Metab*, *98*(5), 2027-2036. doi:10.1210/jc.2012-3876
- Su, Z., Klein, J. D., Du, J., Franch, H. A., Zhang, L., Hassounah, F., . . . Wang, X. H. (2017). Chronic kidney disease induces autophagy leading to dysfunction of mitochondria in skeletal muscle. *Am J Physiol Renal Physiol*, *312*(6), F1128-f1140. doi:10.1152/ajprenal.00600.2016
- Templeton, G. H., Sweeney, H. L., Timson, B. F., Padalino, M., & Dudenhoefter, G. A. (1988). Changes in fiber composition of soleus muscle during rat hindlimb suspension. *J Appl Physiol (1985)*, *65*(3), 1191-1195.
- Tepavcevic, S., Milutinovic, D. V., Macut, D., Stanisic, J., Nikolic, M., Bozic-Antic, I., . . . Koricanac, G. (2015). Cardiac Nitric Oxide Synthases and Na(+)/K(+)-ATPase in the Rat Model of Polycystic Ovary Syndrome Induced by Dihydrotestosterone. *Exp Clin Endocrinol Diabetes*, *123*(5), 303-307. doi:10.1055/s-0035-1548929

- Theilen, N. T., Kunkel, G. H., & Tyagi, S. C. (2017). The Role of Exercise and TFAM in Preventing Skeletal Muscle Atrophy. *J Cell Physiol*, 232(9), 2348-2358. doi:10.1002/jcp.25737
- Thomassen, M., Murphy, R. M., & Bangsbo, J. (2013). Fibre type-specific change in FXVD1 phosphorylation during acute intense exercise in humans. *J Physiol*, 591(6), 1523-1533. doi:10.1113/jphysiol.2012.247312
- Thompson, C. B., & McDonough, A. A. (1996). Skeletal muscle Na,K-ATPase alpha and beta subunit protein levels respond to hypokalemic challenge with isoform and muscle type specificity. *J Biol Chem*, 271(51), 32653-32658.
- Tian, J., Li, X., Liang, M., Liu, L., Xie, J. X., Ye, Q., . . . Xie, Z. (2009). Changes in sodium pump expression dictate the effects of ouabain on cell growth. *J Biol Chem*, 284(22), 14921-14929. doi:10.1074/jbc.M808355200
- van der Velden, J. L., Langen, R. C., Kelders, M. C., Willems, J., Wouters, E. F., Janssen-Heininger, Y. M., & Schols, A. M. (2007). Myogenic differentiation during regrowth of atrophied skeletal muscle is associated with inactivation of GSK-3beta. *Am J Physiol Cell Physiol*, 292(5), C1636-1644. doi:10.1152/ajpcell.00504.2006
- Verhees, K. J., Schols, A. M., Kelders, M. C., Op den Kamp, C. M., van der Velden, J. L., & Langen, R. C. (2011). Glycogen synthase kinase-3beta is required for the induction of skeletal muscle atrophy. *Am J Physiol Cell Physiol*, 301(5), C995-c1007. doi:10.1152/ajpcell.00520.2010
- Walas, H., & Juel, C. (2012). Purinergic activation of rat skeletal muscle membranes increases  $V_{max}$  and  $Na^{+}$  affinity of the Na,K-ATPase and phosphorylates phospholemman and  $\alpha 1$  subunits. *Pflügers Archiv - European Journal of Physiology*, 463(2), 319-326. doi:10.1007/s00424-011-1050-2
- Wang, H., Haas, M., Liang, M., Cai, T., Tian, J., Li, S., & Xie, Z. (2004). Ouabain assembles signaling cascades through the caveolar  $Na^{+}/K^{+}$ -ATPase. *J Biol Chem*, 279(17), 17250-17259. doi:10.1074/jbc.M313239200
- Wang, X., Cai, L., Xie, J. X., Cui, X., Zhang, J., Wang, J., . . . Xie, Z. (2019). A caveolin binding motif in Na/K-ATPase is required for stem cell differentiation and organogenesis in mammals and *C. elegans* [Manuscript submitted for publication]. Marshall Institute for Interdisciplinary Research, Marshall University.

- Wang, X., Pickrell, A. M., Zimmers, T. A., & Moraes, C. T. (2012). Increase in muscle mitochondrial biogenesis does not prevent muscle loss but increased tumor size in a mouse model of acute cancer-induced cachexia. *PLoS One*, 7(3), e33426. doi:10.1371/journal.pone.0033426
- Wang, Z. V., Li, D. L., & Hill, J. A. (2014). Heart failure and loss of metabolic control. *J Cardiovasc Pharmacol*, 63(4), 302-313. doi:10.1097/fjc.0000000000000054
- Wansapura, A. N., Lasko, V. M., Lingrel, J. B., & Lorenz, J. N. (2011). Mice expressing ouabain-sensitive alpha1-Na,K-ATPase have increased susceptibility to pressure overload-induced cardiac hypertrophy. *Am J Physiol Heart Circ Physiol*, 300(1), H347-355. doi:10.1152/ajpheart.00625.2010
- Weihrauch, M., & Handschin, C. (2018). Pharmacological targeting of exercise adaptations in skeletal muscle: Benefits and pitfalls. *Biochem Pharmacol*, 147, 211-220. doi:10.1016/j.bcp.2017.10.006
- Williams, M. W., Resneck, W. G., Kaysser, T., Ursitti, J. A., Birkenmeier, C. S., Barker, J. E., & Bloch, R. J. (2001). Na,K-ATPase in skeletal muscle: two populations of beta-spectrin control localization in the sarcolemma but not partitioning between the sarcolemma and the transverse tubules. *J Cell Sci*, 114(Pt 4), 751-762.
- Wu, Y., & Wang, H. (2019). Convergent evolution of bird-mammal shared characteristics for adapting to nocturnality. *Proc Biol Sci*, 286(1897), 20182185. doi:10.1098/rspb.2018.2185
- Wyckelsma, V. L., McKenna, M. J., Serpiello, F. R., Lamboley, C. R., Aughey, R. J., Stepto, N. K., . . . Murphy, R. M. (2015). Single-fiber expression and fiber-specific adaptability to short-term intense exercise training of Na<sup>+</sup>-K<sup>+</sup>-ATPase alpha- and beta-isoforms in human skeletal muscle. *J Appl Physiol (1985)*, 118(6), 699-706. doi:10.1152/jappphysiol.00419.2014
- Xie, J., Ye, Q., Cui, X., Madan, N., Yi, Q., Pierre, S. V., & Xie, Z. (2015). Expression of rat Na-K-ATPase alpha2 enables ion pumping but not ouabain-induced signaling in alpha1-deficient porcine renal epithelial cells. *Am J Physiol Cell Physiol*, 309(6), C373-382. doi:10.1152/ajpcell.00103.2015
- Xie, Z., & Askari, A. (2002). Na<sup>(+)</sup>/K<sup>(+)</sup>-ATPase as a signal transducer. *Eur J Biochem*, 269(10), 2434-2439.

- Xie, Z., Kometiani, P., Liu, J., Li, J., Shapiro, J. I., & Askari, A. (1999). Intracellular reactive oxygen species mediate the linkage of Na<sup>+</sup>/K<sup>+</sup>-ATPase to hypertrophy and its marker genes in cardiac myocytes. *J Biol Chem*, 274(27), 19323-19328.
- Xu, D., Xu, M., Jeong, S., Qian, Y., Wu, H., Xia, Q., & Kong, X. (2018). The Role of Nrf2 in Liver Disease: Novel Molecular Mechanisms and Therapeutic Approaches. *Front Pharmacol*, 9, 1428. doi:10.3389/fphar.2018.01428
- Xu, H., Ren, X., Lamb, G. D., & Murphy, R. M. (2018). Physiological and biochemical characteristics of skeletal muscles in sedentary and active rats. *J Muscle Res Cell Motil*, 39(1-2), 1-16. doi:10.1007/s10974-018-9493-0
- Yan, Y., Shapiro, A. P., Haller, S., Katragadda, V., Liu, L., Tian, J., . . . Liu, J. (2013). Involvement of reactive oxygen species in a feed-forward mechanism of Na/K-ATPase-mediated signaling transduction. *J Biol Chem*, 288(47), 34249-34258. doi:10.1074/jbc.M113.461020
- Yang, W.-K., Chao, T.-L., Chuang, H.-J., Hu, Y.-C., Lorin-Nebel, C., Blondeau-Bidet, E., . . . Lee, T.-H. (2019). Gene expression of Na<sup>+</sup>/K<sup>+</sup>-ATPase  $\alpha$ -isoforms and FXFD proteins and potential modulatory mechanisms in euryhaline milkfish kidneys upon hypoosmotic challenges. *Aquaculture*, 504, 59-69. doi:<https://doi.org/10.1016/j.aquaculture.2019.01.046>
- Yang, W., Zhang, Y., Li, Y., Wu, Z., & Zhu, D. (2007). Myostatin induces cyclin D1 degradation to cause cell cycle arrest through a phosphatidylinositol 3-kinase/AKT/GSK-3  $\beta$  pathway and is antagonized by insulin-like growth factor 1. *J Biol Chem*, 282(6), 3799-3808. doi:10.1074/jbc.M610185200
- Ye, Q., Lai, F., Banerjee, M., Duan, Q., Li, Z., Si, S., & Xie, Z. (2013). Expression of mutant  $\alpha 1$  Na/K-ATPase defective in conformational transition attenuates Src-mediated signal transduction. *J Biol Chem*, 288(8), 5803-5814. doi:10.1074/jbc.M112.442608
- Young, R. M., & Lingrel, J. B. (1987). Tissue distribution of mRNAs encoding the  $\alpha$  isoforms and  $\beta$  subunit of rat Na<sup>+</sup>,K<sup>+</sup>-ATPase. *Biochem Biophys Res Commun*, 145(1), 52-58.
- Yu, H., Cui, X., Zhang, J., Xie, J. X., Banerjee, M., Pierre, S. V., & Xie, Z. (2018). Heterogeneity of signal transduction by Na-K-ATPase  $\alpha$ -isoforms: role of Src interaction. *Am J Physiol Cell Physiol*, 314(2), C202-c210. doi:10.1152/ajpcell.00124.2017

- Yuan, Z., Cai, T., Tian, J., Ivanov, A. V., Giovannucci, D. R., & Xie, Z. (2005). Na/K-ATPase tethers phospholipase C and IP3 receptor into a calcium-regulatory complex. *Mol Biol Cell*, 16(9), 4034-4045. doi:10.1091/mbc.e05-04-0295
- Zhang, D., Wang, X., Li, Y., Zhao, L., Lu, M., Yao, X., . . . Ying, H. (2014). Thyroid hormone regulates muscle fiber type conversion via miR-133a1. *J Cell Biol*, 207(6), 753-766. doi:10.1083/jcb.201406068
- Zhang, L., Morris, K. J., & Ng, Y. C. (2006). Fiber type-specific immunostaining of the Na<sup>+</sup>,K<sup>+</sup>-ATPase subunit isoforms in skeletal muscle: age-associated differential changes. *Biochim Biophys Acta*, 1762(9), 783-793. doi:10.1016/j.bbadis.2006.08.006
- Zhang, S., Hulver, M. W., McMillan, R. P., Cline, M. A., & Gilbert, E. R. (2014). The pivotal role of pyruvate dehydrogenase kinases in metabolic flexibility. *Nutr Metab (Lond)*, 11(1), 10. doi:10.1186/1743-7075-11-10
- Zhuang, L., Xu, L., Wang, P., Jiang, Y., Yong, P., Zhang, C., . . . Yang, P. (2015). Na<sup>+</sup>/K<sup>+</sup>-ATPase alpha1 subunit, a novel therapeutic target for hepatocellular carcinoma. *Oncotarget*, 6(29), 28183-28193. doi:10.18632/oncotarget.4726
- Zurlo, F., Larson, K., Bogardus, C., & Ravussin, E. (1990). Skeletal muscle metabolism is a major determinant of resting energy expenditure. *J Clin Invest*, 86(5), 1423-1427. doi:10.1172/jci114857

## APPENDIX A

### LETTER FROM OFFICE OF RESEARCH INTEGRITY



Office of Research Integrity

November 12, 2019

Laura Kutz  
Biomedical Sciences PhD Candidate  
Marshall Institute for Interdisciplinary Research (MIIR)  
Marshall University

Dear Ms. Kutz:

This letter is in response to the submitted dissertation abstract entitled "*Role of ATP1A1 in Skeletal Muscle Growth and Metabolism.*" After assessing the abstract it has been deemed not to be human subject research and therefore exempt from oversight of the Marshall University Institutional Review Board (IRB). The Institutional Animal Care and Use Committee (IACUC) has reviewed and approved the study under protocol #609 and #610. The applicable human and animal federal regulations have set forth the criteria utilized in making this determination. If there are any changes to the abstract you provided then you would need to resubmit that information to the Office of Research Integrity for review and a determination.

I appreciate your willingness to submit the abstract for determination. Please feel free to contact the Office of Research Integrity if you have any questions regarding future protocols that may require IRB review.

Sincerely,



Bruce F. Day, ThD, CIP  
Director  
Office of Research Integrity

## APPENDIX B

### ABBREVIATIONS

µg – micrograms; 1/1000000<sup>th</sup> of a gram

2-DG – 2-deoxyglucose

AAC-19 – porcine renal epithelial cell line

Akt – protein kinase B (see also: PKB)

AMP – adenosine monophosphate

AMPK – 5' adenosine monophosphate-activated protein kinase

ANOVA – analysis of variance

ATCC – American Type Culture Collection

ATP – adenosine triphosphate

ATP1A1 – Na/K-ATPase  $\alpha$ 1

AUC – area under the curve

BiNGO – Biological Networks Gene Ontology tool

B-Raf – serine/threonine-protein kinase B-Raf

BW – body weight

C<sub>2</sub>C<sub>12</sub> – immortalized mouse myoblast line

C57J/B16 – commonly used strain of inbred mice

cAMP – cyclic adenosine monophosphate

cDNA – complementary deoxyribonucleic acid

CSA – cross-sectional area

CTS – cardiotonic steroids

DIO2 – type II iodothyronine deiodinase

DMEM – Dulbecco’s modified Eagle’s medium

ECAR – extracellular acidification rate

ECL – enhanced chemiluminescence

EDL – extensor digitorum longus

EDTA – ethylenediaminetetraacetic acid

EGF – epidermal growth factor

EGFR – epidermal growth factor receptor

EGTA – ethylene glycol-bis( $\beta$ -aminoethyl ether)-*N,N,N',N'*-tetraacetic acidethylene

FBS – fetal bovine serum

FCCP – carbonyl cyanide-4-(trifluoromethoxy)phenylhydrazone

FIJI – FIJI is just ImageJ

FVB – albino inbred mouse strain

FXRD1 – phospholemman

GIMP – GNU image manipulation program

GLUT4 – glucose transporter type 4

GSK-3 $\beta$  – glycogen synthase kinase 3 $\beta$

GTT – glucose tolerance test

IP – intraperitoneal

IP3 – inositol triphosphate

ITT – insulin tolerance test

K<sup>+</sup> – potassium

KCl – potassium chloride

LAS/AF – Leica Application Suite/Advanced Fluorescence

LX- $\alpha$ 2 – LLC-PK1-derived cell line

LY-a2 – LLC-PK1-derived cell line

m/min – meters per minute

MAPK – mitogen-activated protein kinase

mg/g – milligram/gram

mg/kg – milligram/kilogram

Mg-ATP – magnesium adenosine triphosphate

MgCl<sub>2</sub> – magnesium chloride

MIIR – Marshall Institute for Interdisciplinary Research

mM – millimolar; millimoles per liter

MRF4 – myogenic factor 6; herculin

mRNA – messenger ribonucleic acid

mTORC – mammalian target of rapamycin complex

Myhc – myosin heavy chain

Na/K-ATPase – sodium-potassium adenosine triphosphatase (see also: NKA)

Na<sup>+</sup> – sodium

NaCl – sodium chloride

NAD(P)H – nicotinamide adenine dinucleotide phosphate and nicotinamide adenine dinucleotide

NADPH – nicotinamide adenine dinucleotide phosphate

NaKtide – peptide based on Src binding site in ATP1A1

NASH – non-alcoholic steatohepatitis

NC – normal chow

NFAT – nuclear factor of activated T-cells

NF- $\kappa$ B – nuclear factor kappa-light-chain-enhancer of activated B cells

NIH – National Institute of Health

NKA – sodium-potassium adenosine triphosphatase (see also: Na/K-ATPase)

nm – nanometer

Nrf2 – nuclear factor erythroid 2-related factor 2

OCR – oxygen consumption rate

OD – optical density

PBS – phosphate-buffered saline

PGC-1 $\alpha$  – peroxisome proliferator-activated receptor gamma coactivator-1 $\alpha$

Pi – inorganic phosphate

PI3K – phosphoinositide 3-kinase

PKA – protein kinase A

PMSF – phenylmethylsulfonyl fluoride

PPAR $\gamma$  – peroxisome proliferator-activated receptor gamma

p-Ser9 – phosphorylated serine 9

PY-17 – LLC-PK1-derived cell line

qPCR – quantitative polymerase chain reaction (see also: qRT-PCR, RT-PCR)

qRT-PCR – quantitative real time polymerase chain reaction (see also: qPCR, RT-PCR)

R Gastroc – red gastrocnemius muscle

Rap1 – Ras-proximate-1 or Ras-related-protein-1

RIPA – radioimmunoprecipitation assay

RNA – ribonucleic acid

ROS – reactive oxygen species

RT – reverse transcriptase

RT-PCR – real-time polymerase chain reaction (see also: qPCR, qRT-PCR)

SDS-PAGE – sodium dodecyl sulfate–polyacrylamide gel electrophoresis

SEM – standard error of the mean

sk $\alpha$ 1<sup>-/-</sup> – skeletal muscle-specific ATP1A1 knockout mouse

Src – proto-oncogene tyrosine-protein kinase Src

SST-MINI tubes – serum separator miniature tubes

SubQ – subcutaneous

T3 – triiodothyronine

T4 – thyroxine

TCA – tricarboxylic acid

Tris-HCl – tris(hydroxymethyl)aminomethane hydrochloride

W Gastroc – white gastrocnemius muscle

WD – Western diet

xg – times gravitational force